

Figure credit: Cover art was created by Reinaldo A. Garcia and Marcos A. Sabino.



# Synthesis and characterization of S-IPN hydrogels of chitosan/PVA/PNIPAm to be used in the design of nucleus pulposus prosthesis

Marcos Antonio Sabino<sup>1\*</sup>; Reinaldo Aandres Garcia<sup>1</sup>

\*Corresponding author: e-mail address: [msabino@usb.ve](mailto:msabino@usb.ve)

**Abstract:** Hydrogels (HG) have been widely used in biomedical applications due to their high-water content which improves their biocompatibility with living tissue. In this study, Chitosan (CS) hydrogels cross-linked with Genipin and semi interpenetrated network (S-IPN) with PVA/PNIPAm were prepared to be used in the design of nucleus pulposus (NP) prosthesis. Chemical structure, morphology, swelling ratio (SR), mechanical properties and cytotoxicity were evaluated through a variation of the Genipin percentage and CS/PVA/PNIPAm proportions. Those experiments were carried out through Fourier-Transform Infrared Spectroscopy, Scanning Electron Microscopy, swelling studies, dynamic rheology, and hemocompatibility tests. The results showed that regardless of the Genipin percentage or polymers proportions, all HGs had interconnected porous structure, and change microstructurally, the pore size, its size distribution and the wall thickness. Firstly, an increment in the Genipin percentage and in the CS proportion concluded in an augmentation of the pore size. Secondly, an augmentation in the PVA proportion ended up producing smaller pores, with larger wall thickness and more homogeneous pore size distribution. The variation in PNIPAm proportion didn't influence the morphology, but did have an impact on the SR and storage modulus ( $G'$ ) augmenting in both cases as the PNIPAm proportion. The swelling ratio turned out to be related to the pore morphology; as smaller the pore size, smaller the SR. Likewise, the storage modulus rose insofar the SR diminished. In these S-IPN HGs,  $G'$  varied between 77 Pa and 27000 Pa, values below and above  $G'$  reported for human NP. Also,  $\delta$  varied between 1.4° and 13.17° while the  $\delta$  reported for NP is 23°–31°. Finally, the hemocompatibility tests did not show cellular lysis for any formulation. These outcomes demonstrated that from the rheological and hemocompatibility point of view, this kind of as semi interpenetrated networks (S-IPNs) HGs can be tailored to attain the NP's properties.

**Keywords:** Chitosan. PVA. PNIPAm. Genipin. LCST.  $\delta$ . Storage modulus. S-IPN and Hydrogel.

## Introduction

The vertebral spine is the structure responsible for providing support to the body and protecting the spinal cord. The structure is linked by 24 mobile vertebral bones, 7 of them in the cervical region, 12 in the thoracic region and 5 in the lumbar region. This latter region is the one that withstands most of the load with up to the 55% of all the load produced by the body mass<sup>1,2</sup>. The intervertebral discs (IVD) are embedded between those vertebral bodies and macroscopically, are composed by the nucleus pulposus (NP) surrounded by the annulus fibrosus and on the top and bottom of NP (and part of the AF) you will find the endplates<sup>3,4</sup>.

The NP is a fibro cartilaginous material, with a water content that varies from 90% (at birth) to 70% or less at the age of 60 years old<sup>5</sup>. This amount of water in the NP allows its deformation while maintaining an incompressible volume. Thus, when a pressure is applied from above, the NP reduces its height and attempts to expand radially (which is prevented by the AF). Therefore, the NP transmits the pressure outwards towards the collagen fibers in the annulus, which stores and absorbs the energy developing tension. NP and AF bear part of the load, the rest is transmitted through the vertebral endplates to the next vertebra. When the load ceases, the stored energy in the collagen fibers is released and exerted back to the NP where it is used to restore any deformation<sup>6</sup>. This combined action of the NP and AF also endows the disc with a great resilience that acts as a shock absorber, lessening the speed transmission of forces from one vertebra to the other<sup>3,6,7</sup>.

After water, the most abundant component of the NP are the proteoglycans with a content of 65% of the dry weight, which decreases up to 30% with aging<sup>5</sup>. These are hydrophilic molecules accountable for the content of water and for the generation of the osmotic pressure<sup>2,8</sup>.

Now, focusing on the specific case of low back pain (LBP), this can

be generated by aging and diseases. The first one is a natural process that evokes changes in the extracellular matrix structure (which alter the synthetic capabilities of the disc cells) and increases the accumulation of degraded products that ultimately result in tissue degeneration<sup>9</sup>. On the other hand, degenerative disc disease (DDD) is the main source of chronic and recurring LBP, a condition that 80% of the population suffer in some part of their lives<sup>10</sup>. This syndrome alters the biomechanics of the disc, decreasing the proteoglycans content, dehydrating and shrinking the NP causing a reduction in the osmotic pressure resulting in an increased range of motion<sup>1,11-14</sup>. Once the NP is damaged, it suffers an increment in the shear modulus and a diminution of the swelling pressure, the relative energy dissipation, and the water content leading to a lessening of the height of the IVD. In extreme cases of failure or total removal of NP, excessive bulge of the AF layers leads to a collapse of the IVD<sup>4,15,16</sup>.

Both aging and DDD can be developed even faster by adverse biomechanical loadings, overloads, loads borne for long times, bad postures and high impacts on the spine<sup>4,17,18</sup>. Studies have estimated the annual work productivity losses for LBP in the UK, Australia and USA in 9.1 billion £, 8.1 billion AUD\$ and 100billion USD respectively<sup>18-20</sup>.

Surprisingly, the most common approach to treat chronic low back diseases is to eliminate or diminish the pain rather than restoring the segment biomechanics<sup>3,4</sup>. When conservative treatments to relieve LBP (like heat and cold therapy, steroid injections, medication, physical therapy, etc.) do not work, surgical interventions are required. The most common surgical procedure in these cases is the intervertebral fusion. This treatment, despite diminishing pain, results in increased stiffness, loss of motion, and altered patterns of stress flow that produce altered biomechanics at adjacent motion segments<sup>21-23</sup>. The second most common surgical treatment is the NP discectomy, but in the same way, this

<sup>1</sup>Grupo B5IDA, Departamento de Química, Universidad Simón Bolívar, Caracas, Venezuela AP 89000.

one greatly alters the biomechanical function of the disc leading to further disc degeneration in the form of circumferential tears in the AF<sup>1,24,25</sup>. Furthermore, after discectomy, the NP space is filled with air, causing larger displacement because air is easily compressed<sup>7,26</sup>. Since these traditional treatments alter the segment biomechanics increasing the risks for adjacent segments degeneration in up to 35% and 45%, are needed new motion-preserving treatments that, according to investigations have less ( 12% ) risk of adjacent segments degeneration<sup>27-29</sup>. Moreover, the risks for symptomatic adjacent segment disease in motion-preserving procedures have been reported in 4.6%, significantly lower than patients that underwent intervertebral fusion<sup>29</sup>.

One promising solution is disc arthroplasty (replacement), whose biomechanical objective is the restoration or preservation the mechanical functions of the disc<sup>30</sup>. This kind of replacement is divided mainly into two groups: nucleus prosthesis and total disc prosthesis. The latter one has been developed for more than 60 years, and in the specific case of lumbar arthroplasty only 3 of them have been approved by the U.S. Food and Drugs Administration (FDA)<sup>31,32</sup>. On the other hand, NP prostheses have been under investigation for fewer years, and none of them have achieved the FDA approval. These prostheses are designed to replace only the NP, maintaining the AF and the end plates intact, with the objective of restoring (indirectly) the biomechanical function of the entire IVD<sup>30,33</sup>.

The development of NP replacement hence relies on the tissue engineering field, which focuses on the regeneration (using scaffolds) or replacement (using prosthesis) of damaged tissue<sup>34</sup>. In the case of scaffolds, it is believed that cells need a supporting material to act as template or substrate to attach and generate new tissue. In this scenario, highly porous structures are needed since they allow vascularization and diffusion of the nutrients and waste products. The tissue regeneration also depends on the pore size, since it has been demonstrated that a large surface area (higher inasmuch as smaller the pores) benefit cell attachment and growth, while a large pore size is also required to accommodate and deliver the sufficient cell mass for tissue regeneration, so an equilibrium in pore size should be attained<sup>35</sup>. Nevertheless, even with an optimum pore size, nutrients and cells migration will be inhibited without an interconnected pores structure. These morphology conditions promoted investigations in hydrogels, porous materials that in some cases like in Chitosan Hydrogels, have interconnective pores.

Another criterion to fulfill in prosthesis design is biocompatibility, and again, Chitosan hydrogels have demonstrated a good biocompatibility for IVD cells<sup>36</sup>, antibacterial activity against a broad spectrum of bacteria and do not generate allergic or inflammatory responses after implantation, injection, ingestion or topical application<sup>37-40</sup>. Nonetheless, the problem with hydrogels is their low load-bearing capacity and their biocompatibility<sup>3</sup>. For those reasons, this investigation evaluated Chitosan-based hydrogels as a nucleus pulposus replacement, with several chemical variations to improve mechanical properties. First, the cross-linking with different Genipin concentrations. Genipin has been reported as a non-cytotoxic, anti-inflammatory, anti-angiogenic, anti-oxidative, antiproliferative, and apoptosis-inducing<sup>41</sup>.

The second variation implemented for the CS based HGs was the insertion of two disperse phases and create and semi-interpenetrated networks hydrogel, using: Polyvinyl Alcohol (PVA) and Poly n-isopropylacrylamide (PNIPAm); in different proportions.

The study of NP replacements should assess mechanical, biocompatibility, bio-durability, cell-materials interaction and assimilation, kinematic testing, and safety testing; notwithstanding, this investigation focuses on the study of the first two characteristics in contrast with the NP properties.

## Materials and methods

### Materials

Chitosan MW 160.000 g/mol, deacetylation degree (DD) of 0,82±0,2 (measured by three different methods: Acid-Base Titration according to Youling et al.<sup>42</sup>, UV-VIS Spectroscopy as stated by Renata et al.<sup>43</sup> and Fourier-transform infrared spectroscopy using Chitosan films and KBr pellets<sup>44,45</sup>); and NIPAm purity 97% were purchased from Sigma Aldrich. Genipin with a MW of 226 g/mol and purity≥98% was provided by Challenge Bioproducts, Polyvinyl Alcohol, MW 160.000 g/mol from Himedia was used. Acetic Acid (purity≥99,8%) from Fluca, and for the hemocompatibility test, Blood agar (base) from Merck and defibrinated blood from male sheep.

### Methods

#### Chitosan/Genipin Stoichiometry Ratio

Having measured the Chitosan DD (0, 82), is fair to say that from every 100 monomers in the Chitosan chain, 82 monomers would correspond to D-glucosamine and 18 to N-Acetyl-Glucosamine. Thus, the molecular weight corresponding to 100 Chitosan monomers would be:

$$W_{100 \text{ Chitosan Monomers}} = \%DD * W_{Dglucosamine} + (100\% - \%DD) * W_{Nacetyl-Dglucosamine}$$

$$W_{100 \text{ Chitosan Monomers}} = 82x179,17gr + 18x221,21gr = 18673,72gr$$

This means that for each 18673g of Chitosan, 14692 g correspond to D-glucosamine or in other words, the percentage in weight of D-glucosamine in the Chitosan is 78,68%.

Since each Genipin molecule reacts with 2 D-glucosamine molecules to generate the cross-linking, for a 100% reaction of the D-glucosamine groups in the Chitosan, the Genipin amount necessary would be:

$$\text{Genipin mol} = 2 \times \text{Dglucosamine mol}$$

But, since this study varied the Genipin percentage from 2,48%–5,4% (theoretically cross-linked percentage), to the former equation was needed to add a factor 0,0248 ≤ n ≤ 0,053, resulting in the following equation:

$$\text{Genipin mol} = 2 \times \text{Dglucosamine mol} * n$$

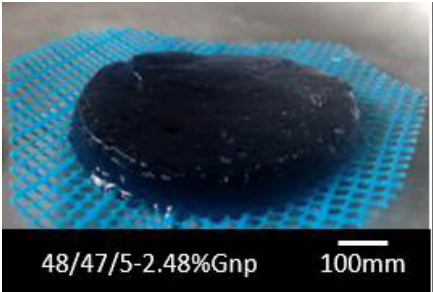
In terms of molecular weight (MW), and replacing  $W_{Dglucosamine}$  in terms of Chitosan results:

$$W_{Genipin} = 2 \times \frac{W_{chitosan} \times 0,7868}{MW_{Dglucosamine}} \times MW_{Genipin}$$

**Hydrogels Preparation**

The synthesis of PNIPAm has been previously published<sup>46</sup>. Three stock solutions were prepared; the first one of Chitosan 1,5% w/v in distilled water, with a concentration of 3% v/v of Acetic Acid. The second of PVA (3% w/v) in distilled water and the latter one of PNIPAm (2,5%w/v) also in distilled water. From these stock solutions, the different HGs formulations were prepared, see table 1.

Each formulation was firstly agitated in a vortex for 10 minutes and then poured in aluminum molds placed in a stove Precision Scientific model Thelco130, at 37°C (with vacuum) for 30h.

%CS	%PVA	%PNIPAm	%Genipin	Experimental Observation
48.0	47.0	5.0	2.480	 <p>48/47/5-2.48%Gnp 100mm</p>
50.0	40.0	10.0	2.792	
54.0	45.0	1.0	3.281	
55.0	45.0	0.0	3.988	
68.0	24.0	8.0	4.058	
95.0	0.0	5.0	4.060	
100	0	0	2.480	
100	0	0	5.300	

**Table 1** – Formulations subjected to different curing conditions.

**Evaluation of solvent evaporation**

First, an aluminum mold with only solvent (water with 3% Acetic Acid) was put into the stove at 37°C for 30h. Secondly, five HGs formulations were poured into different aluminum molds, covered with aluminum film (to avoid the solvent evaporation) and put into the stove at 37°C, also for 30h. In both cases the gelation was monitored (by visual evaluation of percolation). The five HGs formulations selected for this test were two from the lower edge of Chitosan proportion (48%) at the lower and higher Genipin percentage (2.48% and 5.3%); and two formulations from the higher Chitosan proportion (100%) at 3.92% and 2.85% of Genipin. and a formulation with an intermediate value of Chitosan (48%) and the presence of the two dispersed phases PVA and PNIPAm (47 and 5 % respectively). See table 2.

% CS	% PVA	% PNIPAm	% Genipin	Gelled after 30h?
48	52	0	2.48	No
48	52	0	5.30	No
48	47	5	2.71	No
100	0	0	2.48	Yes
100	0	0	5.30	Yes

**Table 2** – Gelation of control samples averting solvent evaporation.

**Swelling Study**

After gelation, the HGs were subjected to lyophilization at -48°C and 0,1mBar for 48h in a lyophilizer Labconco model Freezona 2.5. The xerogels obtained, were weighed to obtain the dehydrated weight ( $w_0$ ), followed by immersion in distilled water (pH 5,9±0,1) at 23°C for 96h. After that, they were weighed again to obtain the hydrated weight ( $w_t$ ) and with those values, the swelling ratio (SR) was measured<sup>47</sup>.

$$S_R = \frac{w_t - w_0}{w_0}$$

Twenty three formulations were evaluated, where three of them were replicates and each formulation had also 3 repeated measures.

**FT-IR Characterization**

Before submerging the xerogels, samples were taken for infrared spectroscopy in a Thermo Scientific model iD3-ATR. Every xerogel was subjected to this study in the spectral region (4000–500) cm<sup>-1</sup>. Nonetheless, those samples with PNIPAm were studied before swelling and after swelling and lyophilization to study whether the interpenetrated phases were leaving from the Chitosan network.

### Morphology evaluation

The xerogels were fractured using  $N_2$ (liquid), and covered with a thin layer of gold through the sputtering process. After that, the samples were subjected to scanning electron microscopy (SEM) with a JOEL instrument model JSM-6390. In each SEM micrograph, approximately 100 pores were measured with the help of the Digimizer® program.

### Rheological Characterization

To characterize viscoelasticity, an oscillatory shear test was carried out with a parallel plate rheometer brand TA instrument model AR2000. For this experiment, swelled hydrogels were placed in the rheometer chamber at 37°C, and a compressive strain of 10% (based on measured specimen thickness) was imposed on the discs for 2 minutes before rheological testing. Firstly, it was necessary to set up the constant strain for dynamic frequency sweep test, to ensure the study in the linear viscoelastic range, a strain sweep was performed. Once the linear viscoelastic region (LVR) of all samples was obtained, a ( $\gamma$ ) strain common for all LVR (0.2%) was selected to carry out the dynamic frequency sweep test from 0.1 rad/sec to 100 rad/sec. The samples studied in this experiment were the swelled samples from the swelling study.

### Hemolysis Test

In these experiments, the S-IPN HGs were put in contact with a blood agar solution to evaluate the hemolytic properties of those materials. Nonetheless, this enriched medium also enhances bacteria growth, altering the study of the material biocompatibility, making the sterilization of all equipment and samples previous to the essay necessary. To sterilize Petri dishes and eppendorfs that would be in contact with the samples and the agar-blood solution, they were put in an autoclave, at 120°C and 1.2psi for 2 hours. To sterilize the xerogels, they were put in the sterilized eppendorfs with a 75% ethanol solution. Those eppendorfs were then placed uncovered inside a UV (enclosed and sterilized) chamber for 24h (allowing the ethanol solution to evaporate). On the other hand, the agar-blood solution was prepared, and under sterile conditions, the medium and each sample were transferred to the sterile Petri dishes and incubated at 37°C with a 5%CO<sub>2</sub> flow. The areas around the hydrogels were observed after 24h and 48h and digital pictures(8MP) for further comparison with the control sample (agar-blood medium). In this experiment, toxicity was indicated by a loss of viable cells around the test device, perceptible by a color change around the sample. A lack of hemolysis (sometimes called  $\gamma$  hemolysis) was indicated when the zone surrounding the sample was indistinct from the rest of the agar-blood. A greenish to brownish discoloration of the medium was a sign of oxidation<sup>48,49</sup>.

### Statistical Analyses

This investigation established a constant concentration of polymers in the initial formulations of 1.5% w/v. Within that polymer's concentration, a variation of proportions in the polymers' components were also established according to table 1.

The Genipin concentration, on the other hand, was studied between 2.48 and 5.4%. In these ranges of mixture components (CS, PVA, and PNIPAm) and numerical factor (Genipin), a design of experiment was carried out using the tool Combined DOE of the program DesignExpert® with a D-Optimally design.

After synthesis and characterization, an analysis of the empirical data obtained from swelling and rheology test were made. First, a normalization of data through Box-Cox transformation<sup>50</sup> was needed and secondly, the statistical model selection was made taking into account Akaike's information criterion (AICc), p-value, model lack of fit, model precision and the difference between  $r^2_{\text{predicted}}$  and  $r^2_{\text{adjusted}}$ <sup>51</sup>.

## Results and Discussion

### Gelation

During the gelation process a decrease in the solution volume of almost all mixtures was observed. This was supported by the decrease in the solution volume of the 100% solvent sample. Because of the solvent evaporation, it is worth mentioning that this concludes in an increment of the solute concentration (polymers and cross-linked).

Regarding the synthesis, Table 2 shows that for samples with 100% of CS, regardless of the Genipin percentage the formulations percolated the mold (even those with the smallest Genipin%). In contrast, formulations with 48% of CS did not attain percolation, not even with the higher Genipin percentage. For these cases, the cure time was greater than 48 hours.

This implies that the critical variable responsible of gelation in less than 30h was the Chitosan proportion. This makes sense since the Chitosan/Genipin system is solely responsible for generating a macromolecule able to percolate all the system (since these two components are the only ones forming chemical bonds)<sup>52-55</sup>. Furthermore, the stoichiometric ratio between CS-Genipin implies that an increment in the Chitosan proportions increments the Genipin concentration in the solution.

Secondly, it could be seen that samples with low Chitosan proportions did not percolate before 30h. The hypotheses that can explain this behavior is that in the formulations with smaller CS amount, this concentration could have been too small to percolate the entire system (to attain sol-gel transition). In that way, allowing solvent evaporation in the system increases the solute concentration up to the point in which the CS/Genipin concentration would be enough to percolate (besides of the five samples during the experiment of "evaluation of solvent evaporation" all the other samples were synthesized uncovered and allowing the solvent evaporation). Furthermore, it has been reported that diminishing the system responsible of gelation (CS/GNP) decreases the kinetic<sup>56</sup> reaction, and the introduction of PVA phase slows down the cross-linking reaction between CS and GNP<sup>57</sup>.

### Hydrogels structure

From FT-IR the first sign of the Genipin presence in the hydrogels structure was the absorption of the internal double bonds of the Genipin-cyclopentane. This might be responsible for the absorption band in 1540cm<sup>-1</sup> (Figure 1). Regularly, unconjugated alkenes show moderate to weak absorption at 1667 cm<sup>-1</sup>– 1640cm<sup>-1</sup> but in the case of cycloalkenes, the C=C stretch vibration is coupled with the C-C stretching of the adjacent bounds, interaction that diminishes inasmuch as the angle within the cycloalkene decrease up to 90° displacing the absorption band to the right<sup>58</sup>.

A second sign of the Genipin presence in the hydrogels was the absorption bands in 795 cm<sup>-1</sup> and 1410cm<sup>-1</sup>, where they correspond to the C-H out-of-plane bending vibrations of the Genipin's alkenes<sup>58,59</sup>.

Regarding the HGs with a PVA phase, most of the bands in this polymer's spectrum were already in the Chitosan, so, the only difference in

the spectrum that allowed the verification of PVA presence in the HGs was the band  $1720\text{ cm}^{-1}$  (Figure 2.a), which was sign of the absorption of the residuals acetate groups during the manufacturing of PVA from hydrolysis of polyvinyl acetate<sup>60,37</sup>.

The hydrogels with an interpenetrated network of PNIPAm also overlapped all its bands with the Chitosan HGs bands, since they had the same functional groups. Nonetheless, it was possible to observe a sharper band in  $1260\text{ cm}^{-1}$  in contrast with the rest of the bands in the hydrogels spectrum (Figure,2.b) consequence of the increment in the methyl groups presents in the PNIPAm.

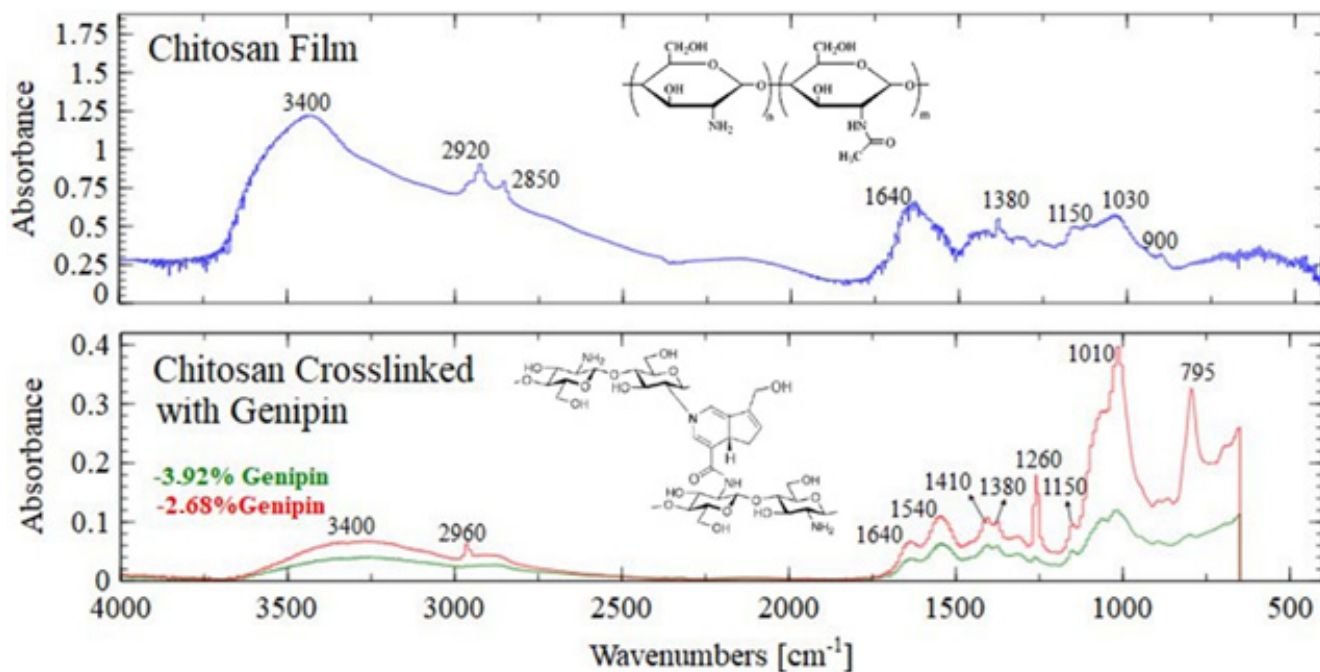


Figure 1 – FTIR Spectra of Chitosan Film and HGs of 100% Chitosan with 3.92 and 2.68% of Genipin.

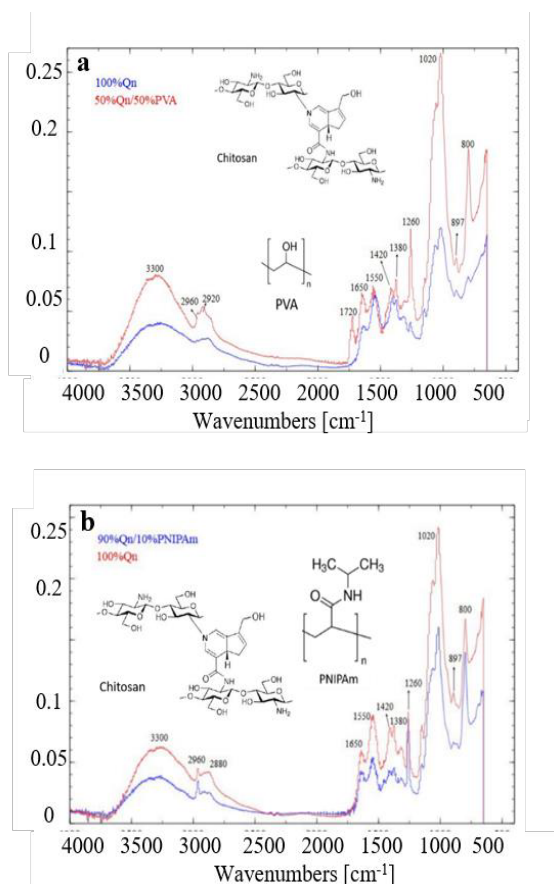


Figure 2 – a) FTIR Spectra of Chitosan HG and Chitosan/PVA HG. b) FTIR Spectra of Chitosan HG and Chitosan/PNIPAm HG.

**Hydrogels morphology**

Variation in the Genipin percentage allowed the modification in the pore size distribution (figure 3-a). In this figure you can see that a decrease in the Genipin percentage narrowed the pore size distribution of the HGs, and furthermore it diminished the pore size<sup>57,58</sup>.

Theoretically, an increment in the Genipin concentration augments the cross-linked density<sup>59</sup>, this might be the cause of the increment in the pore's wall thickness (figure 3-b).

Regarding the polymers composition variation, a diminishing in the Chitosan proportion generated an increment in the wall thickness and a decrement in the pore size (Figure 4). This was a consequence (as before mentioned) of a lessening in the components responsible for the gelation, which augmented evaporation of the solvent producing a densification of the solution.

Another relevant feature in the HGs microstructure was the highly porous and interconnective structure obtained in all HGs.

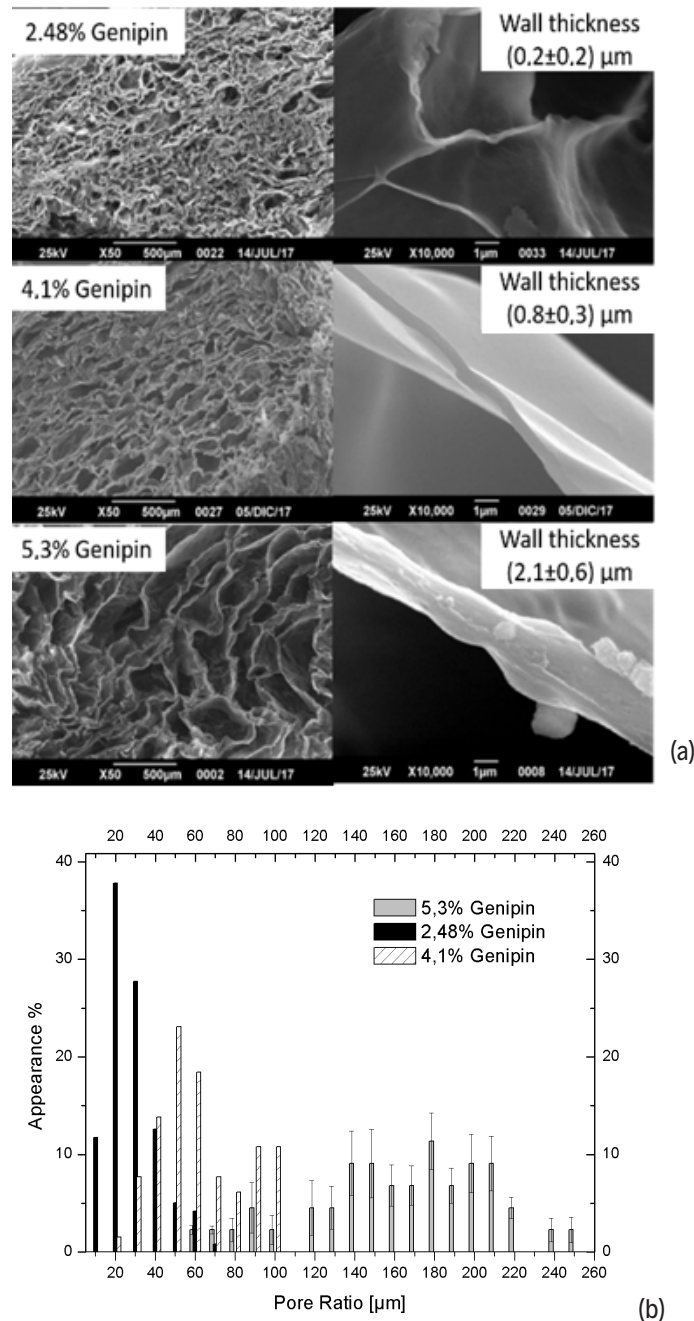


**Figure 3** – Hydrogels with different Genipin concentration and the same polymers composition (48% Chitosan, 47% PVA and 5% PNIPAm): (a) Cross section SEM micrographs. (b) Pore ratio distribution (obtain from SEM micrographs).

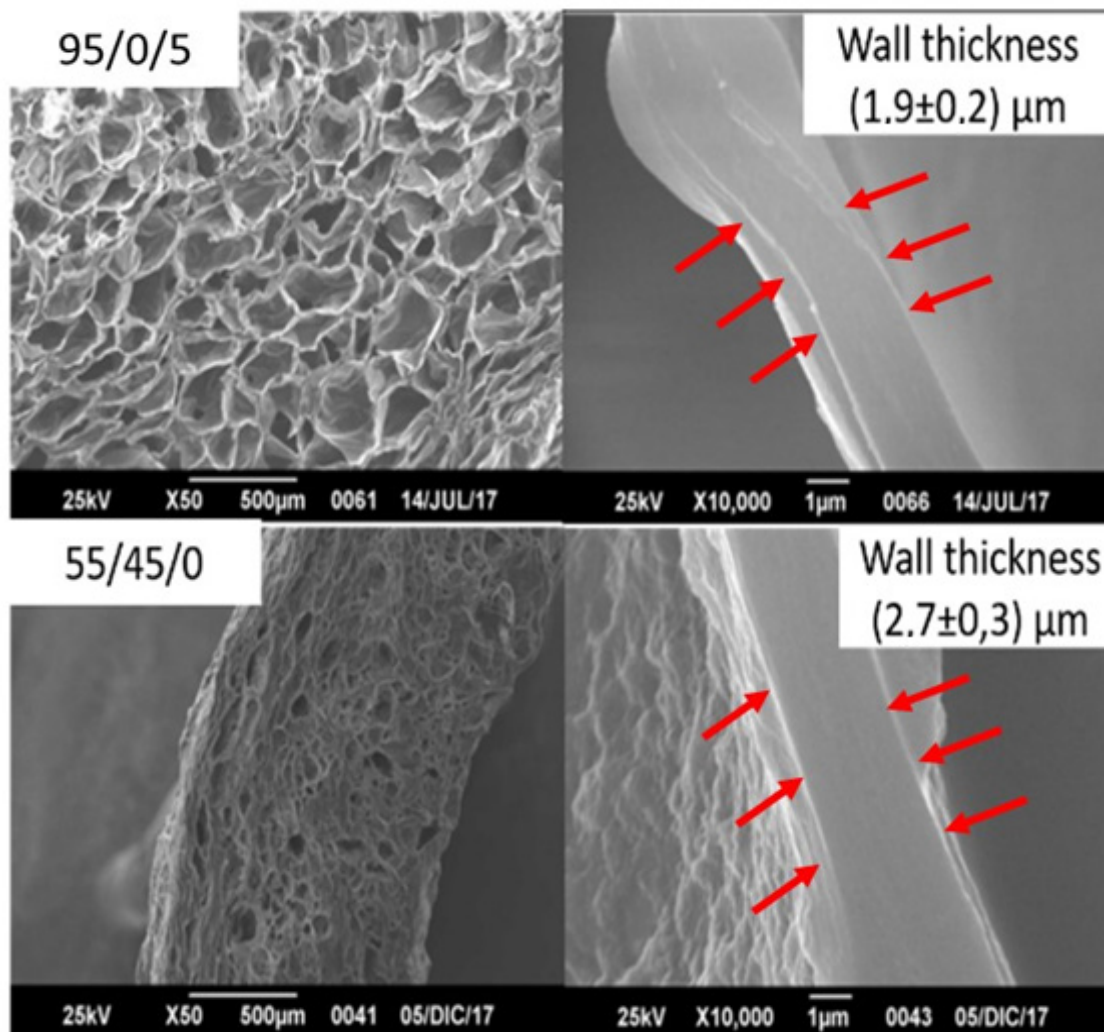


**Figure 4.** Cross section SEM micrographs: S-IPN Hydrogels with different polymers proportions and the same Genipin concentration (~4 %).

#### HGs Swelling Study

The statistical model that better fitted the experimental data was represented by the follow equation:

$$SR = 0.26xCS + 4.58xPVA + 0.54xPNIPAm - 0,07xCSxPVA - 1.74xPVAxGNP \quad (\text{equation 1})$$

Where SR is the swelling ratio this model had a p-value of  $1,4E^{-7}$ , with a lack of fit of 0.36,  $r^2$  of 0.941582 (with  $r^2_{\text{predicted}} - r^2_{\text{adjusted}} = 0,02$ ) and an adequate precision of 23.7.

The first three terms indicate that PVA, PNIPAm, and CS produced an increment in the SR of the HGs. In the case of PVA, it makes sense because of its hydrophilic nature<sup>60</sup>. Regarding Chitosan, this was no surprise either since the distilled water had a smaller pH than the Chitosan's pKa, allowing primary amine groups to be protonated and promoting counter ions (water molecules) to migrate from the surrounding medium to the inside of the HG resulting in an osmotic pressure difference. This process is named Donnan equilibrium<sup>42,54,61</sup>. Results are shown in figure 5.

In the same way, PNIPAm at the temperature of the medium (24°C) was below the lower critical solution temperature (LCST) which implies a linear structure and hydrophilic behavior in this polymer<sup>62,63</sup>.

Even when the lack of strong physical or chemical bonds between PNIPAm and the other phases at temperatures below LCST has been reported as allowing a leakage of this polymer from the S-IPN structure towards the fluid<sup>62</sup>, this was not the case, since the study of the characteristic band ( $1260\text{cm}^{-1}$ ) obtained in the FTIR essay of a xerogel (containing PNIPAm) and then after swelling and lyophilization of the same sample, showed no change in the intensity of that band. This is possible because the physical entanglement between the S-IPN and the chitosan network.

The phenomenon of swelling mentioned before deals only with water type I and II<sup>63,64</sup>. For water type III (also called interstitial water) is necessary to consider the HG pore size since the water type III locates in the free space inside the HG's structure<sup>65</sup>. Thus, while smaller pores hold a smaller amount of water type III in the structure, that might be the reason for the decrease of the SR inasmuch as the GNP percentage diminished. Figure 4 shows graphically the effect of the polymers proportion over the SW in the upper and lower edges of Genipin concentration.



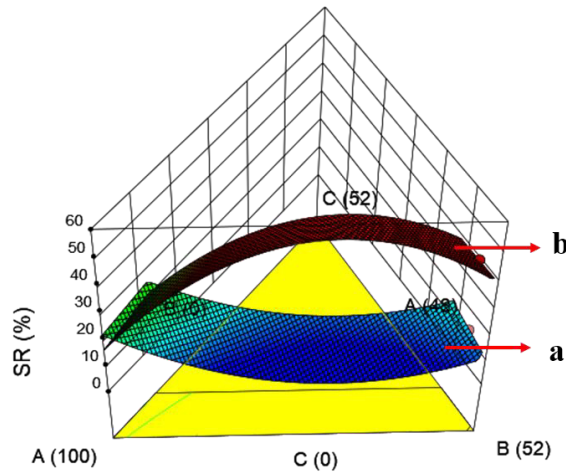


**Figure 5** – Effect of the polymers proportion over the swelling ration in the: (a) lower (2.48%) and (b) upper (5.4%) edges of Genipin concentration. With A, B and C are CS, PVA and PNIPAm proportions respectively.

**Mechanical properties**

In the case of the storage modulus ( $G'$ ) the statistical model that better fitted the experimental data was represented by the following equation:

$$\sqrt{G'} = 2.32xCS + 14.45xPVA + 1.36xPNIPAm - 5.90xPVAxGNP \tag{equation 2}$$

This model had a p-value smaller than 0.0001 with a lack of fit of 1.91,  $r^2$  of 0.91 (with  $r^2_{\text{predicted}} - r^2_{\text{adjusted}} = 0,07$ ) and an adequate precision of 17.68.

The PVA effect showed an increment of  $G'$  inasmuch as the Genipin percentage diminished the concentration (Figure 6). The first explanation for this outcome relies on the fact that increasing the amount of SR decreases the elastic modulus (and other mechanical properties)<sup>54,66-68</sup>, hence, those components that diminished the structure pore size, reduce the SR, producing an increment in the storage modulus (which is the case of diminishing Genipin percentage and augmenting PVA proportion)<sup>69</sup>. Secondly, knowing that a uniform pore structure also improves the mechanical properties of the HG<sup>70</sup>, increasing PVA proportion and diminishing the Genipin concentration, narrows the range of pore size increasing the storage modulus. Third, it has also been reported that an S-IPN of PVA endows the Chitosan network of stiffness owing to the hydrogen bonds between these two polymers<sup>54</sup>. And fourth, even when theoretically, increasing the amount of cross-linking agent, increases the cross-linking density concluding in an improvement of mechanical properties<sup>68</sup>, it has been reported that when the cross-linking overcomes a threshold, highly cross-linked heterogeneities appear, resulting in a diminishing in the number of cross-links formed and then in the mechanical properties<sup>68</sup>. Low et al. located that threshold for CS hydrogels cross-linked with GNP in 1% w/v of Genipin<sup>57</sup>, which agrees with this investigation, where  $G'$  decreased inasmuch as the Genipin concentration rose from 2,48% to 5,4%. Finally, the effect of PNIPAm over  $G'$  was not that relevant in contrast with the effect of PVA and Genipin, nonetheless, it is reasonable to expect an increment in  $G'$  since the PNIPAm at 37°C is contracted due to a collapse of the polymer coil, diminishing the SR of the HG<sup>69-71</sup>.

Regarding the lag between stress and strain ( $\delta$ ), the models tested in the statistical analysis did not give reliable information owing to the lack of fit of models and the difference between  $r^2_{\text{predicted}}$  and  $r^2_{\text{adjusted}}$  which was greater than 0,2 in all cases.

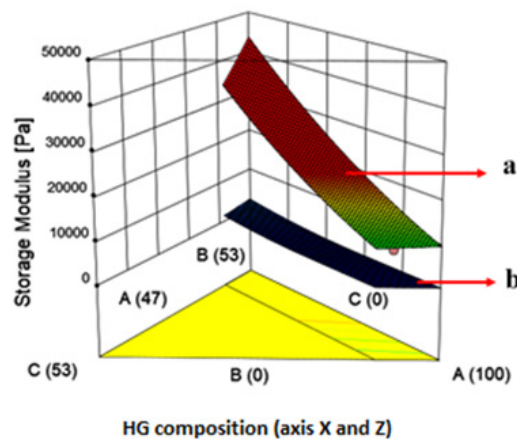


**Figure 6** – Effect of the polymers proportion over the Storage modulus in the: (a) lower (2.48%) and (b) upper (5.4%) edges of Genipin concentration. With A, B and C are CS, PVA and PNIPAm proportions respectively.

### Applications of S-IPN HGs as materials for NP replacement

Table 3 shows  $G'$  and loss tangent ( $\tan\delta$ ) for Nucleus pulposus according to different investigations<sup>5, 73, 74</sup>, as well as those values for the HG S-IPN synthesized in this investigation, specifically those with the highest and smallest mechanical properties.

From table 3 it can be depicted that  $G'$  of the S-IPN HG could be tailored to NP's  $G'$ , nonetheless, the value of  $\tan\delta$  was always smaller than the NP's corresponding value, this means, the S-IPN HG behaved more like an elastic solid than NPs.

Ideally, a NP replacement should guarantee a minimally invasive surgery, looking forward to maintaining the integrity of the annulus fibrosus and end plates; hence, the best option is the injection of the implant into the disc space for in situ healing. Despite that in the S-IPN HG process of gelation they suffered a process of solvent evaporation, further studies are needed to figure out if these HGs can be synthesized allowing evaporation process just before the sol-gel transition (when the solution still flows) but prevented after that point, looking forward to the solution injection before sol-gel transition to in situ healing and still obtaining the S-IPN HG.

The effect over tissue regeneration, shelf life, and degradability of this S-IPN HGs should also be studied to figure out if they are suitable as a prosthesis or as a scaffold. Nonetheless, this investigation proved that the pore morphology can be controlled by modifying the components proportions and crosslinking percentage, feature that can be tailored to improve the process of tissue regeneration, since a more uniform pore size facilitates the spatial distribution of fibroblasts, differentiation of preosteoblasts and diffusion of macromolecules, leading to even distribution of cells and homogeneous differentiation of cells<sup>59,75</sup>.

$G'$ [kPa]	$\tan\delta$	Source	Species
20.8	0.28	[73]	Goats
0.32	0.26	[74]	Porcine
4.7-26.5	0.38-0.53	[5]	Human L4-L5
27.96	0.045	*	HG S-IPN
0.077	0.23	**	HG S-IPN

Where \* represents the formulation 50/40/10 and 2.8%GNP and \*\* the formulation 95/0/5 and 4.1%GNP.

**Table 3** – Comparison between rheological properties of NP and S-IPN HGs.

### Hemocompatibility

Blood is composed of 90% to 95% of water and around 5% of cells (red blood cells, white blood cells, platelets, etc.)<sup>71</sup>. A toxic material could generate hemolysis, which is the rupture of the cellular membrane of the red blood cells killing the cell<sup>43,44</sup>. Every S-IPN HG formulation does not exhibited hemolysis (no appearance of a whitish halo around the samples), a sign of a none-cytotoxic feature, asseveration that can be extrapolated to HGs in the whole range of Genipin percentage and polymers proportions studied<sup>72</sup>. See figure 7 for hemocompatibility results.

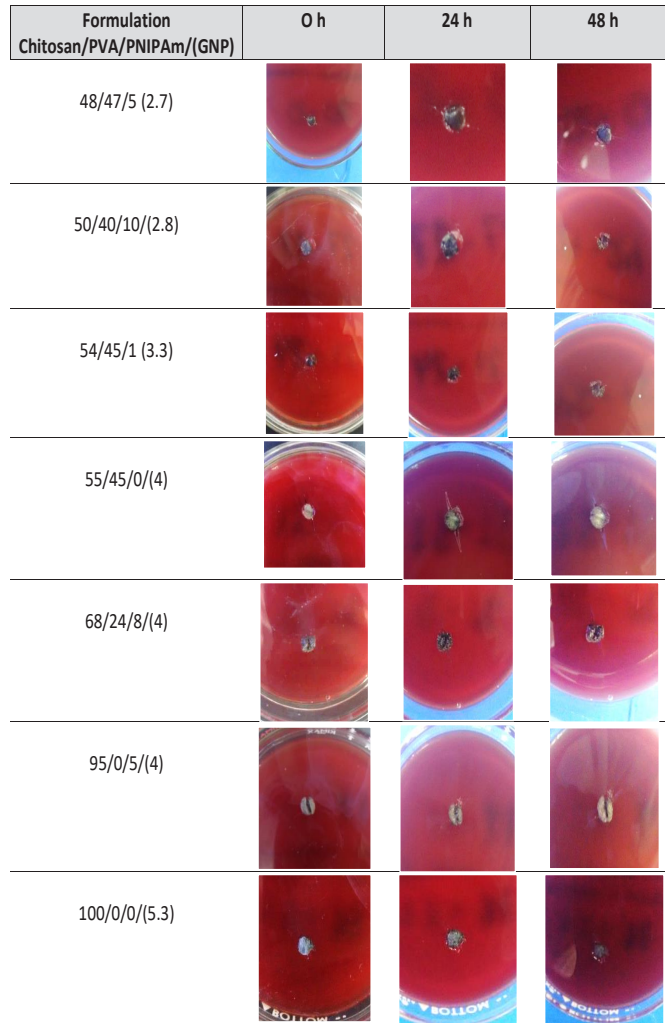


**Figure 7–** Hemocompatibility of agar/ blood gel formulations Evolution for 48 hr at 37°C.

**Conclusions**

Modification in CS/PVA/PNIPAm proportion and GNP percentage can control the pore size and its size distribution, the SR and the storage modulus.

The range of storage modulus obtained by the different S-IPN HGs studied, agree with the values for the storage modulus of human lumbar NPs and other species. Meanwhile, the loss tangent achieved in S-IPN HGs were also close to NPs values. These outcomes alongside with its non-cytotoxic feature, stand up this kind of S-IPN HGs for further study as material for NP prosthesis

**Acknowledgment**

The authors want to thank Lab E-USB through the section of polymers and electron microscopy for the rheology test and SEM respectively. To the laboratory of analytical chemistry for FTIR spectra and the microbiology laboratory for the hemocompatibility tests.

**References**

[1]. Qi-Bin Bao, Geoffrey M. McCullen, Paul A. Higham, John H. Dumbleton and Hansen A. Yuan “Review: The artificial disc: theory, design and materials” *Biomaterials*, Vol. 17, pp. 1157–1167, 1996.

[2]. C. Jongeneelen, *Biomechanics in the intervertebral disc, A literature review*, Eindhoven: University of Technology, pp 1–15, 2006.

[3]. Chan, S. C. y B., Gantenbein Ritter “Intervertebral disc regeneration or repair with biomaterials and stem cell therapy – feasible or fiction?” *Swiss Med Weekly*, vol. 142, pp. 1–12, 2012.

[4]. Iatridis JC1, Nicoll SB, Michalek AJ, Walter BA, Gupta MS. “Role of biomechanics on intervertebral disc degeneration and regenerative therapies: What needs repairing in the disc and what are promising biomaterials for its repair?” *Spine Journal*, vol. 13, n° 3, p. 243–262, 2013.

[5]. Iatridis, James C.; Weidenbaum, Mark; Setton, Lori A.; Mow, Van C., “Is the nucleus pulposus a solid or a fluid? Mechanical behaviors of the

- nucleus pulposus of the human intervertebral disc" *Spine*, vol. 21, n° 10, pp. 1174–1184, 1996.
- [6]. Nikolai Bogduk, "Clinical Anatomy of the Lumbar Spine and Sacrum", London/New York/ Oxford/Philadelphia/St Louis/Sydney/Toronto: Elsevier, pp. 1–77, 2005.
- [7]. Zhiyu Zhou, Manman Gao, Fuxin Wei, Jiabi Liang, Wenbin Deng, Xuejun Dai, Guangqian Zhou and Xuenong Zou, "Shock Absorbing Function Study on Denucleated Intervertebral Disc with or without Hydrogel Injection through Static and Dynamic Biomechanical Tests In Vitro" *BioMed Research International*, pp. 1–7, 2014.
- [8]. Irving M. Shapiro and Makarand V., "The Intervertebral Disc", Philadelphia: Springer, pp.3–52, 109–124 and 139–170, 2014.
- [9]. Peter J. Roughley, "Biology of intervertebral disc aging and degeneration: Involvement of the extracellular matrix" *Spine*, vol. 29, n° 23, pp. 2691–2699, 2004.
- [10]. James N. Parker, and Philip M. Parker, "Degenerative Disc Disease", San Diego: ICON Health Publications, 2004.
- [11]. D.W., Meakin J.R. and Hukins, "Effect of removing the nucleus pulposus on the deformation of the annulus fibrosus during compression of the intervertebral disc" *Biomechanics*, vol. 33, n° 5, pp. 575–580, 2000.
- [12]. Manohar Panjabi, Mark Brown, Sven Lindahl, Lars Irstam, and Martin Hermens, "Intrinsic disc pressure as a measure of integrity of the lumbar spine" *Journal Spine*, vol. 13, n° 8, pp. 913–917, 1988.
- [13]. Richard E. Seroussi, Martin H. Krag, David L. Muller and Malcolm H. Pope, "Internal deformations of intact and denucleated human lumbar discs subjected to compression, flexion, and extension loads" *Orthopaedic Research*, vol. 7, n° 1, p. 122–131, 1989.
- [14]. Iatridis JC, Setton L.A., Weidenbaum M., Mow V.C., "Alterations in the mechanical behavior of the human lumbar nucleus pulposus with degeneration and aging" *J Orthop Res.*, vol. 15, n° 2, pp. 318–322, 1997.
- [15]. Brinkman P, Grootenbore H. , "Change of disc height, radial disc bulge and intradiscal pressure from discectomy" *Spine*, vol. 16, pp. 641–646, 1991.
- [16]. Nishiyama K, Nye T., "Kinematics of whole lumbar spine, effect of discectomy" *Spine*, vol. 10, pp. 543–554, 1985.
- [17]. Michael A. Adams, "Biomechanics of back pain" *Acupuncture in Medicine*, vol. 22, n° 4, pp. 178–188, 2004.
- [18]. Simon Dagenais, Jaime Caro, and Scott Haldeman "A systematic review of low back pain cost of illness studies in the United States and internationally" *The Spine Journal*, vol. 8, pp. 8–20, 2008.
- [19]. Surgeons, American Academy of Orthopaedic "The Burden of Musculoskeletal Diseases in the United States," Rosemont, IL: Bone and Joint Decade, 2008. Available: [http:// www.boneandjointburden.org/](http://www.boneandjointburden.org/).
- [20]. Jensen M.C., Kelly A.P., Brant-Zawadzki M.N., "MRI of degenerative disease of the lumbar spine" *Magn Reson Q.*, vol. 10, n° 3, p. 173–190, 1994.
- [21]. Shono Y., Kaneda K, Abumi K., "Stability of posterior spinal instrumentation and its effects on adjacent motion segments in the lumbosacral spine" *Spine*, vol. 23, pp. 1550–1558, 1998.
- [22]. Lehman T. R., Spratt K. F., "Long-term follow-up of lower lumbar fusion patients" *Spine*, vol. 12, pp. 97–104, 1987.
- [23]. Lee C. K. and Langrana N. A., " Lumbosacral spinal fusion: a biomechanical study" *Spine*, vol. 9, pp. 574–581, 1984.
- [24]. O'Connell G.D., Malhotra N.R., Vresilovic E.J., Elliott D.M., "The Effect of Discectomy and the Dependence on Degeneration of Human Intervertebral Disc Strain in Axial Compression" *Spine*, vol. 36, n° 21, p. 1765–1771, 2011.
- [25]. Judith R. Meakin, Thomas W. Redpath, David W.L. Hukins, "The Effect of Partial Removal of the Nucleus Pulposus from the intervertebral Disc on the Response of the Human Annulus Fibrosus to Compression" *Clinical Biomechanics*, vol. 16, pp. 121–128, 2001.
- [26]. Neil R. Malhotra, Woojin M. Han, Jesse Beckstein, Jordan Cloyd, "An Injectable Nucleus Pulposus Implant Restores Compressive Range of Motion in the Ovine Disc" *Spine*, vol. 37, n° 18, p. 1099–1105, 2013.
- [27]. Gillet P., "The fate of the adjacent motion segments after lumbar fusion" *J Spinal Disorder Tech*, vol. 16, n° 4, pp. 338–45, 2003.
- [28]. Rahm M.D., Hall B.B., "Adjacent segment degeneration after lumbar fusion with instrumentation: a retrospective study" *Spinal Disorder.*, vol. 9, n° 5, pp. 392–400, 1996.

- [29]. Chunpeng Ren, Yueming Song, Limin Liu, Youdi Xue, "Adjacent segment degeneration and disease after lumbar fusion compared with motion-preserving procedures: a meta-analysis," *Orthop Surg Traumatol*, vol. 24, n° 1, p. 245–253, 2014.
- [30]. Casey K. Lee, Vijay K. Goel, "Artificial disc prosthesis: design concepts and criteria" *The Spine Journal*, vol. 4, pp. 209–218, 2004.
- [31]. Aetna, "Intervertebral Disc Prostheses" 17/01/2018. Available: [http://www.aetna.com/cpb/medical/data/500\\_599/0591.html](http://www.aetna.com/cpb/medical/data/500_599/0591.html).
- [32]. Angelo Carpy, "Progress in Molecular and Environmental Bioengineering – From Analysis and Modeling to Technology Applications", Rijeka, Croatia, InTech, 2011, pp. 117–150.
- [33]. Hassan Serhan, Devdatt Mhatre, Henri Defossez, "Motion-preserving technologies for degenerative lumbar spine: The past, present, and future horizons" *SAS Journal*, vol. 5, pp. 75–89, 2011.
- [34]. Raphael M. Otterbrite, Kinam Park, Teruo Okano "Biomedical Applications of Hydrogels Handbook", New York–London: Springer, pp 227–242.
- [35]. Shoufeng Yang, Kah–Ah–Fai Leong, Zhaohui Du y Chee–Kai Chua, "The Design of Scaffolds for Use in Tissue Engineering. Part I. Traditional Factors" *Tissue Engineering*, vol. 7, n° 6, pp. 679–689, 2001.
- [36]. Cheng Y.H., Yang S.H., Su W.Y., Chen Y.C., Yang K.C., Cheng W.T., Wu S.C., Lin F.H., "Thermosensitive chitosan–gelatin– glycerol phosphate hydrogels as a cell carrier for nucleus pulposus re– generation: an in vitro study" *Tissue Eng. Part A.*, vol. 16, n° 2, pp. 695–703, 2010.
- [37]. Youling Yuan, Betsy M. Chesnutt, Warren O. Haggard and Joel D. Bumgardner, "Deacetylation of Chitosan: Material Characterization and in vitro Evaluation via Albumin Adsorption and Pre–Osteoblastic Cell Cultures" *Materials*, vol. 4, pp. 1399–1416, 2011.
- [38]. Renata Czechowska–Biskup, Diana Jarošnińska, Bożena Rokita, Piotr Ułański, Janusz M. Rosiak, "Determination of Degree of Deacetylation of Chitosan – Comparison of methods" *Progress on chemistry and application of chitin and its derivatives*, vol. 17, pp. 5–20, 2012.
- [39]. Mad Rabiul Hussain, Murshid Iman and Tarun K. Maji, "Determination of Degree of Deacetylation of Chitosan and Their effect on the Release Behavior of Essential Oil from Chitosan and Chitosan– Gelatin Complex Microcapsules" *Advanced Engineering Applications*, vol. 2, n° 4, pp. 4–12, 2013.
- [40]. Tanveer Ahmad Khan Kulliyah, Kok Khiang Peh, Hung Seng Chang "Reporting degree of deacetylation values of chitosan: the influence of analytical methods" *Pharm Pharmaceut Sci.*, vol. 5, n° 3, pp. 205–212, 2002.
- [41]. Maria G. Carrero, James J. Posada, Marcos A. Sabino "Intelligent Copolymers Based on Poly (N–Iopropylacrylamide) PNIPAm with potential use in Biomedical Applications. Part. I PNIPAm Functionalization with 3–Butenoic Acid and Piperazine" *International Journal of Advances in Medical Biotechnology*, vol. 1, n° 1, pp. 1–8, 2018.
- [42]. Steve Rimmer, "Biomedical Hydrogels, Oxford, Cambridge, Philadelphia and New: Woodhead Publishing, pp. 35–61, 2011.
- [43]. Brian J. Tindall, Johannes Sikorski, Robert A. Smibert, and Noel R. Krieg "Phenotypic Characterization and the Principles of Comparative Systematics" *de Methods for General and Molecular Microbiology*, Washington, ASM Press, 2007, pp. 335–386.
- [44]. Encyclopedia, "World of Microbiology and Immunology", Available: <https://www.encyclopedia.com/science/encyclopedias-almanacs-transcripts-and-maps/blood-agar-hemolysis-and-hemolytic-reactions>. [last access: 7/4/2018].
- [45]. G. P. Box and D. R. Cox, "An Analysis of Transformations" *Research Methods Meeting of the Society*, pp. 211–252, 1964.
- [46]. Kenneth P. Burnham and David R. Anderson, "Model Selection and Multimodel Inference: A Practical Information– Theoretic Approach", Berlin, Heidelberg, Barcelona, Hong Kong, London, Milan and Paris: Springer, pp. 49–65 y 98–121. 2002.
- [47]. A. Carpi, "Progress in Molecular and Environmental Bioengineering – From Analysis and Modeling to Technology Applications", InTech, pp. 117–141. 2011.
- [48]. John K. Gillham, "Formation and Properties of Thermosetting and High Tg Polymeric Materials" *Polymer Engineering and Science*, vol. 26, n° 20, pp. 1429–1433, 1986.
- [49]. H. S. V. y. R. J. W. Jean Pierre Pscault, *Thermosetting Polymers*, New York: Marcel Dekker, pp. 1–10. 2002.
- [50]. M. José Moura, M. Margarida Figueiredo y M. Helena Gil, "Rheological study of genipin cross–linked chitosan hydrogels" *Biomacromolecules*, vol. 8, pp. 3823–3829, 2007.
- [51]. George Odian, "Principles of Polymerization" New York, John Wiley & Sons, 2004, pp. 39–50.
- [52]. Nand A.V., Rohindra D.R. y Khurma, J.R., "Characterization of genipin crosslinked hydrogels composed of chitosan and partially hydrolyzed

- poly(vinyl alcohol)” E-Polymers, pp. 30–38, 2007.
- [53]. Robert M. Silverstein, Francis X. Webster, David J. Kiemle “Spectrometric identification of organic compounds”, New York: John Wiley & Sons, 81–90. 2005.
- [54]. Tao Wang, Mahir Turhan and Sundaram Gunasekaran “Selected properties of pH-sensitive, biodegradable chitosan–poly(vinyl alcohol) hydrogel” *Polymer International*, vol. 53, pp. 911–918, 2004.
- [55]. A. M. Shehap, “Thermal and Spectroscopic Studies of Polyvinyl” *Egypt. J. Solids*, vol. 31, n° 1, 2008.
- [56]. Christie M. Hassan, and Nikolaos A. Peppas, “Structure and Applications of Poly(vinyl alcohol) Hydrogels Produced by Conventional Crosslinking or by Freezing/Thawing Methods” de *Biopolymers PVA Hydrogels, Anionic Polymerization Nanocomposites*, Berlin Heidelberg, Springer-Verlag, 2000, pp. 37–65.
- [57]. Long Bi, Zheng Cao, Yunyu Hu, Yang Song, Long Yu, Bo Yang, Jihong Mu, Zhaosong Huang y Yisheng Han, “Effects of different cross-linking conditions on the properties of genipin-cross-linked chitosan/collagen scaffolds for cartilage tissue engineering” *J Mater Sci: Mater Med*, vol. 22, pp. 51–62, 2011.
- [58]. Simona Dimida, Amilcare Barca, Nadia Cancelli, Vincenzo De Benedictis, Maria Grazia Raucci, y Christian Demitri, “Effects of Genipin Concentration on Cross-Linked Chitosan Scaffolds for Bone Tissue Engineering: Structural Characterization and Evidence of Biocompatibility Features” *International Journal of Polymer Science*, pp. 1–7, 2017.
- [59]. Jiabing Ran, Lingjun Xie, Guanglin Sun, Jingxiao Hu, Si Chen, Pei Jiang, Xinyu Shen, Hua Tong “A facile method for the preparation of chitosan-based scaffolds with anisotropic pores for tissue engineering applications” *Carbohydrate Polymers*, vol. 152, p. 615–623, 2016.
- [60]. Tayser Sumer Gaaz, Abu Bakar Sulong, Majid Niaz Akhtar, Abdul Amir H. Kadhum, “Properties and Applications of Polyvinyl Alcohol, Halloysite Nanotubes and Their Nanocomposites” *Molecules*, vol. 20, p. 22833–22847, 2015.
- [61]. Sundaram Gunasekaran, Tao Wang, Chunxiang Chai, “Swelling of pH-Sensitive Chitosan–Poly(vinyl alcohol) Hydrogels” *Journal of Applied Polymer Science*, vol. 102, p. 4665–4671, 2006.
- [62]. Mingzhen Wang, Yu Fang, Daodao Hu “Preparation and properties of chitosan–poly(N-isopropylacrylamide) full-IPN hydrogels” *Reactive & Functional Polymers*, vol. 48, pp. 215–221, 2001.
- [63]. Kamiya Jain, Raman Verdarajan, Masaki Watanabe, Masaki Ishikiriya, and Noriyoshi Matsumi, “Tunable LCST behavior of poly(N-isopropylacrylamide/ionic liquid) copolymers” *Polymer Chemistry*, n° 38, pp. 6819–6825, 2015.
- [64]. I. G. Pedley and B. J. Tighe, “Water Binding Properties of Hydrogel Polymers for Reverse Osmosis and Related Applications” *Brit. Polym.*, vol. 11, pp. 130–136, 1979.
- [65]. Hossein Omidian and Kinam Park, “Introduction to Hydrogels” de *Biomedical Applications of Hidrogels Handbook*, New York, Dordrecht, Heidelberg and London, Springer, 2010, pp. 1–15.
- [66]. Victor T. Wyatt, “Effects of Swelling on the Viscoelastic Properties of Polyester Films Made from Glycerol and Glutaric Acid” *Journal of Applied Polymer Science*, vol. 1, pp. 1–10, 2012.
- [67]. H. Bendaikha, S. Chaoui, S. Ould Kada, and A. Krallafa, “Swelling behavior and viscoelastic properties of a Polyacetal Hydrogel” *AIP Conference Proceedings*, vol. 64, 2008.
- [68]. Kristi S. Anseth, Christopher N. Bowman and Lisa Brannon-Peppas, “Mechanical properties of hydrogels and their experimental determination” *Biomaterials*, vol. 17, pp. 1647–5167, 1996.
- [69]. Hye Yun Kim, Ha Neul Kim, So Jin Lee, Jeong Eun Song, Soon Yong Kwon, Jin Wha Chung, Dongwon Lee and Gilson Khang, “Effect of pore sizes of PLGA scaffolds on mechanical properties and cell behavior for nucleus pulposus regeneration in vivo” *Tissue Engineering and Regenerative Medicina*, vol. 11, n° 1, pp. 44–57, 2014.
- [70]. Jorge M. Sobral, Sofia G. Caridade, Rui A. Sousa, João F. Mano, “Three-dimensional plotted scaffolds with controlled pore size gradients: Effect of scaffold geometry on mechanical performance and cell seeding efficiency” *Acta Biomaterialia*, vol. 7, pp. 1009–1018, 2011.
- [71]. Laxman S. Desai and Laurence Lister, “Biocompatibility Safety Assessment of Medical Devices: FDA/ISO and Japanese Guidelines” *Toxikon Corp.*, pp. 1–19, 2016.
- [72]. Marta A. Cooperstein and Heather E. Canavan, “Assessment of cytotoxicity of (N-isopropyl acrylamide) and Poly (N-isopropyl acrylamide) coated surfaces” *Bio interphases*, vol. 8, n° 19, pp. 1–12, 2013.
- [73]. J.L. Bron, G.H. Koenderink, V. Everts, T.H. Smit, “Rheological Characterization of the Nucleus Pulposus and Dense Collagen Scaffolds Intended for Functional Replacement” *Journal of Orthopedic Research*, pp. 620–626, 2009.

- [74]. F. Causa, L. Manto, A. Borzacchiello, R. De Santis, P. A. Netti, L. Ambrosio, L. Nicolais, "Spatial and Structure Dependence of Mechanical Properties of Porcine Intervertebral Disc" *Journal of Material Science: Materials in Medicine*, vol. 13, pp. 1277-1280, 2002.
- [75]. Sung-Wook Choi, Yu Zhang y Younan Xia, "Three-dimensional Scaffolds for Tissue Engineering: The Importance of Uniformity in Pore Size and Structure" *Langmuir*, vol. 26, n° 24, p. 19001-19006, 2010.



# Production and characterization of membranes containing PCL and PVP obtained by simultaneous and blends electrospinning

Ana L. de B. Soares<sup>1\*</sup>; João de Deus. P. de Moraes Segundo<sup>2</sup>; Marcos A. D'Ávila<sup>2</sup>; Fábria K. Andrade<sup>1</sup>; Rodrigo S. Vieira<sup>1</sup>

\*Corresponding author: e-mail address: [lorena.soares@gpsa.ufc.br](mailto:lorena.soares@gpsa.ufc.br)

**Abstract:** Electrospinning can easily produce nano- and micrometer-diameter polymeric fiber membranes. The hydrophilicity of poly ( $\epsilon$ -caprolactone) (PCL) membranes can be improved blending it with another polymers. PCL has biocompatibility and an excellent in vitro and in vivo release mechanism, however, it has limited applications when faster degradation is required. In this work, two blends membranes containing PCL and polyvinylpyrrolidone (PVP) and one membrane containing simultaneously fibers of PVP and PCL were produced by electrospinning. The membranes received morphological characterization by scanning electron microscopy (SEM). The contact angle measurements were used to investigate the wettability of the materials. Fourier Transform Infrared Spectroscopy (FTIR) was used to depict the chemical composition of the materials. The PCL/PVP membrane with a 1:1 ratio (w/w, of the polymer solutions) stood out among the others, because in addition to an increase in wettability, it presented a better balance between the characteristics of these two polymers.

**Keywords:** Poly ( $\epsilon$ -caprolactone). Polyvinylpyrrolidone. Electrospinning. Hydrophobicity. Hydrophilicity.

## Introduction

The use of biomaterial-based fibers has received attention for biomedical applications in the areas of tissue engineering<sup>1</sup> or regenerative medicine<sup>2</sup>. Polymeric membranes can be produced by nano- and micrometer fibers using electrospinning technique, in a relatively inexpensive and easy mechanism<sup>3</sup>.

Electrospinning is a technique in which a viscous polymer solution is intended to force through an electric field to form fibers on a grounded metal surface. The produced fibers from this process are deposited continuously, forming a membrane with high surface area to volume ratio, porous, and flexible<sup>4</sup>.

Poly( $\epsilon$ -caprolactone) (PCL) is a semicrystalline polymer with high mechanical properties and biocompatibility, presenting potential properties for use as biomaterial<sup>5,6</sup>. This polymer is widely used in electrospinning processes<sup>1,7,8</sup> because it is a non-toxic material and *in vitro* and *in vivo* biocompatibility. PCL is a hydrophobic material and it has limited applications for devices which require a faster degradation<sup>9</sup>.

Polyvinylpyrrolidone (PVP) has in its main molecular structural highly hydrophilic groupz (pyrrolidone) and a hydrophobic groups (alkyl) being a hygroscopic and non-toxic biopolymer<sup>10</sup>.

The association of PCL with another polymer, producing polymer blends, can be carried out using using the electrospinning technique, improving PCL hydrophilicity. Kim and collaborators (2013) produced scaffolds by electrospinning using a PCL/PVP blend. The authors produced fibers with good chemical interaction between polymers with potential applications in tissue engineering<sup>11</sup>.

In this study, PCL has been combined with PVP in different ways such as conventional electrospinning using PCL and PVP blending solutions, and simultaneous electrospinning of PCL and PVP solution in order to improve the wettability of the PCL fibers.

## Materials and methods

### Materials

PCL (molecular mass: 80,000 g.mol<sup>-1</sup>) and PVP (molecular mass: 1,300,000 g.mol<sup>-1</sup>) were purchased from Sigma-Aldrich. Chloroform

and acetone were purchased from Labsynth Products for Laboratories Ltda. Ethyl alcohol was purchased from The Scientific Synergy, and methyl alcohol was purchased from Neon Comercial Ltda.

### Membranes production by solution electrospinning

The PCL solution was prepared by the mixture of chloroform and acetone solvents (1:1 mass ratio), under mechanical stirring for 15 minutes at room temperature. Next, PCL 15.82% w/w was added into the flask and subjected to the mechanical stirring until complete solubilization of polymer for 2 hours.

The PVP solution was prepared mixing ethanol and water solvents (4:1 mass ratio) into the flask. The solvents mixture was mechanically stirred for 5 minutes. Then, PVP 8% w/w was added into the flask under mechanical stirring for 2 hours at room temperature.

The PCL/PVP blend solution was prepared by mixing the PCL and PVP solutions, previously described, into an unique flask in the proportion of 1:1 mass ratio. In order to mixture completely the polymers, it was applied a mechanical stirring during 2 hours. The solution prepared by this methodology was called the PP2 solution.

Another PCL/PVP blend solution was prepared as described in the literature<sup>12</sup> and it was called PP3. Chloroform and methanol were mixed into the flask in the proportion 3:1 (volume ratio), and PCL solution with 10% w/v was prepared. Another mixture solution was prepared with the same solvents and proportion to prepare the PVP solution with 30% w/v. After their preparation, the solutions were mixed at a ratio of 7:3 by volume. The PCL/PVP blend solution was mechanically stirred for 2 hours at room temperature called PP3 solution.

In the conventional electrospinning system, a single syringe was used to accommodate the polymeric solution, equipped with an infusion pump, high voltage source with 15 kV capacity, and a rectangular metallic collector cooper that was kept static. The simultaneous electrospinning system was equipped similarly to conventional electrospinning. The difference was in the use of two syringes that accommodated different polymeric solutions.

During electrospinning, the solvents evaporated, and the PCL, PVP,

<sup>1</sup>Dep. of Chemical Engineering, Federal University of Ceará, Pici Campus, Fortaleza (CE), Brazil.

<sup>2</sup>Dep. of Manufacturing and Materials and Engineering, University Of Campinas, Campinas (SP), Brazil.



PP2, and PP3 solutions resulted in the PCL, PVP, PP2, and PP3 membranes, respectively. The membrane PP1 was produced by simultaneous electrospinning system with the PCL solution into a syringe and PVP solution into other syringe and resulted in the PP1 membrane.

The process parameters used were the capillary diameter of  $\varnothing = 0.8$  mm, the flow rate of  $Q = 8$  mL/h, the working distance of  $Wd = 20$  cm, and the applied voltage of  $V = 15$  kV. All these parameters were fixed. The environmental parameters were humidity and temperature of 57% and  $T = 26^\circ\text{C}$ , respectively.

## Characterizations

### Scanning Electron Microscopy (SEM)

Fibers micrographic images of PCL, PVP, PP1, PP2, and PP3 were obtained by scanning electron microscope – SEM (ZEISS, model Evo MA–15). The samples were coated with a thin layer of gold (5–10 nm) using a Sputter Coater (BAL–TEC, model SCD 050).

The fiber diameter measurements were carried out manually from SEM images using ImageJ software, and the mean values and standard deviations (mean  $\pm$  SD) were calculated following the procedure suggested in the literature<sup>13</sup>.

### Wettability and Contact Angle

The contact angle measurements ( $\theta$ ) using a water drop (5  $\mu\text{L}$ ) on the materials surface evaluated the materials wettability. Digital microscope (TQC USB, TQC microscope) was used to monitor water drop behavior for 120 seconds. The contact angle measurements were obtained by ImageJ software. The tests were performed in triplicate at room temperature ( $T = 26^\circ\text{C}$ ) and 57% humidity. In order to investigate the influence of membrane porosity, PCL, PVP, PP2, and PP3 films were prepared using the casting method.

### Fourier Transform Infrared Spectroscopy (FTIR)

Spectroscopic analysis of the materials chemical composition was performed by Fourier Transform Infrared Absorption Spectrometer – FTIR (Spectrum 65, PerkinElmer), equipped with the accessory of Attenuated Total Reflection – ATR was used. The analyzed region was in the range of 4000 to 400  $\text{cm}^{-1}$ .

## Results and Discussions

### Scanning Electron Microscopy (SEM)

All SEM images of this work were obtained with magnitudes at 1,000X and 10,000X with 10 and 1  $\mu\text{m}$  scales, respectively. The diameters values were measured manually and represented as mean  $\pm$  SD, statistical distribution, and data distribution.

In Figure 1 is shown the SEM images of the PCL membrane that showed the behavior of the fibers with random direction and without the presence of pearls, which are considered defects in fibers produced by electrospinning<sup>14</sup>. This result corroborates with the SEM images obtained by Morais Segundo (2015) that produced the fibers using the same process parameters<sup>5</sup>. Besides, we observed by superficial characterization from the SEM image, the rough surface of PCL fibers; this effect may be related to the humidity during its formation<sup>15,16</sup>.

PVP membrane morphology is shown in Figure 2 by the SEM images. The process parameters for its production were the same parameters used in the membrane PCL production; these parameters were not favorable for fibers production without beads. Figure 2.a and Figure 2.b are showed the presence of beads and beads-on-string in the fibers structure. However, we observed considerably thinner fibers than PCL fibers. Vongsetskul et al. (2015) prepared PVP solution using ethanol and water and investigated PVP fibers production by electrospinning using different voltage values. The author reported that higher voltages give finer PVP fibers, with a voltage of 16 kV was able to produce ultrafine fibers<sup>17</sup>. In this study, no optimization was done to eliminate the beads, because it was used as an indicator to locate the PVP fibers in the membrane morphology obtained by simultaneous electrospinning.

The SEM images in Figure 3 show the electrospun PVP and PCL fibers simultaneously (PP1). The morphology showed the PCL fibers identified by large fibers with a rough surface, as shown in Figure 1, and fine fibers identified the PVP fibers with beads that correspond to the same characteristic observed in Figure 2 attributed to PVP fibers. The mixture between PCL and PVP polymers into the PP1 membrane does not exist chemical interaction due to the electrospinning technique used, which can be a differential for specific applications.

The Figure 3 in (c), (d), (e), and (f) contains the fiber morphologies of the PP2 and PP3 membranes that were produced by the formation of PCL and PVP blends. In both materials, the production of beads-free fibers was obtained; this effect may have occurred due to the good chemical interaction between the PCL e PVP polymers, which had already been reported by the work authors that produced the PP3 membrane<sup>11</sup>. In this research, we performed a different methodology from the literature to produce PP2 fibers, which resulted in the formation of finer and more uniform fibers than PP3 fibers, as can be seen in Figure 3d compared with the Figure 3f.

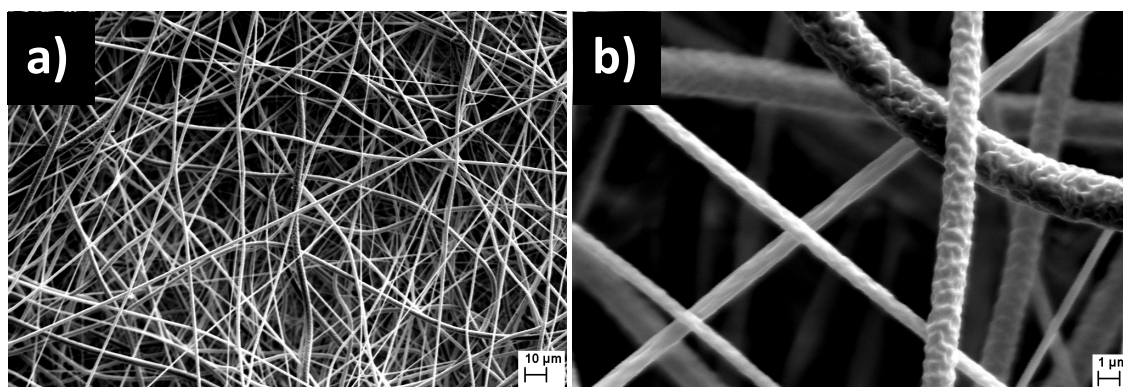


**Figure 1**– SEM images of the PCL membrane with magnitudes of 1,000X (a) and 10,000X (b).

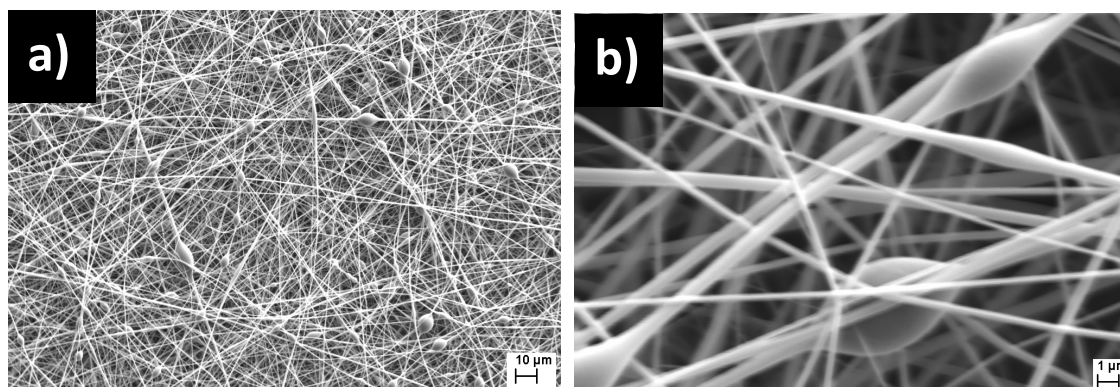


**Figure 2** – SEM images of PVP membrane with magnitudes of 1,000X (a) and 10,000X (b).

Figure 3 in (c), (d), (e), and (f) In Figure 4 is shown the distribution of fiber diameters of PVP, PCL, PP1, PP2, and PP3. The diameters of PVP fibers were more uniform than the PCL fibers. PP3 fibers presented values more disperse of their diameters than the PP2 fibers. On the other hand, the PP1 fiber diameters had its distribution more strengthen due to the PCL fiber diameter participation that presented lower diameters values, as shown in Table 1. The diameters of fibers for PCL, PVP, PP1, PP2, and PP3 were  $1.9 \pm 0.5$ ,  $0.4 \pm 0.2$ ,  $0.5 \pm 0.5$ ,  $1.8 \pm 1.2$ , and  $4.0 \pm 1.0 \mu\text{m}$ , respectively.

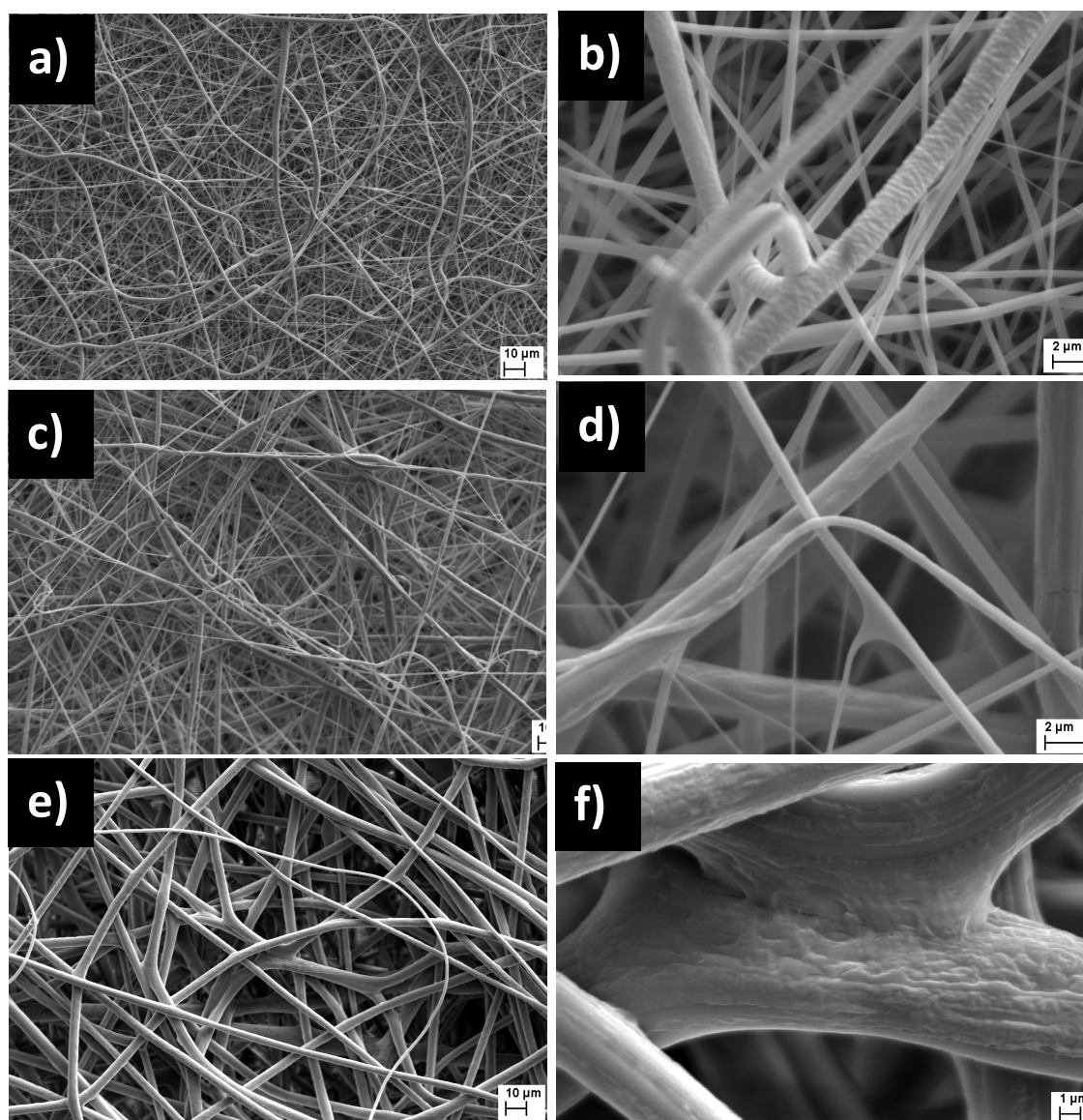


**Figure 3** – SEM images of the membranes of PP1 (a and b), PP2 (c and d) and PP3 (e and f) with magnitudes of 1,000X and 10,000X, respectively.

Table 1 are listed the statistical data on the diameters of the electrospun fibers by different techniques. In the PP1 membrane, we observed the  $D_{min} = 0.04 \mu\text{m}$  and  $D_{max} = 3.30 \mu\text{m}$ ; both values corroborate with the  $D_{min}$  from PVP and  $D_{max}$  from PCL. Obviously, it is clear that the PVP fibers structural dimensions were smaller than the PCL fibers, as showed the Figure 4a and Figure 3b. The participation concomitantly of PVP and PCL fibers was confirmed due to their characteristic unique.

In addition, the PCL/PVP blended fibers into PP2 membrane showed better structural characteristics than the PCL/PVP blended fibers from the PP3 membrane described on literature. This improvement may have occurred due to a reduction in the amount of PCL in the solution blending.

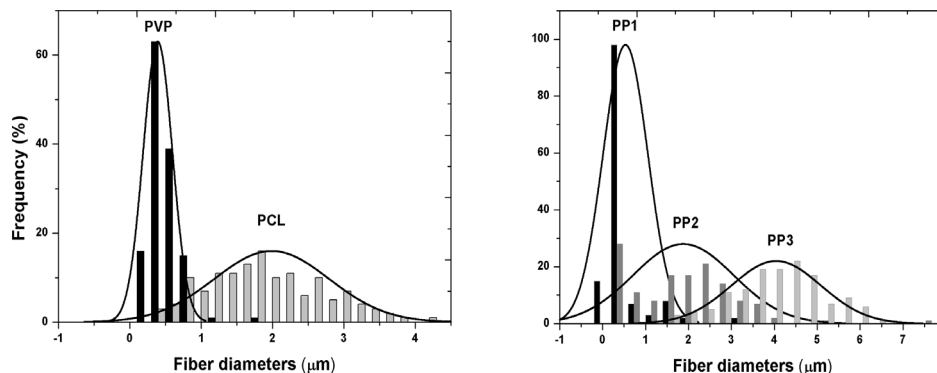


Figure 4 – Distribution curve of (a) PCL and PVP fiber diameters. (b) PP1, PP2, and PP3 fiber diameters.

Statistic data	FIBER DIAMETERS (μm)				
	PCL	PVP	PCL + PVP	BLENDS	
				PCL:PVP 1:1	PCL:PVP 7:3
Mean ± SD	1.9±0.5	0.4±0.2	0.5±0.5	1.8±1.2	4.0±1.0
$D_{max}$	4.3	1.8	3.3	7.5	6.3
$D_{min}$	0.5	0.09	0.04	0.2	1.5

Table 1 – Fiber diameters obtained in different processing ways. Values are in micrometers (μm).

**Wettability and Contact Angle**

In order to compare the effect of wettability were prepared films of PCL, PVP, PP1, PP2, and PP3. Figure 5 is shown the wettability in Table 2 are listed the contact angle measurements ( ).

PCL is considered a hydrophobic polymer<sup>9</sup>, and the PCL membranes produced by electrospinning have their hydrophobicity increased by the presence of air due to membrane porosity<sup>5</sup>. Figure 5.e shows the water drop on the PCL membrane in an almost spherical shape with  $\theta = 136.33 \pm 7.84^\circ$ . On the PCL film, the water drop behavior in the half-moon shape (to see Figure 5.a) and its contact angle was  $\theta = 79.88 \pm 3.25^\circ$ . These results confirmed the air influence in the PCL membrane.

PVP has with the water a friendly relationship because of its hygroscopic property<sup>18</sup>. For this reason, it is considered highly hydrophilic. Figure 5b shows the water drop on the PVP film of scattered form with a contact angle of  $\theta = 49.74 \pm 1.68^\circ$ . The PVP membrane did not have its contact angle value due to the PVP membrane total water drop absorption. In this case, the opposite effect occurred with the water drop on the PCL membrane; due to the PVP membrane porosity, its absorption was slightly rapid and high.

The PP1, PP2, and PP3 membranes acquired the same PVP membrane effect, being highly absorbent to water. In contrast, the contact angles of the films of PP2 and PP3 were  $\theta = 55.23 \pm 2.76^\circ$  and  $\theta = 71.22 \pm 2.20^\circ$ , respectively. The contact angle of PP3 film was larger than PP2 film due to an increase of PCL amount into PP3 film.

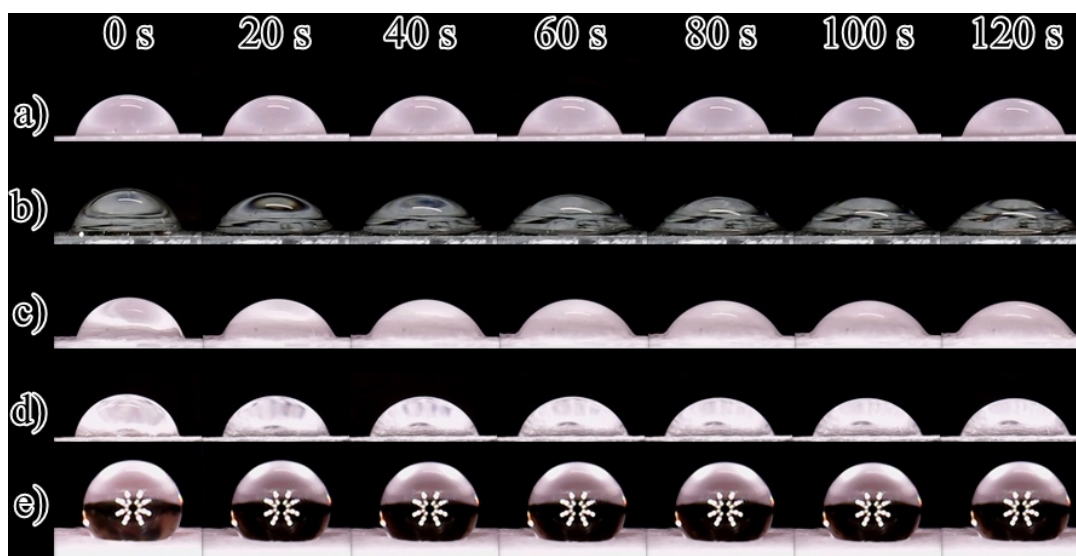


**Figure 5** – Wettability of PCL (a), PVP (b), PP2 (c) and PP3 (d), and PCL membrane (e) films.

Material	Contact Angle	
	Film	Membrane
PCL	79.88 ± 3.25	136.33 ± 7.84
PVP	49.74 ± 1.68	---
PP1	NA	---
PP2	55.23 ± 2.76	---
PP3	71.22 ± 2.20	---

**Table 2** – Contact angle of films and membranes of the studied materials.

#### Fourier Transform Infrared Spectroscopy (FTIR)

In Figure 6 are showed the FTIR spectra and their main bands that represent the vibrational modes of chemical composition of PCL, PVP, PP1, PP2, and PP3 membranes.

The PCL membrane bands are following the literature<sup>19</sup>. Positions at 2946  $\text{cm}^{-1}$  and 2868  $\text{cm}^{-1}$  are attributed to the asymmetrical and symmetrical stretching of  $\text{CH}_2$  group. The bands at 1722  $\text{cm}^{-1}$  correspond to the ester  $\text{C}=\text{O}$  group, at 1293  $\text{cm}^{-1}$  represents the stretching of  $\text{C}-\text{C}$  and  $\text{C}-\text{O}$  in the crystalline phase, and at 1162  $\text{cm}^{-1}$  is attributed to the symmetrical stretching of  $\text{C}-\text{O}-\text{C}$ .

PVP membrane bands such as at 1644  $\text{cm}^{-1}$  represent the stretching of the amide  $\text{C}=\text{O}$  group, at 1287  $\text{cm}^{-1}$  assigns to the amide  $\text{C}-\text{N}$  stretching, at 1495  $\text{cm}^{-1}$  corresponds to the  $\text{CH}_2$  deformation of linear chain, and at 1422  $\text{cm}^{-1}$  associates to the  $\text{CH}$  asymmetric deformation and  $\text{CH}_2$  cyclic groups<sup>20, 21, 22</sup>. The band at 3419  $\text{cm}^{-1}$  represents the stretching of  $\text{O}-\text{H}$  group due to its hygroscopicity.

Figure 6 shows bands around 3419  $\text{cm}^{-1}$ , 1722  $\text{cm}^{-1}$ , and 1644  $\text{cm}^{-1}$  in the PP1, PP2, and PP3 membranes, which confirms PVP presence in the membranes and chemical interaction between the polymers. Moreover, it explains the rapid absorption of water, as shown in the wettability study. Therefore, the PP1, PP2, and PP3 membranes acquired the hygroscopic property of PVP.

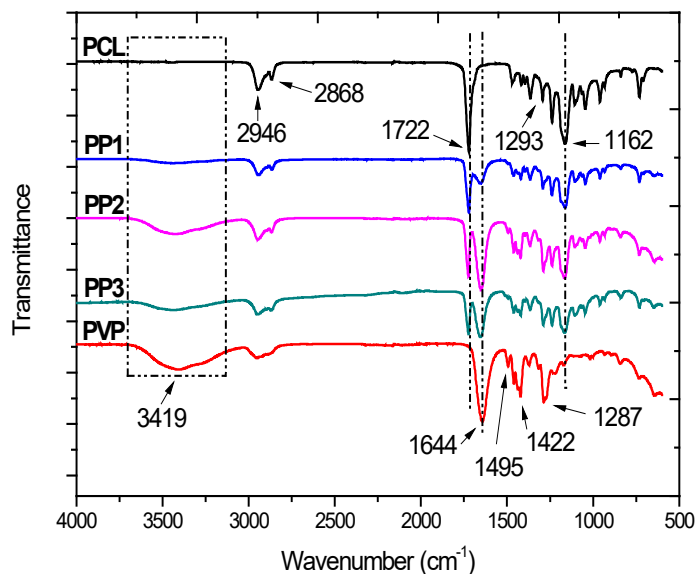


**Figure 6** – FTIR spectra and positions of the PCL, PVP, PP1, PP2, and PP3 vibrational modes.

### Conclusion

Electrospinning produced membrane containing PCL and PVP using different techniques of preparation. SEM images showed the morphology of PVP and PCL fibers and revealed nanometric dimensions for the PVP fibers. The PP1 membrane preserved the PCL and PVP fibers structural characteristics, and the fibers of PP2 and PP3 membranes presented different aspects. The presence of PVP into the PCL membrane considerably improved its wettability. The bands at 3419 and 1644  $\text{cm}^{-1}$  confirmed PVP in the PP1, PP2, and PP3 membranes. The PP1 and PP2 membranes produced in this work have great potential for pharmaceutical and biomedical applications.

### Acknowledgments

We thank the Higher Education Personnel Improvement Coordination – CAPES, National Academic Cooperation Program – PROCAD, Amazonas State Research Support Foundation – FAPEAM for financial support, National Council for Scientific and Technological Development – CNPq (proc. 308660/2015–3 and 421745/2016–9), and Biomaterials Laboratory of the Pontifical Catholic University of São Paulo – PUC–SP, Faculty of Medical and Health Sciences – Campus Sorocaba.

### References

- [1]. Løvdal A, Vange J, Nielsen LF, Almdal K. Mechanical properties of electrospun PCL scaffold under in vitro and accelerated degradation conditions. *Biomedical Engineering – Applications, Basis and Communications*, vol. 26, n° 3, pp. 1–13, 2014.
- [2]. Vurat MT, Elçin AE, Elçin YM. Osteogenic composite nanocoating based on nanohydroxyapatite, strontium ranelate and polycaprolactone for titanium implants. *Transactions of Nonferrous Metals Society of China (English Edition)*, vol. 28, n° 9, pp. 1763–1773, 2018.
- [3]. Gao C, Zhao K, Wu Y, Gao Q, Zhu P. Fabrication of strontium/calcium containing poly( $\gamma$ -glutamic acid)–organosiloxane fibrous hybrid materials for osteoporotic bone regeneration. *RSC Advances*, vol. 8, n° 45, pp. 25745–25753, 2018.
- [4]. Zhijiang C, Ping X, Shiqi H, Cong Z. Soy protein nanoparticles modified bacterial cellulose electrospun nanofiber membrane scaffold by ultrasound–induced self–assembly technique: characterization and cytocompatibility. *Cellulose*, vol. 26, n° 10, pp. 6133–6150, 2019.
- [5]. Moraes Segundo JDP. Influência da Adição de Surfactantes em Fibras Altamente Alinhadas de Poli (caprolactona) obtidas por Eletrospiação. Campinas. Dissertação (Mestrado em Engenharia Mecânica) – Universidade Estadual de Campinas; 2015.
- [6]. Roa JPB, Mano V, Faustino PB, Felix EB, Silva MESR, Souza Filho JD. Síntese e Caracterização do Copolímero Poli(3 Hidroxibutirato co Caprolactona) a Partir de Poli(3 Hidroxibutirato) e Poli( $\epsilon$  Caprolactona). *Polímeros*, vol. 20, n° 3, pp. 221–226, 2010.
- [7]. Ghasemi–Mobarakeh L, Prabhakaran MP, Morshed M, Nasr–Esfahani MH, Ramakrishna S. Bio–functionalized PCL nanofibrous scaffolds for nerve tissue engineering. *Materials Science and Engineering C*, vol. 30, n° 8, pp. 1129–1136, 2010.
- [8]. Souza MA, Carobolante JPA, Almeida RS, d’Ávila MA, Walker RS, Popat KC, Claro APRA. Immobilisation of apatite on Ti30Ta alloy surface by electrospinning of PCL. *Surface Innovations*, vol. 5, n° 2, pp. 68–74, 2017.
- [9]. Nair BP, Sindhu M, Nair PD. Polycaprolactone–laponite composite scaffold releasing strontium ranelate for bone tissue engineering applications. *Colloids and Surfaces B: Biointerfaces*, vol. 143, pp. 423–430, 2016.

- [10]. Jadhav SV, Nikam DS, Khot VM, Thorat ND, Phadatare MR, Ningthoujam RS, Salunkhe AB, Pawar SH. Studies on colloidal stability of PVP-coated LSMO nanoparticles for magnetic fluid hyperthermia. *New Journal of Chemistry*, vol. 37, n° 10, pp. 3121–3130, 2013.
- [11]. Kim GM, Le KHT, Giannitelli SM, Lee YJ, Rainer A, Trombetta M. Electrospinning of PCL/PVP blends for tissue engineering scaffolds. *Journal of Materials Science: Materials in Medicine*, vol. 24, n° 6, pp. 1425–1442, 2013.
- [12]. Shadamarshan RP, Balaji H, Rao HS, Balagangadharan K, Chandran SV, Selvamurugan N. Fabrication of PCL/PVP Electrospun Fibers loaded with Trans-anethole for Bone Regeneration in vitro. *Colloids and Surfaces B: Biointerfaces*, vol. 171, pp. 698–706, 2018.
- [13]. Moraes Segundo JDP, Moraes MOS, Brito WR, d'Ávila MA. Incorporation of molecularly imprinted polymer nanoparticles in electrospun polycaprolactone fibers. *Materials Letters*, vol. 275, pp. 1–4, 2020.
- [14]. Kostakova E, Seps M, Pokorny P, Lukas D. Study of polycaprolactone wet electrospinning process. *Express Polymer Letters*, vol. 8, n° 8, pp. 554–564, 2014.
- [15]. Katsogiannis KAG, Vladisavljević GT, Georgiadou S. Porous electrospun polycaprolactone (PCL) fibres by phase separation. *European Polymer Journal*, vol. 69, pp. 284–295, 2015.
- [16]. Nezarati RM, Eifert MB, Cosgriff-Hernandez E. Effects of humidity and solution viscosity on electrospun fiber morphology. *Tissue Engineering – Part C: Methods*, vol. 19, n° 10, pp. 810–819, 2013.
- [17]. Vongsetskul T, Chantarodsakun T, Wongsomboon P, Rangkupan R, Tangboriboonrat P. Effect of solvent and processing parameters on electrospun polyvinylpyrrolidone ultra-fine fibers. *Chiang Mai Journal of Science*, vol. 42, n° 2, pp. 436–442, 2015.
- [18]. Kariduraganavar MY, Kittur AA, Kamble RR. *Polymer Synthesis and Processing*. In: Kumbar SG, Laurencin CT, Deng M. *Natural and Synthetic Biomedical Polymers*. Elsevier; 2014. pp. 1–31.
- [19]. Faria PC, Martin AA, Alves NP. Caracterização no Infravermelho (IV) e Eletrônica de superfície (MEV) de membranas assimétricas à base de Poli(acrilonitrila-co-acetato de vinila). *Matéria*, vol. 22, n° 1, pp. 2017.
- [20]. Elzein T, Nasser-Eddine M, Delaite C, Bistac S, Dumas P. FTIR study of polycaprolactone chain organization at interfaces. *Journal of Colloid and Interface Science*, vol. 273, n° 2, pp. 381–387, 2004.
- [21]. Silva LG. Caracterização físico química e avaliação da liberação in-vitro dos conjugados poli( $\epsilon$ -caprolactona)/tetraciclina e poli( $\epsilon$ -caprolactona)/ácido acetilsalicílico. Itajubá. *Dissertação (Mestrado em Materiais para Engenharia) – Universidade Federal de Itajubá*; 2012.
- [22]. Zhang X, Sun N, Wu B, Lu Y, Guan T, Wu W. Physical characterization of lansoprazole/PVP solid dispersion prepared by fluid-bed coating technique. *Powder Technology*, vol. 182, n° 3, pp. 480–485, 2008.



## Effect of galvanic coupling between titanium alloy and stainless steel on behavior of corrosion of dental implants

Larissa O. Berbel<sup>1\*</sup>; Bárbara V. G. de Viveiros<sup>1</sup>; Ana Lígia Micelli<sup>1</sup>; Jesualdo Rossi<sup>1</sup>; Frederico Nigro<sup>1</sup>; Luis C. Aranha<sup>1</sup>; Isolda Costa<sup>1</sup>

\*Corresponding author: e-mail address: [lari\\_berbel@yahoo.com.br](mailto:lari_berbel@yahoo.com.br)

**Abstract:** Titanium and its alloys are widely used in dental implant manufacturing due its favorable properties, such as, biocompatibility, high mechanical strength and high corrosion resistance. This last one, is a result of the ability of titanium to form an oxide film (TiO<sub>2</sub>) in contact with oxygen. However, a several factors can accelerate the corrosion process of implants in contact with the oral environment, such as, acidification of the medium, differential aeration, inflammatory conditions, presence of protein and the junction of diferent metals. The goals of this research is to investigate the corrosion effect of galvanic coupling between titanium alloy (grade V) and stainless steel 316L. The investigative technique adopted was the scanning vibrating electrode technique (SVET) in phosphate buffer solution simulating inflammatory conditions. The results showed detrimental effects of acidity of the environment, induced by inflammatory conditions, accelerate the oxidation of Ti-6Al-4V. SVET maps and SEM images for the junction of the different metals showed that the region with the highest electrochemical activity it is at the interface between the metals, mostly concentrated on the Ti-6Al-4V alloy, depending on the conditions of the medium.

**Keywords:** Biomaterials. Corrosion. Dental implants.

### Introduction

Studies using metallic biomaterials have been conducted since the 19th century. In the beginning, the metals commonly used for organ replacement in the orthopedic area were iron, gold and silver. However, over the years, many researches have selected metallic materials capable of meeting the necessary requirements for use in the orthopedic and dental applications<sup>1</sup>. It is necessary to attend the requirements for biomaterials to contact body fluids since the application of biomaterials requires biocompatibility, high corrosion resistance, high mechanical resistance, osseointegration, besides properties such as durability, fatigue strength and ductility are also required<sup>1,2</sup>.

According to Manan *et al.*<sup>3</sup>, metals of high corrosion resistance may corrode when in contact with body fluids, depending on the environment conditions. The corrosion resistance of metallic biomaterials used in dentistry needs to be studied, since the buccal region presents favorable conditions to promote and accelerate the corrosive processes in dental implants. Metals inserted in oral region might be exposed to pH changes<sup>4</sup>. Also, the temperature and the presence of proteins<sup>5</sup>, bacteria<sup>6</sup>, might vary and the salts concentration might reach high values<sup>7</sup>. Also, fluoride ions in mouthwash affect the corrosion behavior of the material<sup>6</sup>.

According to the American Society for Testing and Materials (ASTM) G15-93<sup>8</sup>, corrosion occurs through chemical or electrochemical reactions between the metal and the environment to which it is exposed, resulting in the degradation of its properties. The environment conditions are of major importance the corrosion behavior of dental implants.

Several types of corrosion can be observed in dental implants, such as, pitting, crevice and galvanic corrosion. Galvanic corrosion in dental prostheses occurs when they are manufactured with dissimilar alloys. When different materials come into contact with corrosive fluids a potential difference is established between metals, creating in vivo galvanic cells<sup>9,10</sup>.

The potential difference produces electric current flow that accelerates anodic dissolution of the less noble metal. Furthermore, electric current passing through the metal and tissue junction causes pain to the patient<sup>10</sup>.

In order to understand the behavior of metallic biomaterials when in contact with the buccal region it is necessary to evaluate the in vitro corrosion behavior of these metals by simulating inflammatory conditions around the dental implant.

The present study was carried out to evaluate the corrosion behavior of Ti-6Al-4V dental implant galvanically coupled with 316L stainless steel prosthetic abutment. The corrosion behavior was evaluated by open circuit potential measurements and scanning vibrating electrode technique (SVET), once the corrosion process is driven by electrochemical reactions between the metal and the medium to which it is exposed<sup>11</sup>.

### Materials and methods

The material used in this study consisted of a Ti-6Al-4V (Ti grade V) dental implant connected to a stainless steel 316 L prosthetic abutment. Samples of the connected materials were embedded in a cold curing resin and then sequentially ground with SiC paper #800, #1200, #2000 and #4000. Subsequently, the surface of the samples was polished with 1 µm diamond paste. Finally, the samples were degreased with acetone in a sonifier, rinsed with deionized water and dried under a hot air stream.

The tests were performed in phosphate buffered solution (PBS) with addition of 1% (mass) hydrogen peroxide (34 % Standard) and pH adjusted to 3. These characteristics are typical of inflammatory conditions. The area exposed to the electrolyte (test medium) was 0.05 cm<sup>2</sup>. Hydrogen peroxide acts as a substitute for reactive oxygen species (ROS) often present in inflammatory processes<sup>12</sup>. Under these conditions, pH are in the range of 3 to 4<sup>13</sup>.

<sup>1</sup>Instituto de Pesquisas Energéticas e Nucleares (IPEN – CNEN/SP), São Paulo, SP, Brazil.



**Figure 1**– Dental implant of Ti grade V and a prosthetic abutment of stainless steel 316L.

### Open circuit potential measurements

The open circuit potential was monitored as a function of immersion time in the electrolyte used in this study that comprised a phosphate buffer solution with 1% hydrogen peroxide and pH adjusted to 3 to simulate inflammatory conditions. Electrochemical tests were carried out using a three-electrode set up consisting of Ag/AgCl (3M KCl), as reference electrode, a platinum wire as counter electrode and the sample of Ti grade V and stainless steel 316 L, separately or coupled, as working electrode.

### Scanning vibration electrode technique (SVET)

Scanning vibration electrode technique tests were carried out using an Applicable Electronics™, controlled by the Automated Scanning Electrode Technique ASET 4.0 software (Science Wares™). Insulated Pt–Ir probes (Microprobe Inc.) with a platinum black deposited were used as vibration electrode for the SVET system. The probe was placed ( $100 \pm 3$ )  $\mu\text{m}$  above the surface, vibrating in the planes perpendicular (Z) and parallel (X) to the samples surface. The amplitude of vibration was 19  $\mu\text{m}$ , vibration frequencies of the probe were 174 Hz (X) and 73 Hz (Z). A time lag between acquiring each current density data-point was 0.5 s. All experiments were performed in a Faraday cage at  $(20 \pm 2)$  °C. The tests were carried for 24h.

### Surface Characterization

After immersion tests, the exposed surface of the samples was characterized by optical microscopy, using a Leica DMLM, and scanning electron microscope (SEM), using a TM–3000, with 15 keV acceleration voltage, tabletop model, located at the Center of Lasers and Applications (CLA– IPEN–CNEN/SP).

### Results e Discussions

Figure 2 shows the open circuit potential variation as a function of time of immersion of Ti–6Al–4V and 316 L stainless steel, either separately or coupled, in the electrolyte of this study.

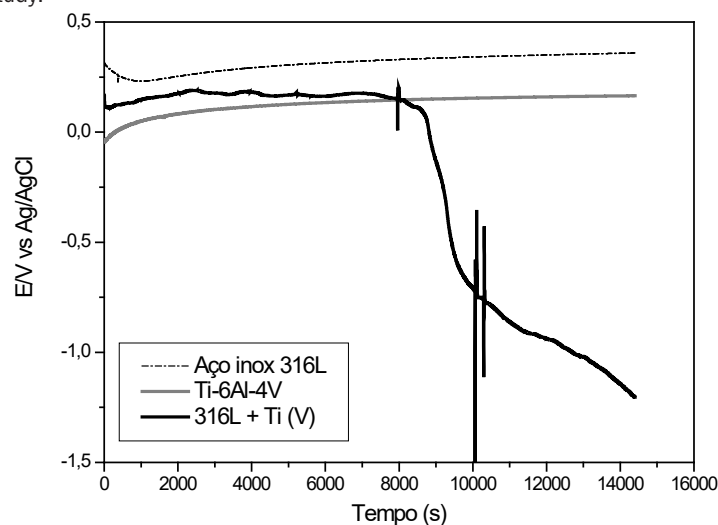


**Figure 2** – Open circuit potential variation as a function of time of immersion of a dental implant (Ti grade V) and a prosthetic abutment of stainless steel, either separately or coupled.

According to OCP measurements, the stainless steel 316 presented more positive potentials compared to the titanium alloy, throughout the test. Therefore, when the Ti alloy is electrically connected to the SS 316L and exposed to the electrolyte of this study, the grade V titanium acts as anode while the stainless steel, behaves as cathode.

As expected, the open circuit potential of the sample with Ti alloy coupled to SS 316L showed an intermediate value between the two materials



tested separately, up to 8000 seconds (s) of the test. After this period of test, strong corrosion attack occurred in the sample with the galvanic couple that was evidenced by potential oscillations (indicated in Figure 2). Consequently, for longer periods than 8000 s, the potential largely decreased and values well below those of the two isolated alloys were measured. These results indicate a harmful effect of galvanically coupling the two tested alloys to the passive film promoting its attack when exposed to aggressive environments, and, consequently, corrosion of the material. The oscillations in potential of the galvanically coupled samples were supported by the intense localized attack observed at the exposed surface.

Figure 3 shows SVET maps of the galvanic couple during exposure to the electrolyte for 2h (A), 10h (B) and 14h (C). The immersion times corresponding to the maps of Figure 3(A), (B) and (C).

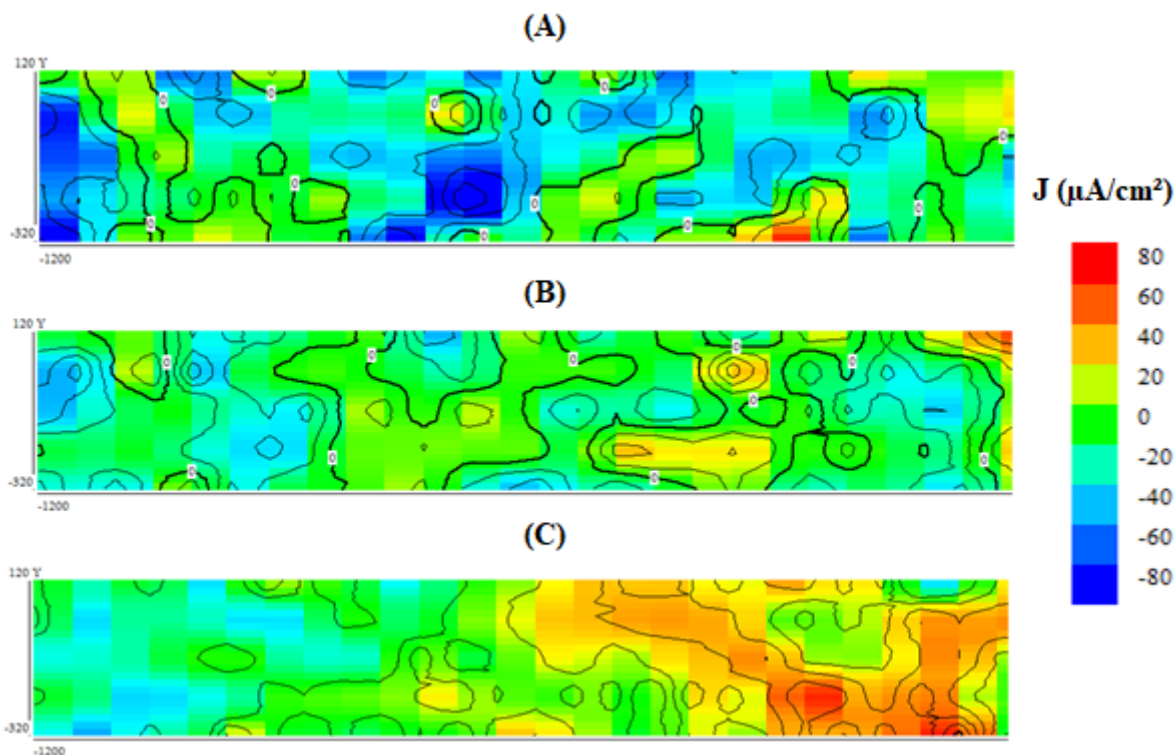


**Figure 3** – SVET maps of the region of the galvanic coupling between the stainless steel 316 L abutment and the Ti grade V dental implant after (A) 2 hours, (B) 10 hours e (C) 14 hours of immersion in a PBS solution pH 3 and addition of 1%  $H_2O_2$ .

After 2h of immersion, anodic areas were identified in the Ti alloy (see arrows). SVET maps (Fig. 3) showed that the anodic regions were related with the Ti-6Al-4V alloy. Anodic areas were clearly identified in the Ti alloy after 14h of test. Also, the anodic currents were related to the Ti-6Al-4V alloy. Consequently, the SS 316L was cathodically protected (blue regions). It is noteworthy that the conditions used in this study may occur in the buccal region in case of inflammatory processes.

Figure 4 shows the surface of the dental implants connected to the prosthetic abutment by (A) optical microscope and (B) scanning electron microscope (SEM) after the SVET assay.

The surface images of the galvanic coupling by scanning electron microscopy and optical microscopy (Fig. 4) after 24 hours of immersion test shows a large amount of corrosion products in the galvanic coupling region, mainly on Ti-6Al-4V alloy. Comparing the results of open circuit potential and SVET maps, it is observed that in acid medium (pH 3) and hydrogen peroxide addition, the titanium alloy grade V used with implant acts as anode in relation to stainless steel 316 L used as a prosthetic abutment, and latter being protected cathodically while Ti alloy corrosion is accelerated.

Mellado-Valero et al.<sup>14</sup> analyzed the electrochemical behavior of five different alloy used to the manufactured of prosthetic abutments coupled to a titanium grade 2 used as dental implant from electrochemical assays in a solution of artificial saliva under different pH conditions (6.5 and 3.0) with the addition of fluoride ions. After the tests, was observed acceleration of corrosion of titanium alloy (grade 2) when coupled galvanically to the Co-Cr prosthetic abutment. The authors concluded that the effect of galvanic coupling is highly dependent on the conditions of the medium and the material in contact.

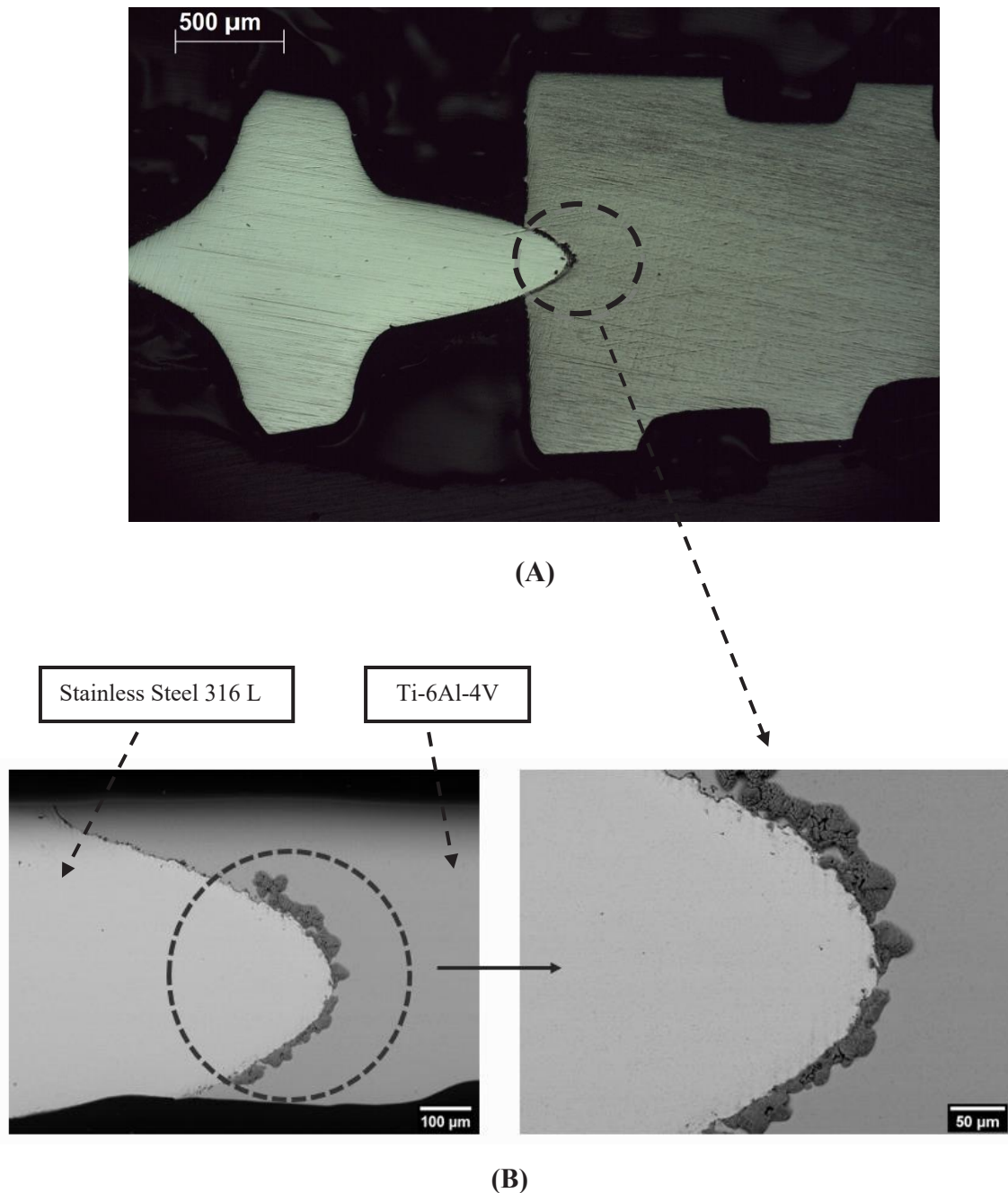


**Figure 4** – Images of (A) optical microscopy and (B) scanning electron microscopy (SEM) after 24 hours of immersion in a phosphate buffer solution pH 3 and 1% H<sub>2</sub>O<sub>2</sub>.

### Conclusions

The results of this study allow to concluding that Ti-6Al-4V alloy in galvanic contact with stainless steel 316 L acts as the anode in contact with a solution simulating inflammatory conditions in the oral environment. Galvanic coupling promotes an attack on the Ti alloy by attacking the passive film on the Ti alloy grade V when in contact with SS 316L, resulting in an intense attack on the coupling, as observed by a large amount of corrosion products under the area between these alloys.

### Acknowledgement

The authors thank the “Coordination of Superior Level Staff Improvement”– CAPES for the scholarship granted to the lead author for this study. And the support given by the Center for Lasers and Applications’ Multiuser Facility at IPEN–CNEN/SP.

### References

- [1]. Asri, R. I. M.; Harun, W. S. W.; Samykano, M.; Lah, N. A. C.; Ghani, S. A. C.; Tarlochan, F.; Raza, M. R. Corrosion and surface modification on biocompatible metals: a review. *Materials Science and Engineering C*, v. 77, 2017.

- [2]. Ravoiu, A.; Benea, L.; Chiriac, A. Metabolic albumin and its effect on electrochemical behavior on titanium implant alloy. *Materials Science and Engineering*, v. 374, 2018.
- [3]. Manan, N. S.; Harun, W. S. W.; Shri, D. N. A.; Ghani, S. A. C.; Kurniawan, T.; Ismail, M. H.; Ibrahim, M. H. I. Study of corrosion in biocompatible metals for implants: a review. *Journal of alloys and compounds*, v. 701, 2017.
- [4]. Moreno, J. M. C. Vasilescu, E.; Drob, P.; Osiceanu, P.; Vasilescu, C.; Drob, S. I.; Popa, M. Surface and electrochemical characterization of a new ternary titanium based alloy behaviour in electrolytes of varying pH. *Corrosion Science*, v. 77, 2013.
- [5]. Silva–Bermudez, P.; Rodil, S. E. Na overview of protein adsorption on metal oxide coatings for biomedical implants. *Surface & Coatings Technology*, v. 233, 2013.
- [6]. Apaza–Bedoya, K.; Tarce, M.; Benfatti, C. A. M.; Henriques, B.; Mathew, M. T.; Teughels, W. Souza, J. C. M. Synergistic interactions between corrosion and wear at titanium–based dental implant connections: A scoping review. *Journal of Periodontal Research*, v. 52(6), 2017.
- [7]. Revathi, A.; Magesh, S.; Balla, V. K.; Das, M.; Manivasagam, G. Current advances in enhancement of wear and corrosion resistance of titanium alloys: a review. *Materials Technology*, 2016.
- [8]. ASTM G15–93. Standard terminology relating to corrosion and corrosion testing.
- [9]. Bhola, R.; Bhola, S. M.; Mishra, B.; Olson, D. Corrosion in titanium dental implants/prostheses – a review. *Trends in Biomaterials and Artificial Organs*, v. 25(1), 2011.
- [10]. Chaturvedi, T. P. An overview of the corrosion aspect of dental implants (titanium and its alloys). *Indian Journal for Dental Research*, v. 20(1), 2009.
- [11]. Guo, H.; Callaway, J. B.; Ting, J. P–Y. Inflammasomes: mechanism of action, role in disease, and therapeutics. *Nature Medicine*, v. 21, n. 7, 2015.
- [12]. Izquierdo, J.; Bolat, G.; Mareci, D.; Munteanu, C.; González S.; Souto, R. M. Electrochemical behaviour of ZrTi alloys in artificial physiological solution simulating in vitro inflammatory conditions. *Applied Surface Science*, v. 313, 2014.
- [13]. Konstantinidis, I. A.; Kotsakis, G. A.; Gerdes, S.; Walter, M. H. Cross–sectional study on the prevalence and risk indicators of peri–implant diseases. *European Journal of Oral Implantology*, v. 8, n. 1, 2015.
- [14]. Mellado–Valero, A.; Muñoz, A. I.; Pina, V. G.; Sola–Ruiz, M. F. Electrochemical behaviour and galvanic effects of titanium implants coupled to metallic suprastructures in artificial saliva. *Materials*, v. 11, 2018.



# Industrial Revolution 4.0 and the 3D printing in Biotechnology of tissue re-generation

Lucas Noboru Fatori Trevizan<sup>1\*</sup>; Mayté Paredes Zaldivar<sup>2</sup>; Antônio Carlos Massabni<sup>3</sup>

\*Corresponding author: e-mail address: [noboro\\_trevizan@hotmail.com](mailto:noboro_trevizan@hotmail.com)

**Abstract:** When portrayed to the current society, the industry is considered as part of the society economically responsible for the development and production of consumer goods. The processes of industrial revolution were highlighted by phases of improvement and technological advances (1st Industrial Revolution), the use of electric energy (2nd Industrial Revolution), and the dissemination of the digitalization of technology (3rd Industrial Revolution). In addition, nowadays such developments can be associated with the use of the internet and the automation of processes by artificial intelligence, thus reaching the 4th Industrial Revolution. The concept of Industry 4.0 is directly linked to the concept of intelligent fabrics, starting from factors such as innovation, which allows companies to have complex production models including mainly sustainable character and applied biotechnologies. In addition, both the 4th Industrial Revolution and biotechnology can be correlated in terms of 3D bioprinting. Thus, the work shows a brief history of 3D printers and their potential in applications in the area of tissue engineering. It reveals the need for multidisciplinary and increasingly qualified professionals in the face of the new phase of socioindustrial evolution.

**Keywords:** 3D printing. Additive manufacturing. Biotechnology. Tissue engineering.

## Introduction

In the context of social technological developments, areas such as the industrial sector undergo direct modifications as technological advances develop. Thus, more significant changes in the market in the worldwide result in major changes. In the last decades, one of these transformations that marked all scenarios was the insertion of the internet. Together with the internet, the industry entered a new stage in its evolutionary process, with the emergence of the Industrial Revolution 4.0. This process has brought great scientific technical advances where processes have become more reproducible and agile, with this, the growth of the market for 3D printers, especially in relation to rising areas such as biotechnology.

Thus, the objective of this review is to highlight the main points of Industrial Revolution 4.0, relating the area of biotechnology by its presenting concepts, and relating points to the professional future for such technological junction in tissue engineering.

## Industrial revolution 4.0

Following the terms of the industrial revolution, the industry is considered as part of the society, which is economically responsible for the development, and production of consumer goods, using highly mechanized procedures to achieve this goal.<sup>1</sup> When portrayed the vision of future in industrial production, the tendency of modular application and high efficiency manufactured industrial systems rose, which has its self-control of production quality and standardization.<sup>2</sup>

In addition, the evolution of industrial processes has been highlighted by phases of improvement and technological advances, such as mechanization of manufactures (1st Industrial Revolution), intense electricity use (2nd Industrial Revolution), and the spread of technology digitization (3rd Industrial Revolution).<sup>2</sup> However, combining such technologies with the use of the internet, artificial intelligence and processes automation, it is possible to achieve the 4th Industrial Revolution.

Thus, the internet becomes a key factor in the advances of this revo-

lution, especially because it is a public technology and not a technology owned by a single owner.<sup>3</sup> Based on this factor, the application of the internet in economic scenarios causes their total transformation, as mentioned by Rifkin.<sup>4</sup> This trend is confirmed by the concept of zero marginal cost, emphasizing connectivity in anticipation of a collaborative economy. For this reason, it replaces the capital system in its current form, especially when it comes to internet products, that helps directly the faster progress and a more collaborative world, resulting in increasingly intelligent cities.<sup>5</sup>

In view of these claims, the 4th Industrial Revolution affects political, social and mainly economic organizations around the globe. Moreover, its main scope modifies the production structure, enabling its increase, and supplying previously unseen pressures such as the sustainability and protection of the environment.<sup>1</sup>

In addition to this new production structure, new structuring models are also required with regard to resource preservation and management. The development directly affects the industrial model, so the final disposal of products and waste is also affected. Thus, the model of Industrial Sustainability 4.0 emerges on the global stage.<sup>6</sup>

When referring to this term, Industrial Sustainability 4.0 is primarily the basis of the concept of sustainability in its entirety, emphasizing that it find out the requirements of the current generation without compromising the future generations.<sup>7,8</sup> Thus, the base pillars that form sustainability as a simple structure are constituted by economic, social and environmental factors. The pillars adhere to the transition circle between technological innovation and social innovation, of which they are responsible for providing sustainable solutions that meet the three sustainability criteria, and can also act as a mechanism for assessing any related Industry 4.0.<sup>8</sup>

Moreover, when associated with the evolution of these technologies, the cyber-physical union makes this revolution increasingly applied to the areas related to computational technology. Thus, as an example of industries that grew exponentially with the development of this new stage

<sup>1</sup>PhD student of the Graduate Program in Biotechnology in Regenerative Medicine and Medicinal Chemistry of University of Araraquara (UNIARA).

<sup>2</sup>Postdoctoral Program in Biotechnology in Regenerative Medicine and Medicinal Chemistry at the University of Araraquara (UNIARA).

<sup>3</sup>Professor of the Graduate Program in Biotechnology in Regenerative Medicine and Medicinal Chemistry of University of Araraquara (UNIARA).

of technological advancement, it is possible to mention the industries of smartphones, internet services and related goods, and improvements of services previously considered basic.<sup>2,9</sup>

Therefore, the concept of Industry 4.0 is directly linked to the concept of intelligent manufacturing, or smart factory. Presenting as essential feature, factors such as innovation, which allows companies to have complex production models as well as ensure the possibility of unexpected interruptions as well more efficient products. In short, in a smart factory, staff, machinery, and production resources have communication that flows naturally and constantly as if they were directly interconnected.<sup>10</sup>

In addition, areas that grew together with the 4th Industrial Revolution are the areas of biological sciences and health. Unlike previous revolutions, these areas have had a great scientific technical support, which generated great expectation in the development of technology.<sup>11</sup> Together with the rise of Revolution 4.0 to the joining of biological and math areas, the rise of a previously existing but still developing area, the Biotechnology has gained momentum across the globe.

**Biotechnology definition**

With the beginning of the twentieth century, great scientific technical advances allowed the development of new technologies. Mainly when related to areas of genetics, which the application of Mendel’s laws, along with Morgan’s discoveries provided new models of knowledge. Based on this assumption, the rediscovery of biological inheritance followed by gene localization became even more applicable, as gene manipulation allowed great progress in the scientific community.<sup>12</sup>

Moreover, in 1990, with the sequencing of the human genome, the use of genetic engineering became even more popular, opening fields not previously explored in the political–social–scientific scenario.<sup>13</sup> Since then, biotechnology has become increasingly noticeable in scientific circles, gaining greater prominence in the areas of food production and health.

However, when related to the term “Biotechnology”, there is still a great divergence about its concept, in short, as quoted by Faleiro, Andrade and Reis Junior,<sup>14</sup> “Biotechnology is a set of techniques that uses living beings, or part of them, in the development of processes and/or products that have an economic and (or) social function”.

In addition, other definitions are presented as: “It is the use of knowledge about biological processes and the properties of living things in order to solve problems and create utility products.”<sup>15</sup> When related to classical biotechnology, we can also find even broader definitions: “It is the industrial use of fermentation processes ... technology that allows the use of biological material for industrial purposes.”<sup>16</sup> “It is a set of techniques that use living things, or part of them, to produce or modify products, increase plant and animal productivity efficiently, or produce microorganisms for specific uses.”<sup>17</sup>

In portraying modern biotechnology, we can find definitions as: “It’s the use of cells and biomolecules for problem solving or product transformation. It is a set of techniques that enhances the best characteristics of cells, such as productive capacities, and makes available biological molecules, such as DNA and proteins, to be used”.<sup>18</sup> “It is the development of products by biological processes using recombinant DNA technology”.<sup>19</sup> “Spectrum or set of molecular technologies applied to the study of microorganisms, plants and animals.”<sup>20,21</sup>

**Biotechnology application areas**

When looking at to the term biotechnology, it is noted that it has a wide spectrum of actions, including the need for a multidisciplinary professional, precisely due to the union of areas such as biology, engineering and chemistry for applications in the production of goods (Figure 1).

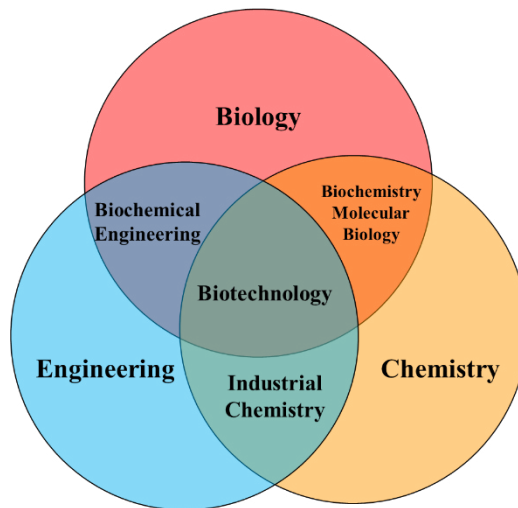


**Figure 1** – Outline of the major constituent areas of biotechnology. Source: Biotechnology Information Council.<sup>21</sup>

Thus, the use of biotechnology associated with its various factors applicable to industry 4.0 has been highlighted in the current scenario, in which numerous biotechnological methodologies bring about and new production systems, increasing the economic, social and environmental benefits, besides the industrial application.<sup>14</sup>

Finally, the parallel growth of biotechnology coupled with the Industrial Revolution 4.0, especially in healthcare, leads to increasingly sophisticated new techniques and their broader applicability using the most advanced and efficient technological methodologies. For this reason, the use of nano-technology, nanobiotechnology, gene therapy, molecular biology, genetic engineering and mainly the area of tissue engineering can be mentioned.<sup>22</sup>

**Tissue engineering concept**

The term tissue engineering was first described in 1988 as: “the application of engineering and life science principles and methods, toward the fundamental understanding of structure–function relationships in normal and pathological mammalian tissues, and the development of biological

substitutes to restore, maintain or improve tissue function".<sup>23</sup>

In short, the tissue engineering is related to the use of principles from the cell transplants, associated with the material science with the objective to develop biological substitutes leading to regeneration to a normal tissue function. Moreover, it is possible to divide it in two classifications: the first is the use of acellular matrices, the regeneration depends directly of the body's natural ability to orientate the tissue regeneration; normally this technique use scaffolds application followed by chemical stimuli for starting the tissue reconstruction. The second is related to the use of cellular matrices that are correlated to applications of material contend incorporated cells, these cells can be heterologous (such as bovine), allogeneic (same species, different individual), or autologous. In this case, the use of autologous cells is preferred because of the lower rejection possibility, and avoids the deleterious side effects caused by the immunosuppressive medication after application.<sup>24,25</sup>

In addition, it has a multidisciplinary character, encompassing chemical, physical, biological and medical knowledge for the development of viable biological substitutes for their restoration, maintenance and suitability. Thus, it aims to develop therapeutic options to be applied under specific clinical conditions, by tissue replacement and/or regeneration using biomaterials.<sup>26-28</sup>

### Tissue engineering applications

Tissue engineering directly utilizes porous 3D supports to condition the most conducive environments for tissue and organ regeneration. These supports, called scaffolds, essentially function as a model for tissue formation, where they are typically cultured with cells and growth factors, or occasionally subjected to biophysical stimuli in the form of a bioreactor.<sup>29</sup> These cell scaffolds are cultured *in vitro* to synthesize tissues that can be implanted at the wound site or directly at the site of injury using the patient's own body as a system, in which tissue or organ regeneration is induced *in vivo*. This combination of cells, growth factors and scaffolds is often referred to as the tissue engineering triad.<sup>23</sup>

The success of this methodology depends directly and mainly on the nature of these biomaterials, which can be modified to mimic the extracellular matrix (ECM) architecture of the target tissues, which are characterized by a complex organization of structural proteins and fibers such as collagen and a diversity of proteoglycans and polysaccharides.<sup>26,27</sup> Thus, biomaterials are used to act in the biological interface of systems enabling, treating, increasing, improving or replacing any tissue, organ or function of the body, partially or totally.<sup>30</sup>

Following this reasoning, when considering an ideal biomaterial, characteristics such as the variety of sizes and shapes, as well as the resistance to places where they may suffer impact loads should be taken into account. Another point to be emphasized is biocompatibility, material resorption and possible substitution by the formation of a new tissue.<sup>31</sup> Due to the fact that after implantation of the "substitute" tissue would occur an increase in cellular functions, and the induction of cell growth on the porous surface and internal pores, resulting in the tissue formation process.<sup>32</sup>

When related to the types of biomaterials, two types can be found: natural and synthetic. Natural biomaterials simulate the structure and composition of the native extracellular matrix, allowing the insertion of growth factors and other proteins capable of boosting cellular functions. However, they easily deteriorate and allow the transfer of pathogens to the host, their variability depends on the structure of the original natural polymer.<sup>33,35</sup> Synthetic biomaterials, on the other hand, do not have the characteristic of simulation of the native extracellular matrix, and generally consist of self-assembling peptides that can be modified in order to acquire biologically active characteristics. In addition, they are easy to handle since they have a controlled degradation rate and do not allow the transfer of pathogens to the host. However, they often require signaling molecules to aid in the interaction between cells and material, and further degradation can produce undesirable byproducts.<sup>33,35</sup>

Tissue engineering involves culturing cells by sowing them in biocompatible scaffolds, allowing them to grow and mature (*in vitro* or via bioreactor) to form the desired tissues. Today, 3D bioprinting technology enables systems to obtain greater precision in the spatial relationship between individual elements of the desired tissue, and holds great promise for applications in biotechnology and regenerative medicine.<sup>35</sup> However, to portray 3D bioprinting, a prior background on the technique of additive manufacturing or 3d printing is required.

### Additive manufacture or 3D printing

#### Definition of additive manufacturing or 3D printing

Three-dimensional printing is a method whereby materials such as plastics, metals or polymers are deposited in layers to produce an object in three dimensions.<sup>36</sup> Its use has been applied for the most diverse purposes.<sup>37</sup> In addition, the advancement of technologies driven by the evolution of production processes, such a technology has been explored further as even in biomedical areas.<sup>38</sup>

#### 3D printing company history

When related to 3D printing companies, the story begins with Helisis, founded by Feygin in 1985. Its main product is the sheet lamination process. Its first delivery was in 1991, however the company closed in 2000.<sup>39</sup> Also in 1985, Deken (Japan) introduced its first stereolithography machine (SLP-3000) in 1993.<sup>39,40</sup> In 1986, Hull and Freed formed 3D Systems, which was considered the first modern additive manufacturing machine, the SLA-1, and was launched in 1987, with its first sale taken place in 1988, and its patent approved in 1992.<sup>41</sup> In 1988, Stratasys was founded as the first company to develop fused deposition modeling in 1991 and its patent was accepted in 1992.<sup>42,39</sup>

According to Dipaola<sup>43</sup>, the evolution of bioprinting companies is divided into ages, in which the first era (1970-1980) is marked by the first demonstration of a prototype additive manufacturing. Followed by the second era (1980-1990), marked by the emergence of models of stereolithography and selective laser sintering, along with the birth of 3D Systems. The third era (1990-2005) was marked by the increase in computing resources and the maturation of industrial 3D printing spurred the emergence of other new printing companies in the world. The fourth era (2005-2012) has the rapid expansion and greater awareness of 3D printing as its main factor, which results in an expansion of the printing area, especially with the increasing applicability of the technique. The fifth and sixth eras (2012-2017) were the period where second-generation 3D printers and the beginning of medical application of this technology appear. Finally, with the end of the patent period, 3D printing became very popular across the globe, reaching even domestic sectors, and, under the influence of the Industrial Revolution 4.0, became a much-targeted tool in all areas of knowledge.

#### 3D printing evolution perspective

According to a study by the US National Center for Manufacturing Sciences (1998), 3D printing techniques were unified in mid-1998, process trifurcation was expected to occur by the year 2010, and considerable increased production volume when referring to prototype applications.<sup>44</sup>

In this way, the use of 3D printers, are increasing as technologies are discovered. Thus, by associating such technology with the evolution brought about by the computer age, new part design methodologies emerge. Which guarantees the reproducibility of the process, relating the customization, mass and volume of the part without the loss of quality of the final product.<sup>40</sup> In this context, the various applications of 3D printers because the

differences between their models can be highlighted, which may vary directly or indirectly depending on their purpose and/or used material.

### Types of 3D printers

Among 3D printer development models, there is a great diversity of shapes and models. However, despite its wide range of applications the basis of printing is the same, from a virtual image (usually in computer aided design or CAD format) to obtains a real object in three dimensions. Thus, the foundation of this "3D printing" is differentiated by its application methodology as described below.

#### Selective laser fusion

Selective laser fusion (SLF) arose from the need to manufacture full-density parts in which the mechanical properties similar to those of bulk materials are guaranteed, as well as avoiding long post-processing cycles.<sup>45,46</sup>

During SLF processing, the beam is scanned over a thin layer of a powder (usually metallic or ceramic). Thus, the process of object formation continues along the direction of the laser beam. Later, each layer is sequentially filled with elongated fillets of melted powders. As a result, the object is constructed from overlays of fillets and layers.<sup>47</sup>

#### Deposition of molten material

Fused deposition modeling is based on the principle of depositing a thermoplastic material on a platform. Subsequently, the layers are deposited on the previously printed layers, while the other wires support the new layer, thus forming the new object.<sup>48</sup>

#### Electron beam fusion

Electron beam melting (EBM) is given by melting the pulverized material layer by layer using an electron beam in a high vacuum condition. Thus, this technique can delineate high density parts, without extremely strong voids, which differs from some metal sintering techniques. Moreover, this technique is generally used for metals that have high reactivity with oxygen, which makes it an advantage, since the vacuum is used, preventing interaction with it.<sup>49,50</sup>

#### Digital light processing

Digital light processing is characterized by the use of UV light to solidify a liquid photo polymer.<sup>51</sup> Such technique is widely used due to its high print speed and its simple mechanisms when related to its software. In which, photocurable liquid polymerization is performed layer by layer, thus obtaining the object in three dimensions.<sup>52</sup>

#### 3D bioprinting

Three-dimensional bioprinting technology is directly related to the deposition of biomaterials, cells, biological structures and layer-by-layer growth factors in order to produce biosimilar and biocompatible tissues and organs. In addition, such technology enables the use of cell suspension printing in a scaffolded or nonscaffolded structure.<sup>35,53</sup>

One of the main points to be emphasized in the process of bioprinting is its soft and friendly characteristic to the cells, since such technique should allow the impression of them without damage, which would allow the maintenance of cell survival after the procedure. Thus, this requirement limits many 3D printing techniques that are suitable for such purpose. These techniques include direct ink writing, which allows the extrusion of high viscosity solutions, hydrogels, colloidal suspensions, cell suspensions and/or aggregates with or without chargers.<sup>53</sup>

Unlike other conventional printing techniques, the main advantages of using 3D bioprinting are accurate deposition, repeatability, simplicity and controlled cell distribution, and the constant development of this technique in recent years. Thus, bioprinting has become a major field of application, being represented mainly as the great technical-scientific advance in the face of the Industrial Revolution 4.0.

### Conclusion

The Industrial Revolution 4.0 has become a major factor in perfecting previously unexplored techniques. In addition, the use of new technologies associated with biotechnology has contributed to a better quality of life. Nowadays, in the age of computerization and technological improvement, the increase in development, especially in areas such as engineering, reflects enhancement and advances not previously aimed at all areas of application and knowledge. In other words, this evolution tends to need more and more qualified professionals, mainly due to the multidisciplinary required to new production processes.

### Acknowledgements

The authors thank Fundação Nacional de Desenvolvimento do Ensino Superior Particular (Funadesp), Fundação de Amparo à Pesquisa do Estado de São Paulo (Fapesp), Conselho Nacional de Desenvolvimento Científico e Tecnológico (CNPq) and Coordenação de Aperfeiçoamento de Pessoal de Nível Superior – Brasil (CAPES) – Finance Code 001 for financial support.

### References

- [1]. Magalhães R, Vendramini A. Os impactos da Quarta Revolução Industrial. *GV Executivo*. 2018;**17**(1):40–3. <https://doi.org/10.12660/gvexec.v17n1.2018.74093>
- [2]. Lasi H, Fettke P, Kemper H-G, Feld T, Hoffmann M. *Industrie 4.0*. *Wirtschaftsinf*. 2014;**56**(4):261–4. <https://doi.org/10.1007/S11576-014-0424-4>
- [3]. Carr NG. IT doesn't matter. *Harv Bus Rev*. 2003;**81**(5):41–9. [cited 2020 Feb. 18]. <https://hbr.org/2003/05/it-doesnt-matter>
- [4]. Rifkin J. *The zero marginal cost society: the internet of things, the collaborative commons, and the eclipse of capitalism*. New York: St. Martin's Press; 2014.
- [5]. Kanter RM, Litow SS. *Informed and interconnected: a manifesto for smarter cities*. Harvard Business School General Management Unit Working

- Paper No. 09–141; 2009. <https://doi.org/10.2139/ssrn.1420236>
- [6]. Morrar R, Arman H, Mousa S. The Fourth Industrial Revolution (Industry 4.0): a social innovation perspective. *Technol Innov Manag Rev.* 2017;**7**(11):12–20. <http://doi.org/10.22215/timreview/1117>
- [7]. Adams WM. The future of sustainability: re-thinking environment and development in the twenty-first century. In: IUCN Renowned Thinkers Meeting. Gland: IUCN; 2006. [cited 2020 Feb. 21]. Available at: <https://portals.iucn.org/library/node/12635>
- [8]. Adams WM, Jeanrenaud S. Transition to sustainability: towards a humane and diverse world. Gland: IUCN; 2008.
- [9]. Almada-Lobo F. The Industry 4.0 revolution and the future of manufacturing execution systems (MES). *Int J Innov Manag.* 2016;**3**(4):16–21. [https://doi.org/10.24840/2183-0606\\_003.004\\_0003](https://doi.org/10.24840/2183-0606_003.004_0003)
- [10]. Kagermann H, Wahlster W, Helbig J. Recommendations for implementing the strategic initiative INDUSTRIE 4.0 -- Securing the future of German manufacturing industry. Final report of the Industrie 4.0 working group. München: National Academy of Science and Engineering; 2013. [cited 2020 Feb. 21]. Available at: [http://forschungsunion.de/pdf/industrie\\_4\\_0\\_final\\_report.pdf](http://forschungsunion.de/pdf/industrie_4_0_final_report.pdf)
- [11]. Yoon D. What we need to prepare for the fourth industrial revolution. *Healthc Inform Res.* 2017;**23**(2):75–6. <https://doi.org/10.4258/hir.2017.23.2.75>
- [12]. Watson JD, Berry, A. DNA: o segredo da vida. São Paulo: Companhia das Letras; 2005.
- [13]. Pereira LV. Seqüenciaram o genoma humano... E agora? São Paulo: Moderna; 2001.
- [14]. Faleiro FG, Andrade SRM, Reis Junior FB. Biotecnologia: estado da arte e aplicações na agropecuária. Planaltina: Embrapa Cerrados-Livro técnico; 2011. [cited 2020 Feb. 21]. Available at: <https://www.embrapa.br/busca-de-publicacoes/-/publicacao/916213/biotecnologia-estado-da-arte-e-aplicacoes-na-agropecuaria>
- [15]. United Nations (UN). Convention on Biological Diversity [Internet]. 1992. [cited 2019 Oct. 30]. Available at: <https://www.cbd.int/doc/legal/cbd-en.pdf>
- [16]. Borém A, Romano ES, Sá MFG. Fluxo gênico e transgênicos. Viçosa: UFV; 2007.
- [17]. Torres AC, Ferreira AT, Sá FG, Buso JA, Caldas LS, Nascimento AS, et al. Glossário de biotecnologia vegetal. Brasília (DF): Embrapa Hortalças; 2000. [cited 2019 Oct. 30]. Available at: <http://www.infoteca.cnptia.embrapa.br/infoteca/handle/doc/769141>
- [18]. Agência Brasileira de Desenvolvimento Industrial (ABDI) [Internet]. [cited 2019 Oct. 30]. Available at: <https://www.abdi.com.br/>
- [19]. Borém A, Santos FR. Biotecnologia simplificada. Viçosa: Suprema; 2004.
- [20]. Borém A, Vieira MLC, Colli W. Glossário de biotecnologia. Viçosa: Suprema; 2009.
- [21]. Conselho de Informações sobre Biotecnologia (CIB). Campus Virtual de Saúde Pública (CVSP) [Internet]. [cited 2019 Oct. 30]. Available at: <https://brasil.campusvirtuaisp.org/taxonomy/term/9453>
- [22]. Chang TMS. Artificial cells: biotechnology, nanomedicine, regenerative medicine, blood substitutes, bioencapsulation, and cell/stem cell therapy. Singapore: World Scientific; 2007. <https://doi.org/10.1142/6395>
- [23]. O'Brien FJ. Biomaterials & scaffolds for tissue engineering. *Mater Today.* 2011;**14**(3):88–95. [https://doi.org/10.1016/S1369-7021\(11\)70058-X](https://doi.org/10.1016/S1369-7021(11)70058-X)
- [24]. Atala A. Tissue engineering and regenerative medicine: concepts for clinical application. *Rejuvenation Research.* 2004;**7**(1):15–31. <https://doi.org/10.1089/154916804323105053>
- [25]. Langer R. Biomaterials in drug delivery and tissue engineering: one laboratory's experience. *Accounts of Chemical Research.* 2000;**33**(2):94–101. <https://doi.org/10.1021/ar9800993>
- [26]. Cai X-J, Xu Y-Y. Nanomaterials in controlled drug release. *Cytotechnology.* 2011;**63**(4):319–23. <https://doi.org/10.1007/s10616-011-9366-5>
- [27]. Shi Q, Li Y, Sun J, Zhang H, Chen L, Chen B, et al. The osteogenesis of bacterial cellulose scaffold loaded with bone morphogenetic protein-2. *Biomaterials.* 2012;**33**(28):6644–9. <https://doi.org/10.1016/j.biomaterials.2012.05.071>
- [28]. Shi D, Somberg J. Biomaterials and tissue engineering. *Am J Ther.* 2014;**13**(1):88–91. <https://doi.org/10.1097/01.mjt.0000203908.45949.90>
- [29]. Martin I, Wendt D, Heberer M. The role of bioreactors in tissue engineering. *Trends Biotechnol.* 2004;**22**(2):80–6. <https://doi.org/10.1016/j.tibtech.2003.12.001>
- [30]. Williams DF. On the nature of biomaterials. *Biomaterials.* 2009;**30**(30):5897–909. <https://doi.org/10.1016/j.biomaterials.2009.07.027>
- [31]. Chapekar MS. Tissue engineering: challenges and opportunities. *J Biomed Mater Res.* 2000;**53**(6):617–20. <https://doi.org/10.1002/1097->



4636(2000)53:6<617::AID-JBM1>3.0.CO;2-C

- [32]. Spector M. Basic principles of scaffolds in tissue engineering. In: Lynch SE, Marx RE, Nevins M, Wisner-Lynch LA (Eds.). Tissue engineering. Applications in oral and maxillofacial surgery and periodontics. Batavia: Quintessence; 2008.
- [33]. Holmes TC. Novel peptide-based biomaterial scaffolds for tissue engineering. Trends Biotechnol. 2002;**20**(1):16–21. [https://doi.org/10.1016/s0167-7799\(01\)01840-6](https://doi.org/10.1016/s0167-7799(01)01840-6)
- [34]. Ng KW, Khor HL, Huttmacher DW. *In vitro* characterization of natural and synthetic dermal matrices cultured with human dermal fibroblasts. Biomaterials. 2004;**25**(14):2807–18. <https://doi.org/10.1016/j.biomaterials.2003.09.058>
- [35]. Bishop ES, Mostafa S, Pakvasa M, Luu HH, Lee MJ, Wolf JM, et al. 3-D bioprinting technologies in tissue engineering and regenerative medicine: Current and future trends. Genes Dev. 2017;**4**(4):185–95. <https://doi.org/10.1016/j.gendis.2017.10.002>
- [36]. Schubert C, van Langeveld MC, Donoso LA. Innovations in 3D printing: a 3D overview from optics to organs. Br J Ophthalmol. 2014;**98**(2):159–61. <https://doi.org/10.1136/bjophthalmol-2013-304446>
- [37]. Hager I, Golonka A, Putanowicz R. 3D printing of buildings and building components as the future of sustainable construction? Procedia Eng. 2016;**151**:292–9. <https://doi.org/10.1016/j.proeng.2016.07.357>
- [38]. Chia HN, Wu BM. Recent advances in 3D printing of biomaterials. J Biol Eng. 2015;**9**(4):1–14. <https://doi.org/10.1186/s13036-015-0001-4>
- [39]. Beaman JJ, Barlow JW, Bourell DL, Crawford RH, Marcus HL, McAlea KP. Solid freeform fabrication: a new direction in manufacturing. Boston: Springer; 1997. <https://doi.org/10.1007/978-1-4615-6327-3>
- [40]. Bourell DL. Perspectives on additive manufacturing. Annu Rev Mater Res. 2016;**46**:1–18. <https://doi.org/10.1146/annurev-matsci-070115-031606>
- [41]. Hull CW. Lewis CW, inventors; 3D Systems Inc., assignee. Methods and apparatus for production of three-dimensional objects by stereolithography. United States patent US 4999143A. 1988 Apr 18.
- [42]. Crump SS, inventor; Stratasys Inc., assignee. Apparatus and method for creating three-dimensional objects. United States patent US 5121329A. 1984 Aug 8.
- [43]. Jakus AE. An introduction to 3D printing – past, present, and future promise. In: Dipaola, M (Ed.). 3D Printing in Orthopaedic Surgery. Amsterdam: Elsevier Health Sciences; 2018.
- [44]. National Center for Manufacturing Sciences, The road to manufacturing: 1998 industrial roadmap for the rapid prototyping industry, NCMS Report 0199RE98, Ann Arbor, 1998.
- [45]. Badrossamay M, Childs THC. Further studies in selective laser melting of stainless and tool steel powders. Int J Mach Tools Manuf. 2007;**47**(5):779–84. <https://doi.org/10.1016/j.ijmachtools.2006.09.013>
- [46]. Marques S, Souza AF, Miranda JR, Santos RFF. Evaluating the conformal cooling system in moulds for plastic injection by CAE simulation. In: 9<sup>th</sup> International Conference on Industrial Tools and Material Processing Technologies. Ljubljana: TECOS, Slovenian Tool and Die Development Centre; 2014.
- [47]. Yadroitsev I, Smurov I. Surface morphology in selective laser melting of metal powders. Phys. Procedia. 2011;**12**(A):264–70. <https://doi.org/10.1016/j.phpro.2011.03.034>
- [48]. Mello CHP, Guedes FN, Noronha VJM, Kawasaki AA, Rocha TES, Ferreira JR, et al. Análise da qualidade superficial e dimensional em peças produzidas por modelagem por deposição de material fundido (FDM). Rev Prod Online. 2010;**10**(3):504–23. <https://doi.org/10.14488/1676-1901.v10i3.237>
- [49]. Taminger KM, Hafley RA. Electron beam freeform fabrication for cost effective near-net shape manufacturing. Hampton: NATO UNCLASSIFIED; 2006 May 15. 19 p. Report No.: 20080013538. [cited 2019 Feb. 21]. Available at: <https://ntrs.nasa.gov/search.jsp?R=20080013538>
- [50]. Sing SL, An J, Yeong WY, Wiria FE. Laser and electron beam powder bed additive manufacturing of metallic implants: A review on processes, materials and designs. J Orthop Res. 2016;**34**(3):369–85. <https://doi.org/10.1002/jor.23075>
- [51]. Gibson I, Rosen D, Stucker B. Additive manufacturing technologies: 3D Printing, rapid prototyping, and direct digital manufacturing. New York: Springer; 2014. <https://doi.org/10.1007/978-1-4939-2113-3>
- [52]. Wu C, Yi R, Liu Y-J, He Y, Wang CCL. Delta DLP 3D printing with large size. In: 2016 IEEE/RSJ International Conference on Intelligent Robots and Systems (IROS). Daejeon: IEEE; 2016. <https://doi.org/10.1109/iros.2016.7759338>
- [53]. Ji S, Guvendiren M. Recent advances in bioink design for 3D bioprinting of tissues and organs. Front Bioeng Biotechnol. 2017;**5**(23):1–8. <https://doi.org/10.3389/fbioe.2017.00023>



## Cell viability evaluation of vero cells viability cultured on different chitosan films: development of functional biodressings possibilities

Victor Campana Leite<sup>1</sup>; Warley Wagner Pereira Filho<sup>1</sup>; Ênio Nazaré de Oliveira Junior<sup>2</sup>; Daniela Leite Fabrino<sup>2\*</sup>

\*Corresponding author: e-mail address: danifabrino@ufsj.edu.br

**Abstract:** Biomaterials used in regenerative medicine must have biocompatibility and be non-toxic, as they are used in contact with living tissues for repair or replacement. Therefore, they must provide a suitable microenvironment for ex vivo cell culture. Chitosan is a biomaterial highly used in cell culture research because it is non-toxic, biocompatible, biodegradable, exhibits high hydrophilicity, and has important antibacterial characteristics. This work has studied the interaction of VERO cells with chitosan films produced with different crosslinking agents, by evaluating the viability and cell morphology. Assays were followed for 96 hours for analysis of cell proliferation, viability, and morphology. The cells presented different developments in the different films, being the film with acetic acid the least suitable for cultivation showing cell viability of 58%, on the other hand, films made from chitosan solutions with lactic or citric acid had cell viability of around 70%. Therefore, chitosan films can be explored as biomaterials for the production of biodressings, for example, by exploiting the best crosslinking agent in their production (ie different acids).

**Keywords:** Chitosan. Films. Cell culture. Biomaterial.

### Introduction

#### Cell culture in two dimensions

Cell culture refers to cultures derived from dispersed cells obtained from tissues, primary cultures, or from a cell line<sup>14</sup>. This technique allows the maintenance of living cells under controlled laboratory conditions and enables a better understanding of the molecular mechanisms of the cell, allowing important scientific advances in, for example, vaccine production and tumor cell biology<sup>1</sup>.

The controlled conditions occur through the conditioning of the culture media, nutrient mixtures such as mineral salts [macro and micronutrients], carbohydrates, vitamins, and regulators necessary for cell growth, always maintained with pH, temperature, and oxygenation appropriated to the specific lineage keeping cells and tissues active for longer periods. Sometimes, the media also contain fetal bovine serum [FBS], whose main functions are to stimulate growth and other cellular activities through hormones and growth factors, increase cell adhesion by specific proteins, and provide proteins for hormone transport, minerals, and lipids<sup>21</sup>.

Biopolymers are macromolecules produced by living organisms such as polysaccharides, proteins, nucleic acids, and lipids<sup>11</sup>. These biomaterials have the advantages of being abundant, affordable, similar to ECM, biodegradable and their degradation products are non-toxic and biocompatible. Due to this set of factors, the use of these biomaterials is abundant in numerous sectors of the biomedical industry<sup>17</sup>. Bioresorbable polymers are polymeric materials and solid devices that show degradation through size reduction and which are reabsorbed *in vivo*, materials that are eliminated by metabolic pathways in the body. Bioreaction is a concept that reflects the total elimination of low molar mass degradation by-products and by-products without residual side effects<sup>22</sup>. Bioresorbable devices have been used *in vitro* as a support for cell growth and proliferation of various cell types<sup>6</sup>. Among the several known bioresorbable biomolecules, chitosan occupies a prominent position in cell culture due to its particular characteristics.

Chitosan is a biopolymer obtained by the deacetylation reaction of chitin in alkaline medium. It is the second most abundant biopolymer in nature and can be extracted mainly from the crustacean and insect

exoskeleton. It is insoluble in an aqueous medium and most organic solvents and has low chemical reactivity<sup>9</sup>. The main difference between chitosan and chitin is the average content of the 2-acetamido-2-deoxy-D-glucopyranose [GlcNAc] and 2-amino-2-deoxy-glucopyranose [GlcN] units present in the polymer chains, with effects on the solubility of these polymers. The degree of acetylation [GA] is defined as the average fraction of GlcNAc units present in the polymer chains. The product of chitin deacetylation is considered chitosan when soluble in dilute acid solution<sup>3</sup>.

The main properties of chitosan that lead to its high use as a biomaterial in cell culture research are (1) high hydrophilicity, due to a large number of hydroxyl groups and amino groups present in the polymer chain, which allows its use as a biomaterial in the form of films, gels and membranes<sup>9</sup>; (2) non-toxicity, biocompatibility; and (3) biodegradability<sup>8</sup>. At neutral pH, chitosan acquires a positive global charge by protonating its amino groups. This property is of great importance for cell culture because it gives to chitosan the ability to electrostatically bind to glycosaminoglycans, proteoglycans, and other negatively-charged molecules<sup>4</sup>.

Chitosan has been widely studied as a start material due to its antimicrobial properties and ability to manage the inflammatory response, besides promoting fibroblasts migration<sup>10,15</sup>.

Analysis of the healing process from a macroscopic point of view reveals that chitosan plays an important role in the recovery of acute skin lesions on rats, accelerating the healing process and providing reduced lesion width, which reinforces its potential for medical application<sup>5</sup>.

However, it has been shown that the presentation of the chitosan biomaterial, for example, gels, sponges, scaffolds, nanoparticles, films, or combined dressings influences its performances<sup>16</sup>.

Preliminary results from our group indicate that cells do not reject collagen, hyaluronic acid, and chitosan-based support structures<sup>18</sup>. However, this work tested the interaction of cells in chitosan films made with different acids as reticulate agents, aiming to study the interaction of VERO cells with this biomaterial through morphological analysis and cell viability and point out a better starting presentation of a chitosan film for a biodressing development.

<sup>1</sup>Bioprocess Engineering Undergrad students, Federal University of São João del-Rei, Ouro Branco (MG), Brazil.

<sup>2</sup>Chemistry, Biotechnology and Bioprocess Engineering Department, Federal University of São João del-Rei, Ouro Branco (MG), Brazil.

## Methodology

### Production of chitosan films

The chitosan films used were kindly provided by Prof. Dr. Enio Nazaré de Oliveira Junior, from the Department of Chemistry, Biotechnology and Bioprocess Engineering of the Federal University of São João del-Rei. The production of chitosan-based films followed the procedure described by YOSHIDA et al. (2009). Different films were prepared by dissolving commercial chitosan samples, with the degree of acetylation from 5.8 to 6.3%, in 1% (v/v) of acetic acid (AA), lactic acid (AL), or citric acid (AC) solutions at 0.5% (w/v) concentration. The solutions were homogenized on a magnetic stirrer at room temperature for 24 hours until complete dissolution. They were then filtered using an 11 µm filter under vacuum and 100 mL of the filtrate was added to glass plates with a length of 29 cm and width of 21 cm. The films were dried at room temperature.

### Preparation of the cell population

The tubes containing VERO cells were thawed in a water bath and the cells were resuspended in 8 mL RPMI culture medium (SIGMA), 20% fetal bovine serum (FBS) (SIGMA), and 1% of an antibiotic solution (10mg penicillin; 10mg streptomycin; 25µg amphotericin B per ml – SIGMA). The cell solution was centrifuged at 1150xg for 5 minutes and the supernatant was discarded. The pellet was resuspended in 5 mL of the same culture medium used for centrifugation and the cell suspension was transferred to a T-25 culture flask. Then the culture was incubated in a 5% CO<sub>2</sub> incubator at 37°C. After acclimatization of the cells, the FBS concentration was reduced to 10% and the cells were transferred to a T-75 flask, once a suitable confluence has been reached the experiments were performed. Thus, the medium used in all experiments was the 10% FBS and 1% antibiotics RPMI

### Sterilization and preparation of chitosan films for cultivation

Chitosan films were cut into squares (1 cm<sup>2</sup>) and deposited individually, in triplicate, under the bottom of the wells of a 24-well culture plate.

For sterilization, the films remained dipped in 70% alcohol at room temperature. After 3 days the alcohol solution was discarded and the wells containing the films were washed thoroughly with sterile phosphate-saline buffer (PSB). Then 450µL of penicillin/streptomycin antibiotic was added to each well allowing it to act for 30 minutes to eliminate any remaining contamination. The films were washed 3 times with PSB and acclimated in 500µL RPMI 10% FBS and 1% antibiotic culture medium.

### Cell cultivation

The VERO culture at 80% of confluence was trypsinized and resuspended in RPMI culture medium, as described above.

To quantify cell concentration, the cell count was performed in a Haemocytometer. The culture plate containing the different films and the controls were seeded with 0.5 x 10<sup>5</sup> cells and the volume of each well was raised to 1 mL with the culture medium in use. The plates were incubated in a 37°C/CO<sub>2</sub> incubator.

### Morphological analysis by microscopy

For morphology and confluence analysis, VERO cell cultures were observed using the phase-contrast inverted microscope (BX41 Olympus) shortly after the beginning of cultivation, and at 24, 48, and 96 hours of cultivation at magnitudes of 100, 200, and 400x.

### Viability test

The culture medium was discarded and the wells were washed with 2 mL of sterile PSB three times. The films were transferred to another identical plate so that the counting would only occur for cells that were adhered to the biomaterial. 250 µL of 0.25% trypsin (SIGMA) was added to each well and the plate was incubated for 3 minutes at 37 °C. Then 250µL of culture medium was added to all wells. The suspensions were transferred to 2 mL Eppendorf® tubes. 10µL of each suspension was removed and 10µL of 0.4% Trypan blue was added. Thus, 20µL solutions were obtained from each well containing the dye. 10µL of each sample was transferred to Haemocytometer and counted under an optical microscope. After counting the four quadrants in each reticulum, Equation 1 was used to obtain cell concentration in cells / mL. Equation 1:

$$N = \frac{n \times D \times 10^4}{8} \quad (1)$$

Being:

N = number of cells/ml; “N” is the number of cells counted in the quadrants of the two Neubauer chamber reticles and “D” the dilution factor. Cell viability was calculated by the percentage of viable unstained cells by Trypan blue dye during counting.

## Results and Discussion

### Cell growth in chitosan movies

The RPMI culture medium used had in its composition the phenol red pH indicator, therefore, it was possible to monitor qualitatively the pH of the medium during the tests, once it was possible to observe color changes according to the pH variation. Immediately after cell seeding on chitosan films, a sudden change in pH was observed, with a more prominent change in AL films, followed by AC and AA, as can be seen in Figure 1.

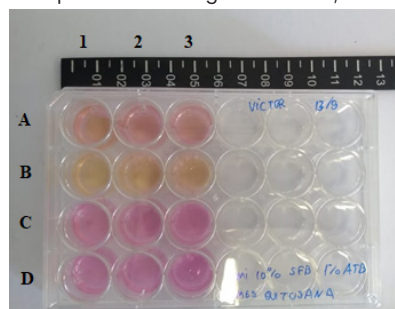


**Figure 1** – 24-well plate containing chitosan films immediately after cell population passage. Chitosan 0.5% in lactic acid [A1 and A2 and A3]; Chitosan 0.5% in citric acid [B1, B2 and B3]; Chitosan 0.5% in acetic acid [C1, C2 and C3]; Negative control [D1, D2 and D3].

This pH variation can be explained by the different pKa values for these acids (Table 1). The lower the pKa value of an acid, the greater the acid dissociation constant ( $K_a$ ).

Acids	pK <sub>a</sub> 25°C
Acetic acid	4.75
Citric acid	pK <sub>a1</sub> =3.15
	pK <sub>a2</sub> =4.77
	pK <sub>a3</sub> =6.40
Lactic acid	3.85

**Table 1** – pKa at 25 °C for acids used in film production.

Source: IUPAC Gold Book, 1997.

In the cell culture system, it is important to control the optimal pH (7.0–7.6) using a buffer and supplementing the culture medium to resist pH variations, especially in the lag phase of cell growth<sup>14</sup>. Therefore, the sudden variation in the pH of the culture medium can affect the culture development, decreasing the cell viability, and increasing the lag phase duration.

**Cell number count**

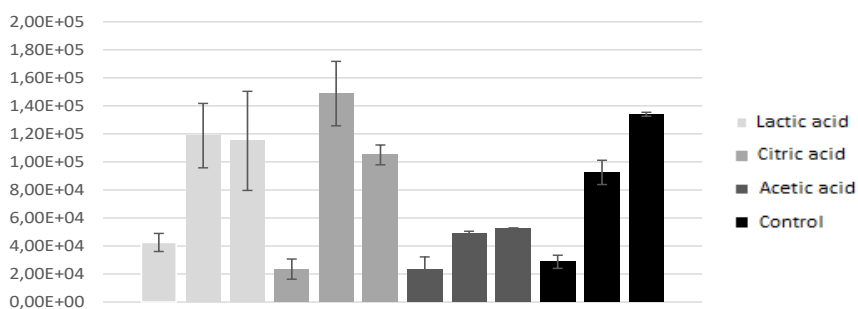
It was found that cells can interact well with chitosan films until they reach a high confluence especially the films which had AL and AC as reticulate agents. Chitosan films in AA were less favorable for cell multiplication (Graph 1).

At 24 hours there was initial cellularization in all films, but the AC and AA films exhibited a low number of cells when compared to the control. The acidification of the medium, generated after the contact of the films with the culture medium and the toxicity of these acids, especially the acetic and citric acids, may have interfered in the initial development of the cells. Utyama (2003), when studying the cytotoxicity of acetic acid on *Artemia salina* Leach, founds that the acid was cytotoxic at all concentrations studied.

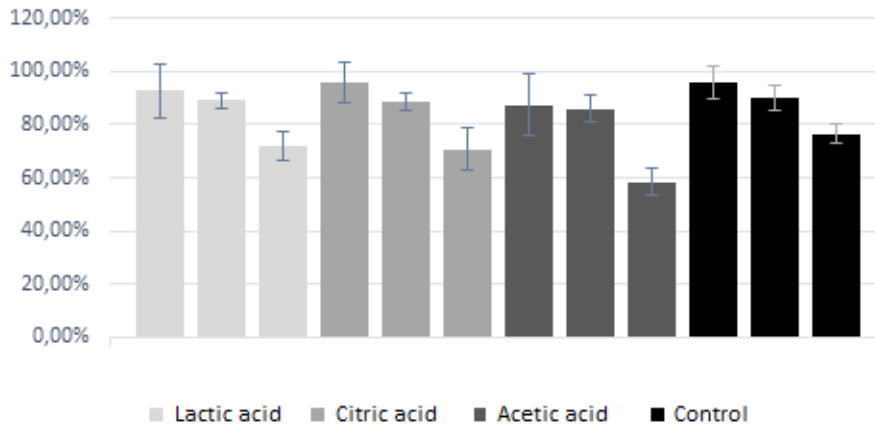
After 48h, it was observed that the cellularization of the films reached similar numbers to the control. In general, it is found around  $1 \times 10^5$  cells/cm when cells are cultured in monolayer<sup>19</sup>. Once the films are about 1cm, the cell concentration values for AL and AC films were compatible with those in the literature. The considerable improvement in cellularization within 48 hours can be explained by the pH control system in the CO<sub>2</sub> incubator. The dissolved CO<sub>2</sub> in equilibrium with bicarbonate ions generates a buffering system in the important medium in the lag phase of cell growth<sup>13</sup>. AA films, on the other hand, were not fit for cellularization and had about half cell numbers compared to other films and the control.

At 96 hours, the cellularization was kept stable for the AL and AC films. AA films maintained the same low cell concentration of 48h, proving to be less viable.

Data from cell viability analysis corroborate with the indication of the AA film as the least viable for cellularization, once at 24 hours of cultivation the viability of the cells cultured in it was 10% lower than the viability found in cells grown in the other films. AL (92.6%) and AC (96%) had results aligned with the control (96%). This decrease in cell viability in AA films becomes more evident at 96h when cell viability in AA films was only around 58%, while in the other films, including control, cell viability was up to 76%. This corroborates the toxicity of these films and the results found in cell count and light microscopy. Graph 2 presents the results for the observed cell viability.



**Graph 1** – Cell concentration [cells / mL] of monolayer cultures on the different films tested and in the control comparing the same acids at different interaction times.



**Graph 2** – Cell viability of monolayer growing cultures on different films tested and on control comparing different acids at different interaction times.

**Analysis of VERO cells culture development in chitosan films**

Figure 2 – shows the morphology of the VERO cell population in each film after 24, 48, and 96 hours after seeding.

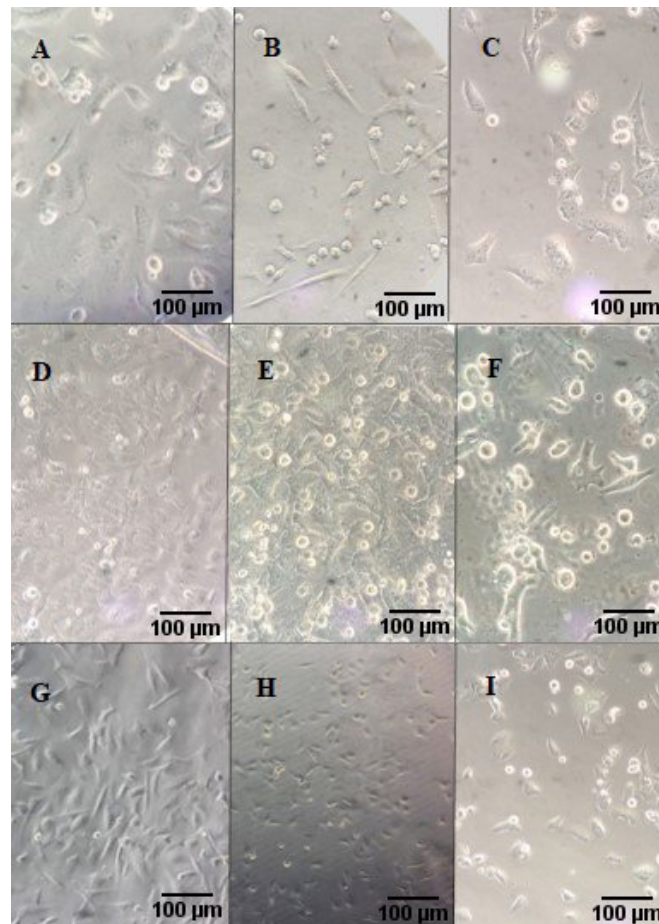


**Figure 2** – Optical microscopy of triplicate wells containing 0.5% chitosan films after 24 hours [A, B, C], 48 hours [D, E, F], and 96 hours [G, H, I] of culture. A, D and G represent the lactic acid films, B, E, H the citric acid films, and C, F, I the acetic acid films. Source: Own author.

Spread cells exhibiting fibroblast conformation were observed within 24 hours of incubation, which corroborates the morphological characterization mentioned in the literature, where fibroblasts are described as regenerating cells with a tendency to grow rapidly <sup>7</sup>.

Besides, it was possible to observe that immediately upon contact with the films, the culture medium acidifies rapidly due to the pKa of the acids used in the preparation of the films. This fact may have interfered in viability and cell number in the first 24h of culture.

One factor that should be considered is that the films were not produced in a sterile and controlled environment, therefore had impurities that could be observed by phase-contrast optical microscopy and according to PATRULEA et al. 2015 this may have an impact on the material performance

and work on this issue is still necessary on the field, as well as better characterization. This way, a more detailed analysis of the films and a better evaluation of the cellular interaction process with the film will require scanning electron microscopy (SEM) analysis.

It is valuable to note that, despite a bulk of data about chitosan as a successful biomaterial used on the wound healing process, there are few works on chitosan-based films and the available products based on different chitosan presentations don't include any film-based one<sup>12</sup>.

Once films are stable and easy to handle this presentation turns out to be interesting on patronization and further studies.

### Conclusion

VERO cells showed satisfactory late viability when grown on chitosan films. These were also biocompatible and capable of providing adhesiveness to VERO cells which achieved a population close to maximum confluence in AL and AC films. On the other hand, AA films maintained a low number of cells along with all the cultivation and showed low cell viability at the end of 96h, proving to be unviable and cytotoxic to the cells. This way we call attention to the fact that chitosan films are a good supply to manufacture biodressings once it is a cheap, easy, and safe biomaterial to be used in contact with cells, however, it is necessary to choose carefully the reticulate agent used in its fabrication.

### Acknowledgments

Acknowledgment to the Research Bureau of the Federal University of São João del-Rei (PROPE / UFSJ) for financial support in the form of a scientific initiation scholarship.

### References

- [1]. Amaral JB, Machado-Santelli G. A cultura de células em 3 dimensões e a sua aplicação em estudos relacionados a formação do lúmen. *Naturalia*. **34**: 1–20 (2011).
- [2]. Bhadriraju K, Chen CS. *Engineering cellular microenvironments to improve cell-based drug testing*. Drug Discov Today. **11**:612–620 (2002). DOI:10.1016/s1359-6446(02)02273-0.
- [3]. Campana-Filho S, Britto D, Curti E et al. Extração, estruturas e propriedades de alfa- e beta-quitina. *Química Nova*. **30** :644–650 (2007). DOI:10.1590/s0100-40422007000300026
- [4]. Chandy T, Sharma C. Chitosan—as a Biomaterial. *Biomaterials, Artificial Cells, and Artificial Organs*. **18**:1–24 (1990). DOI:10.3109/10731199009117286
- [5]. Fráguas RM, Simão AA, Faria PV, Queiroz ER, Junior ENO, Abreu CMP. Preparo e caracterização de filmes comestíveis de quitosana. *Polímeros*. **25**: 48–53 (2015). DOI:10.1590/0104-1428.1656
- [6]. Junior ARS, Wada MLF. Polímeros biorreabsorvíveis como substrato para cultura de células e engenharia tecidual. *Polímeros*. **17**: 308–317 (2007). <https://dx.doi.org/10.1590/S0104-14282007000400010>.
- [7]. Junqueira LC.; Carneiro J. *Biologia celular e molecular*. 9.ed. Rio de Janeiro: Guanabara Koogan, pp. 3–4, (2013).
- [8]. Kim SK, Park PJ, Yang HP, Han SS. Subacute toxicity of chitosan oligosaccharide in Sprague–Dawley rats. *Arzneimittelforschung*, **51**: 769–774 (2001). DOI:10.1055/s-0031-1300113
- [9]. Laranjeira MCM, Fávère VT. Quitosana: biopolímero funcional com potencial industrial biomédico. *Química Nova*. **32** : 672–678 (2009). DOI:10.1590/s0100-40422009000300011
- [10]. Matica MA, Aachmann FL, Tøndervik A, Sletta H, Ostafe V. Chitosan as a Wound Dressing Starting Material: Antimicrobial Properties and Mode of Action. *Int J Mol Sci*. **20** :5889 (2019). DOI:10.3390/ijms20235889
- [11]. McNaught AD, Wilkinson A. IUPAC Compendium Of Chemical Terminology. [Cambridge, England]: *Royal Society of Chemistry* (2000). <https://doi.org/10.1351/goldbook>.
- [12]. Miguel SP, Moreira AF, Correia IJ. Chitosan-based-asymmetric membranes for wound healing: A review. *Int J Biol Macromol*. **127**: 460–475 (2019). DOI:10.1016/j.ijbiomac.2019.01.072
- [13]. Molinaro EM, Caputo LFG, Amendoeira MRR. *Conceitos e métodos para a formação de profissionais em laboratórios de saúde vol. 3*. Fundação Oswaldo Cruz, Rio de Janeiro, pp 1 – 304. (2013). ISBN: 85-98768-41-0.
- [14]. Moraes AM, Augusto EFP, Castilho LR. Tecnologia do cultivo de células animais: de biofármacos à terapia gênica. 1 ed. São Paulo, pp. 15–41 (2008).
- [15]. Oryan A, Sahwieh S. Effectiveness of chitosan scaffold in skin, bone, and cartilage healing. *Int J Biol Macromol*, **104**:1003–1011 (2017). DOI:10.1016/j.ijbiomac.2017.06.124
- [16]. Patrúlea V, Ostafe V, Borchard G, Jordan O. Chitosan as a starting material for wound healing applications. *Eur J Pharm Biopharm*, **97**:417–426 (2015) DOI:10.1016/j.ejpb.2015.08.004
- [17]. Pires ALR, Bierhalz ACK, Moraes AM. Biomaterials: types, applications, and market. *Química Nova*. **37**: 957–971(2015). DOI:10.5935/0100-4042.20150094

- [18]. Rabello L, Trindade V, Oliveira E, Fabrino DL. Development of scaffolds based on chitosan, type I collagen, and hyaluronic acid as a biomaterial for three-dimensional cell culture. *Congresso Da Sociedade Latino Americana De Biomateriais, Orgãos Artificiais E Engenharia De Tecidos*. São Paulo. **14**: 348–357 (2017)
- [19]. Ryan JA. Growing more cells: A simple guide to small volume cell culture scale-up. Presentation presented at the: Massachusetts. (2005). <https://www.corning.com/catalog/cls/documents/application-notes/CLS-AN-064.pdf>
- [20]. Utyama IKA. Avaliação da atividade antimicrobiana e citotóxica in vitro do vinagre a ácido acético: perspectiva na terapêutica de ferida. Escola de Enfermagem de Ribeirão Preto, Universidade de São Paulo, Ribeirão Preto (2003). DOI: 10.11606/D.22.2003.tde-21052004-114541
- [21]. Valk JVD, Brunner D, Smet KD et al. Optimization of chemically defined cell culture media – Replacing fetal bovine serum in mammalian in vitro methods. *Toxicology in Vitro* **24**:1053–1063 (2010). DOI:10.1016/j.tiv.2010.03.016
- [22]. Vert M, Li SM, Spenlehauer G, Guerin P. Bioresorbability and biocompatibility of aliphatic polyesters. *Journal of Materials Science: Materials in Medicine*. **3**: 432–446 (1992). DOI:10.1007/bf00701240
- [23]. Yoshida CMP, Maciel VBV, Mendonça MED, Franco TT. Chitosan tailor-made films: the effects of additives on barrier and mechanical properties. *Packaging Technology and Science*. **22**:161–170 (2008). DOI:10.1002/pts.839



## Fibrous PCL scaffolds as tissue substitutes

Luciana P. Giorno<sup>1\*</sup>; Leonardo R. Rodrigues<sup>2</sup>; Arnaldo R. Santos Jr<sup>1</sup>

\*Corresponding author: e-mail address: [giorno.l@ufabc.edu.br](mailto:giorno.l@ufabc.edu.br)

**Abstract:** Burns are characterized by high clinical complexity. Large skin wounds reduce the body's defenses and activate the inflammatory cascade, resulting in complications such as multiple organ dysfunction syndrome. In an attempt to improve techniques for burn management, tissue engineering has emerged as a viable alternative in which biocompatible materials are used to mimic the extracellular matrix. Scaffolds were fabricated using a poly( $\epsilon$ -caprolactone) polymer matrix (PCL) and PCL combined with gelatin. The solutions were submitted to rotary jet spinning and then crosslinked. All materials were characterized following recommended technical standards (biological and physical). The results showed satisfactory homogenization of the solutions. We observed the formation of PCL and PCL/gelatin fibers. Fourier-transform infrared spectroscopy confirmed the material used in the scaffolds. In conclusion, rotary jet spinning was found to be effective for fiber production and the scaffolds obtained were non-toxic

**Keywords:** Burns. Biocompatible Materials. Rotary Jet Spinning.

### Introduction

Burns are a public health problem of high clinical complexity and are associated with prolonged hospital stay, immune system disorders, susceptibility to infections, and high morbidity and mortality.<sup>1,2</sup> Depending on the extent and characteristics of the burn injury, skin transplantation is the gold standard treatment to ensure patient survival because of the limitations of the tissue repair process.<sup>3,4</sup> However, the imbalance between effective organ donors and recipients indicated by the National Transplant System has encouraged the search for therapeutic alternative to overcome this shortage.<sup>3,4,5</sup>

Among emerging technologies, tissue engineering is a field aimed at elucidating the structure-function relationship between normal and diseased tissues in order to repair or replace tissue using bioresorbable scaffold with specific physical characteristics that mimic human morphofunctionality. Mimicking human tissues, the physiological reactions in response to biomaterials are expected to favor the good integration of these materials in the organism. Thus, research constantly seeks to change the surface of materials in order to improve the capacity of cell adhesion, growth, proliferation and differentiation in the tissues for which they are destined.<sup>6,7,8,9,10,11</sup>

Poly( $\epsilon$ -caprolactone) (PCL) is a bioresorbable material that was approved by the Food and Drug Administration (FDA) for use in humans. PCL is characterized by properties such as flexibility, good mechanical strength, and moderate undesirable host reactions. In addition, PCL is compatible with a wide range of other polymers and is a candidate for grafting and for stimulating cell regeneration.<sup>12,13</sup> Gelatin, which is derived from collagen, is widely used in tissue engineering and cell culture, representing a common substrate for cells.<sup>14</sup>

We aimed to develop a polymer scaffold (PCL/gelatin) via rotary jet spinning that can be used in the future for the filling and repair of injured tissues.

### Materials and methods

#### Materials

CAPA 6500 PCL [Aldrich 440744-250G, Mn 70000-90000; reported molar mass of 50,000 grams per molecule (g/mol)] and gelatin from bovine skin [Sigma-Aldrich, CAS Number: 9000-70-8 MDL: MFCD00081638;

Type B] were used. The pH of a 1.5% solution ranges from 5.0-7.5 at 25°C.

#### Sample Preparation

PCL was dissolved in chloroform (Vetec Química) and stirred in a magnetic stirrer (model 753A, Fisatom) for 24 h. The homogenized solution was transferred to the rotary jet spinning chamber.<sup>15,16,17</sup> The formation of fibers was observed by the flow of the polymeric solution in the collector through capillaries on the lateral surface of the equipment using a maximum power of 950 W and a motor of 210/3,400 (W/rpm).<sup>18</sup> After solvent evaporation, the fibers were removed from the collector and stored in a desiccator before use. Gelatin was dissolved at 20% in distilled water at  $\pm 60^\circ\text{C}$  under constant agitation (magnetic GO stirrer MS-H-Pro) for 20 min. Next, 1% glutaraldehyde solution (Sigma-Aldrich) was added and the mixture was incubated for 24 h to permit crosslinking. For the PCL/gelatin scaffold, PCL and gelatin were prepared as described above. The PCL fibers were immersed in gelatin solution, followed by glutaraldehyde also as described above.<sup>14,19</sup>

The crosslinked gelatin and PCL materials were disinfected with 70% ethanol for 24 h and kept in medium 199 (Lonza) without fetal bovine serum (FBS) in an incubator for 24 h at 37°C (ISO-10993-5). The PCL/gelatin scaffold was sterilized by autoclaving (Stermax) at a pressure of 15 lbs and temperature of 121°C for  $\pm 20$  min.<sup>20</sup>

#### Morphological Characterization of the Scaffolds by Light Microscopy

The samples were examined under a phase-contrast inverted light microscope (Axio Vert.A1, Zeiss) for analysis of the fibers produced by rotary jet spinning. Fragments of the materials were mounted between a slide and coverslip. Drops of distilled water were used to reduce light refraction and to improve resolution.<sup>21</sup>

#### Characterization of the Scaffolds by Fourier-Transform Infrared Spectroscopy (FTIR)

The functional groups and characteristic vibrational modes of each polymer were evaluated with the Spotlight 400 FTIR Imaging System. The parameters adopted were a measurement range of 4000 to 500  $\text{cm}^{-1}$  using the attenuated total reflectance (ATR) technique in the transmittance mode,

<sup>1</sup>Centro de Ciências Naturais e Humanas (CCNH), Universidade Federal do ABC, São Bernardo do Campo, SP, Brazil.

<sup>2</sup>Centro de Engenharia, Modelagem e Ciências Sociais Aplicadas (CECS), Universidade Federal do ABC, Santo André, SP, Brazil.



with a resolution of  $1\text{ cm}^{-1}$  in four scans per measurement.<sup>22</sup>

### Cell Culture

Vero cells, a cell line established from African green monkey (*Cercopithecus aethiops*) kidney cells, were used. These cells were cultured in medium 199 (Lonza) with 10% FBS (Nutricell Cellular Nutrients, Campinas, SP, Brazil) at 37°C in an incubator with 5% CO<sub>2</sub>. The medium was changed whenever it was acidified and subcultures were obtained once or twice a week. Vero cells are recommended for studies of cytotoxicity and cell–cell interactions on biomaterials.<sup>23,24</sup>

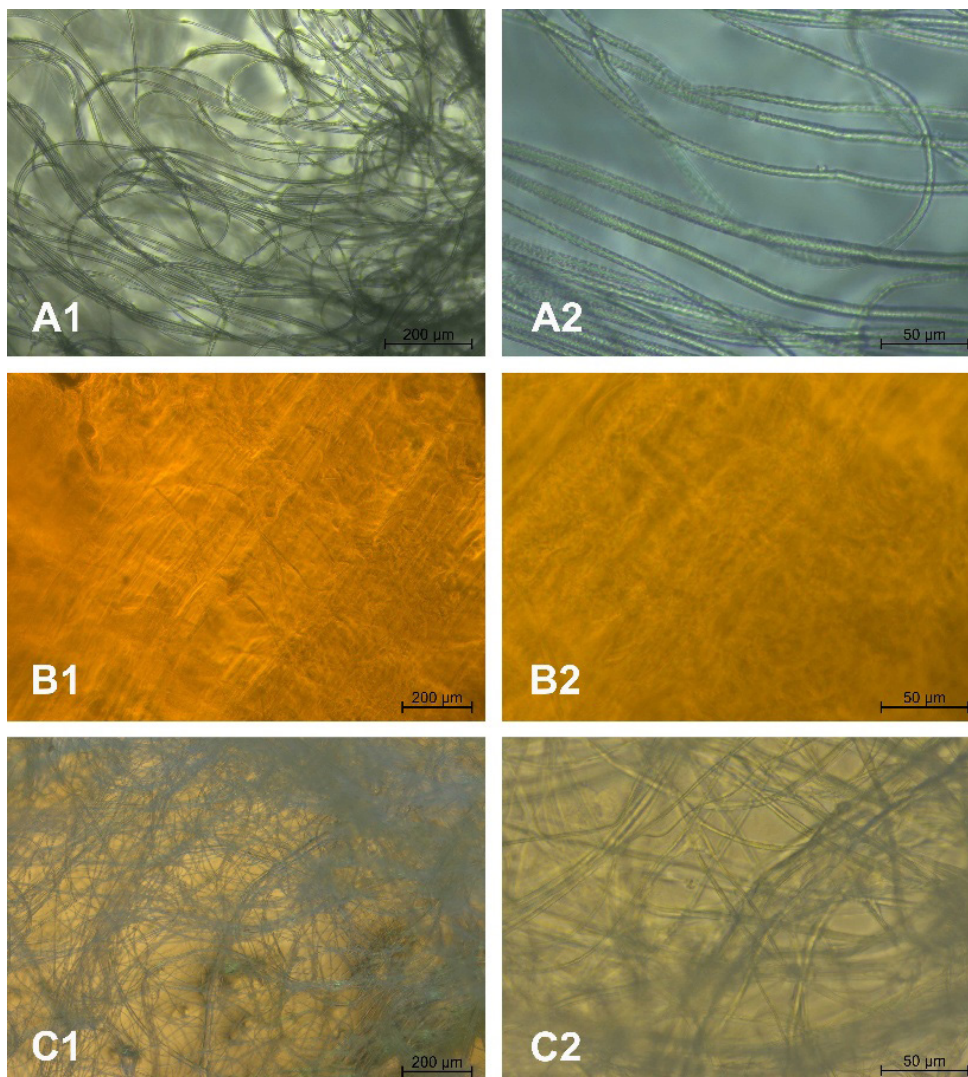
### In Vitro Direct Contact Toxicity

Fragments of each material (PCL, gelatin, and PCL/gelatin) were placed in 24–well culture plates and incubated in FBS–free medium for 24 h at 37°C in a 5% CO<sub>2</sub> atmosphere. After this period, Vero cells were inoculated at a concentration of  $1.0 \times 10^5$  cells/ml in medium with 10% FBS. The cells were kept for 24 h in direct contact with the tested materials under the same culture conditions as described above. Images were obtained with an inverted light microscope (Axio Vert.A1, Zeiss) during the culture period and before fixation.<sup>24</sup>

## Results and discussion

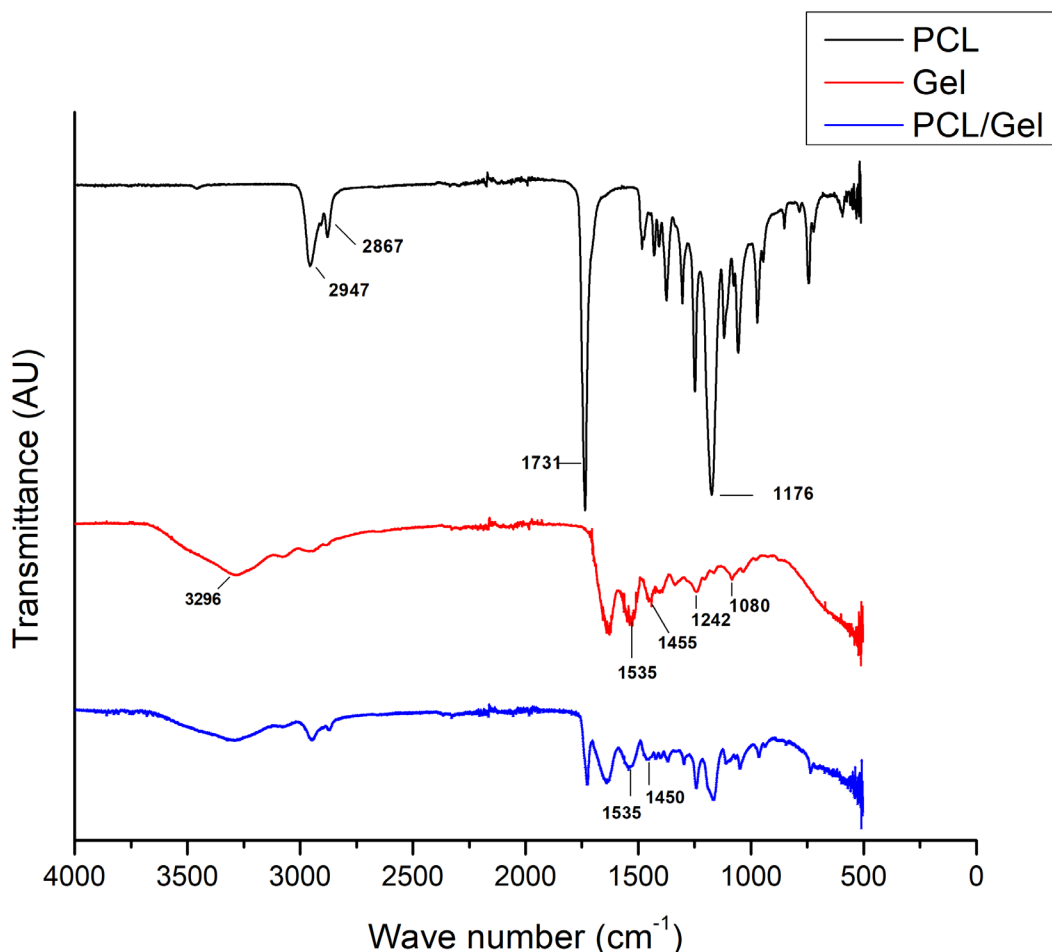
### Fiber Characterization

Figure 1 shows the morphology of the materials studied by light microscopy at different magnifications (A1 and A2: PCL; B1 and B2: gelatin; C1 and C2: PCL/gelatin; scale bar = 200 and 50  $\mu\text{m}$ , respectively). Regarding qualitative characteristics, the PCL/gelatin fibers were thicker and fiber spacing was smaller compared to pure PCL. The gelatin scaffold took on a non–porous form.



**Figure 1** – Light microscopy analysis of the materials studied. A) PCL; B) gelatin; C) PCL/gelatin. Scale bar: 200  $\mu\text{m}$  for A1–C1; 50  $\mu\text{m}$  for A2–C2.

The results of FTIR analysis of PCL, gelatin, and PCL/gelatin fibers are shown in Figure 2. For PCL, we observed a vibrational mode at  $2947\text{ cm}^{-1}$ , characteristic of asymmetric  $\text{CH}_2$  stretching, and at  $2867\text{ cm}^{-1}$  corresponding to symmetric  $\text{CH}_2$  stretching. A  $\text{C}=\text{O}$  stretch can be seen at  $1731\text{ cm}^{-1}$  and symmetric  $\text{C}-\text{O}-\text{O}$  stretching at  $1176\text{ cm}^{-1}$ .<sup>25</sup> In the gelatin scaffold, we observed a peak at  $3296\text{ cm}^{-1}$  characteristic of vibrational  $\text{O}-\text{H}$  and  $\text{N}-\text{H}$  stretch overlap; at  $1535\text{ cm}^{-1}$  we have a  $\text{C}-\text{N}$  stretch and  $\text{N}-\text{H}$  bending (amide II); at  $1455\text{ cm}^{-1}$  we have  $\text{CH}_2$  bending;<sup>26</sup> at  $1242\text{ cm}^{-1}$  we have a  $\text{C}-\text{N}$  stretch and  $\text{N}-\text{H}$  bending (amide III); at  $1080\text{ cm}^{-1}$  we have a  $\text{C}-\text{N}$  stretch and amide III.<sup>27</sup> The same vibrational modes observed for the pure polymers (PCL and gelatin) were found for the PCL/gelatin scaffold, in addition to peaks at  $1450\text{ cm}^{-1}$  and  $1535\text{ cm}^{-1}$  (Figure 2).<sup>20,26</sup>



**Figure 2** – FTIR analysis of PCL, gelatin and PCL/gelatin fibers.

### **In Vitro Direct Contact Toxicity**

Figure 3 shows the phase-contrast microscopy analysis of the direct contact toxicity of Vero cells incubated for 24 h with the different materials (A: negative control; B: positive control; C: PCL; D: gelatin; E: PCL/gelatin; scale bar =  $50\ \mu\text{m}$ ). The images show no contact toxicity.

The quantitative data did not reveal direct contact toxicity and we did not observe cellular changes promoted by the materials.

Depending on the severity of burn injury, which is classified based on the percentage of total body surface area involved, resistant materials are needed because the injury can extend beyond the dermis and can even expose bone components.<sup>1,2</sup> We therefore chose to use PCL, which is bio-resorbable and is classified as a temporary material. In addition to stimulating material-guided extracellular matrix production of the individual, PCL is later degraded, allowing tissue recovery. This material can confer structural stability to mechanical stresses of the system, prevent hydroelectrolyte losses, and minimize the body's susceptibility to infections. We combined PCL with gelatin to improve its features and interaction with human cells. It should be noted that uncrosslinked gelatin usually solubilizes in aqueous medium and is easily eliminated by the body *in vivo*. In addition, it is poorly resistant to mechanical stresses.<sup>13,14,28,29</sup>

The advantages of the rotary jet spinning technique include its low cost, easy construction of the equipment, and high fiber yield.<sup>30</sup>

Many factors were considered to choose the most suitable cell type, including mitotic stability, function, and plasticity. Adequate laboratory practices ranging from the inoculation of the material to medium changes are also necessary since they can affect the results of the experiment. We used Vero cells in this study, which are recommended for the analysis of cytotoxicity and initial cell-cell interactions on biomaterials.<sup>24</sup>

Considering the satisfactory production of fibrous material, our results suggest that PCL/gelatin is a potential scaffold for tissue engineering. Our data were consistent with those reported by Vida et al.<sup>25</sup> who studied PCL, PLLA, and PCL/PLLA fibers, and by Liu et al.<sup>19</sup> in a review on gelatin. Cardoso et al.<sup>31</sup> observed Vero cells spreading on PCL and PCL/chitosan fibers, a morphological pattern similar to that found in our study.

Taken together, the present results suggest that a fibrous scaffold, which structurally resembles extracellular matrix fibers, would represent a more physiological environment for cells. Further research will be conducted to confirm this suggestion.

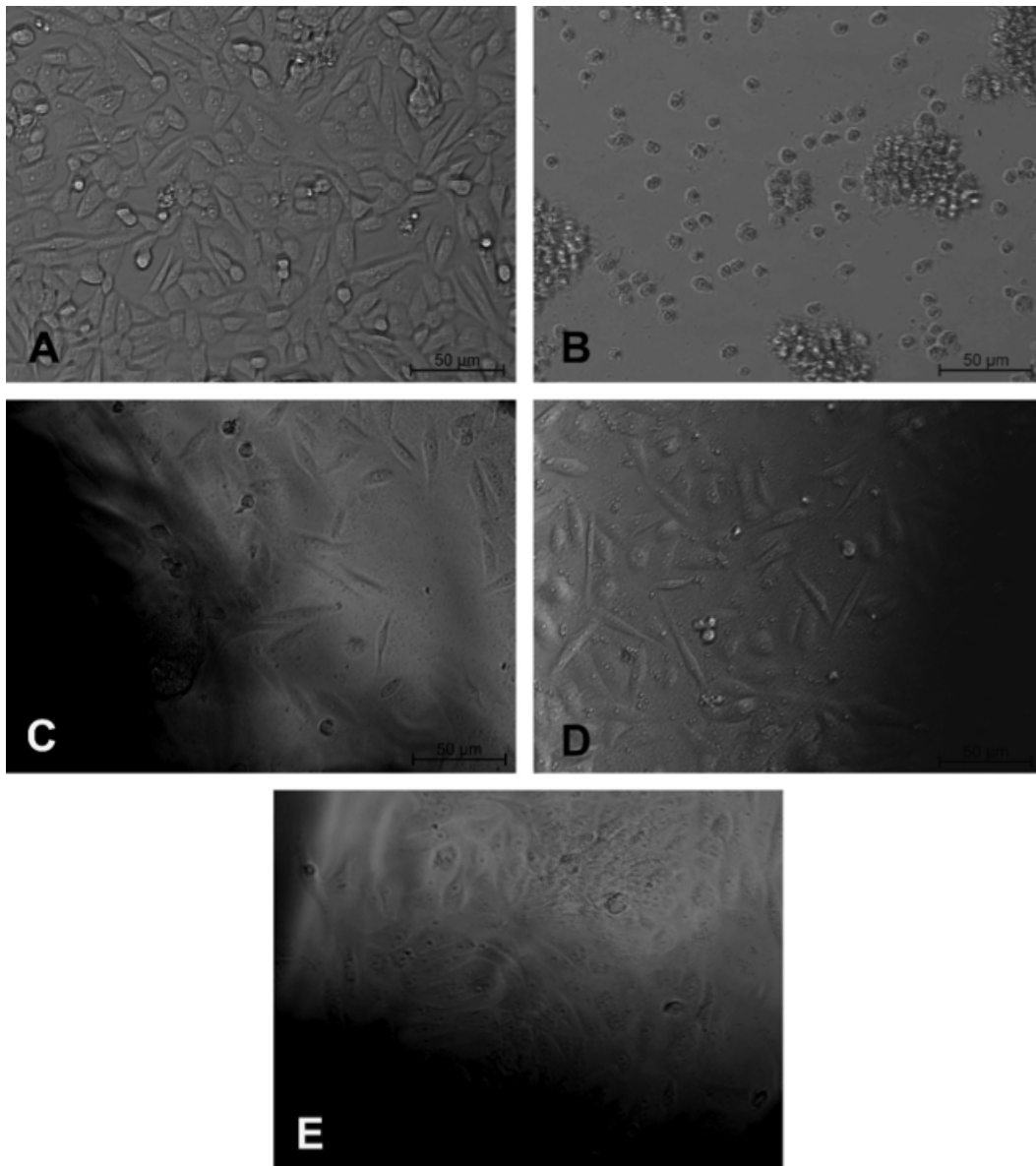


**Figure 3** – Phase-contrast microscopy analysis of the direct contact toxicity of Vero cells in the different experimental groups after 24 h of incubation. A) Negative control; B) positive control; C) PCL; D) gelatin; E) PCL/gelatin. The images show no contact toxicity. Scale bar = 50 µm.

### Conclusion

The rotary jet spinning technique permitted the production of fibers and the coating of gelatin on PCL fibers. The scaffolds were non-toxic and are promising for tissue engineering.

### References

- [1]. Associação Brasileira de Transplantes de Órgãos (ABTO) Registro brasileiro de transplantes (RBT). Ano XXIII N° 3. (2017). Available at: <<http://www.abto.org.br/abtov03/Upload/file/RBT/2017/rbttrim3-leitura.pdf>> Accessed 21 January 2018.
- [2]. World Health Organization (WHO). Burns. World Health Organization: Media centre> Fact sheet > Updated August (2017). Available at: <<http://www.who.int/mediacentre/factsheets/fs365/en/>> Accessed 21 January 2018.
- [3]. Brito TSA. Tratamento de queimados graves com transplante de pele homóloga: revisão sistemática. 2016. 47f. Monografia (Graduação em Medicina) – Faculdade de Medicina da Bahia da Universidade Federal da Bahia. Salvador (Bahia) (2016).
- [4]. Instituto Nacional de Traumatologia e Ortopedia (INTO) Abr. (2017). Available at: <<https://www.into.saude.gov.br/area-de-imprensa/noticias/610-banco-de-pele-comeca-a-funcionar-no-into>> Accessed 21 December 2017.
- [5]. Paggiaro AO, Cathalá BS, Isaac C, Carvalho VF, Oliveira R, Gemperli R. Perfil epidemiológico do doador de pele do Banco de Tecidos do Hospital das Clínicas da Universidade de São Paulo. *Rev Bras Queimaduras* **16**: 23–27 (2017).

- [6]. Park J. Biomaterials Science and Engineering. New York: Plenum Press, pp.193–233 (1984).
- [7]. Liu C, Xia Z, Czernuszka JT. Design and development of three–dimensional scaffolds for tissue engineering. *Chem Eng Res Des* **85**: 1051–1064 (2007).
- [8]. Brasil. Conselho Nacional de Secretários de Saúde. Sistema Único de Saúde: Coleção para entender a gestão do SUS (2011), volume 1. Brasília: CONASS, 2011. p. 291. Available at: <[http://www.conass.org.br/bibliotecav3/pdfs/colecao2011/livro\\_1.pdf](http://www.conass.org.br/bibliotecav3/pdfs/colecao2011/livro_1.pdf)> Accessed 30 January 2018.
- [9]. Tenório M, Mello GA, Viana ALD. Políticas de fomento à ciência, tecnologia e inovação em saúde no Brasil e o lugar da pesquisa clínica. *Ciênc. Saúde Coletiva* **22**: 1441–1454 (2017).
- [10]. Giorno LP, Rodrigues LR, Santos Jr AR. Métodos avançados para tratamento de queimaduras: uma revisão. *Rev Bras Queimaduras* **17**: 1–6 (2018).
- [11]. Giorno LP, Rodrigues LR, Santos Jr AR. Biomedical graft technologies: An overview. *Stem Cell Res Th* **4**: 135–141 (2019).
- [12]. Casarin SA, Malmonge SM, Kobayashi M, Agnelli JAM. Study on in vitro degradation of bioabsorbable polymers poly (hydroxybutyrate–co–valerate) (PHBV) and poly (caprolactone) (PCL). *J Biomater Nanobiotech* **2**: 207–215 (2011).
- [13]. Qin X, Wu D. Effect of different solvents on poly(caprolactone) (PCL) electrospun nonwoven membranes. *J Therm Anal Calorim* **107**: 1007–1013 (2012).
- [14]. Gang Y, Xiao Z, Long H, Ma K, Zhang J, Ren X, Zhang J. Assessment of the characteristics and biocompatibility of gelatin sponge scaffolds prepared by various crosslinking methods. *Sci Rep* **8**: 1616 (2018).
- [15]. Zavaglia CA, Dias CGBT, Avila MAD, Lombello CB, Rodrigues LR, Perea GNR. Dispositivo modular de rotofiação, método de operação e uso. Número do registro: PI1020120084040, Instituição de registro: INPI – Instituto Nacional da Propriedade Industrial, Brasil, 2012.
- [16]. Rigon GR. Matrizes de compósitos de PLDLA com hidroxiapatita obtidas por rotofiação para utilização em engenharia tecidual. 48f. Dissertação (Mestrado). Faculdade de Engenharia Mecânica, Universidade Estadual de Campinas. Campinas, SP: (2013).
- [17]. Brito TAV. Preparação e Caracterização de Nanofibras da Blenda PLLA/PCL obtidas pelos Processos de Eletrofiação e Rotofiação. 90f. Dissertação (Mestrado). Faculdade de Engenharia Mecânica, Universidade Estadual de Campinas, Campinas (2013).
- [18]. Badrossamay MR, McIlwee HA, Goss JA, Parker KK. Nanofiber assembly by rotary jet–spinning. *Nano Lett.* 2010;10(6):2257–61.
- [19]. Liu D, Nikoo M, Boran G, Zhou P, Regenstein JM. Collagen and gelatin. *Annu Rev Food Sci Technol* **6**: 527–57 (2015).
- [20]. Ferraraz DC, Rodrigues LR, Lombello CB. Avaliação da gelatina como arcabouço para células Vero. In: 8º Simpósio de Instrumentação e Imagens Médicas (SIIM) e o 7º Simpósio de Processamento de Sinais (SPS), 2017, São Bernardo do Campo. 8º Simpósio de Instrumentação e Imagens Médicas (SIIM) e o 7º Simpósio de Processamento de Sinais (SPS), 2017.
- [21]. Ryan J, Gerhold AR, Boudreau V, Smith L, Maddox, PS. Introduction to modern methods in light microscopy. In: Markaki Y, Harz H. (eds), *Light Microscopy. Methods in Molecular Biology*, vol 1563, New York: Humana Press, pp. 1–15, 2017 (2017).
- [22]. Castro PAA. Espectroscopia de absorção no infravermelho em pele queimada: avaliação de potenciais biomarcadores para o reparo tecidual. Dissertação (Mestrado em Tecnologia Nuclear – Materiais) Instituto de Pesquisas Energéticas e Nucleares (IPEN) da Universidade de São Paulo (2018).
- [23]. Kirkpatrick CJ. Biological testing of materials and medical devices – a critical view of current and proposed methodologies for biocompatibility testing: cytotoxicity in vitro. *Reg Affairs* **4**: 13–32 (1992).
- [24]. ISO 10993–5 I (E): Biological evaluation of medical devices. Part 5: Tests for cytotoxicity: in vitro methods (2009)
- [25]. Vida TA, Motta AC, Santos Jr. AR, Cardoso GBC, Brito CC, Zavaglia CAC. Fibrous PCL/PLLA scaffolds obtained by rotary jet spinning and electrospinning. *Mater Res* **20**: 910–916 (2017).
- [26]. Zhuang C, Tao F, Cui Y. Anti–degradation gelatin films crosslinked by active ester based on cellulose. *RSC Advances* **5**: 52183–52193 (2015).
- [27]. Movasaghi, Z.; Rehman, S.; Rehman, I.U. Raman spectroscopy of biological tissues. *Appl Spectrosc Rev* **42**: 493–541 (2007).
- [28]. Woodruff MA, Hutmacher DW. The return of a forgotten polymer – Polycaprolactone in the 21st century. *Prog Polym Sci* **35**:1217–1256 (2010)
- [29]. Cipitria A, Skelton A, Dargaville TR, Dalton PD, Hutmacher DW. Design, fabrication and characterization of PCL electrospun scaffolds – a review. *J Mater Chem* **21**: 9419–9453 (2011).

- [30]. Rogalski JJ, Bastiaansen CW, Peijs T. Rotary jet spinning review – a potential high yield future for polymer nanofibers. *Nanocomposites* **3**: 97–121 (2017).
- [31]. Cardoso GB, Machado-Silva AB, Sabino M, Santos Jr AR, Zavaglia CA. Novel hybrid membrane of chitosan/poly (ε-caprolactone) for tissue engineering. *Biomatter* **4**: e29508 (2014).



# Finite element analysis of temporomandibular joint: effect of detachment of the lateral pterygoid muscle

Anita G. Mazzocco<sup>1\*</sup>; André I. Jardini<sup>2</sup>; Elifas I. Nunes<sup>3</sup>; Rubens Maciel Filho<sup>4</sup>

\*Corresponding author: E-mail address: [anitagiaia.mazzocco@gmail.com](mailto:anitagiaia.mazzocco@gmail.com)

**Abstract:** In biomedical engineering field, Temporomandibular joint (TMJ) is considered as a bi-component joint composed by fossa and condyle. It is considered the most active human joint and it performs daily activities such as speaking and chewing. Due to cyclic loading, TMJ disorders impair TMJ function so that it is necessary to replace the natural joint with an alloplastic prosthesis. TMJ orthopedic prosthesis are made of metal alloys and ultra high molecular weight polymers. According to the literature, TMJ replacement surgery is commonly performed worldwide achieving good outcomes. However clinical outcomes point out that TMJ prosthesis present reduced joint kinematics with a limited translational mobility compared to natural joint. In case of unilateral TMJ replacement, this result generates a unilateral hypomobility and a contralateral overload. According to previous studies, this is caused by lateral pterygoid muscle detachment during condylectomy of replacement surgery. To investigate this phenomenon, this study use computational simulation with Ansys software. Finite element analysis is performed with the aim of evaluating effect of unilateral and bilateral pterygoid muscle detachment on mechanical behaviour of a natural human mandible subjected to molar and incisal bite.

**Keywords:** Temporomandibular Joint. Finite Element Analysis. Ansys. Lateral Pterygoid muscle.

## Introduction

Temporomandibular Joint (TMJ) is a bilateral joint that connects mandibular bone to temporal bone. TMJ is a diarthrodial joint composed by condyle, at mandible extremities, and glenoid fossa, at temporal bone. The main TMJ function is to perform chewing and speaking activities so that TMJ diseases impair normal daily activities and have a psychosocial impact on life of individual (1) pain duration, psychological impairment and demographic characteristics. Methods A total of 75 patients with TMD and 75 healthy controls were recruited. The short version of Oral Health Impact Profile (OHIP-14). The study published in 2017 by Lotesto (2) revealed that TMJ replacement surgery is commonly performed internationally with an high success rate. TMJ replacement surgery is the end-stage solution to treat TMJ disorders after previous conservative surgical treatments (3). The two most implanted TMJ replacement devices are TMJ Concepts custom-made system and TMJ Biomet stock system. TMJ Concept is patient-fitted device, manufactured from Computed Tomographic (CT) data of patient, while TMJ Biomet presents different sizes to be adapted to patient anatomy. Both devices are bi-component systems replacing condyle and fossa components. Condyle component is made of metallic alloy (Ti-alloy or CoCr-alloy) and fossa component is composed of metallic mesh and UHMWPE, in case of TMJ Concepts system, or entirely made of UHMWPE for TMJ Biomet system. The history of use of these TMJ replacement devices is around 20 years so that several clinical studies have been carried out. Recently, Zou et al. (4) realized a review study about postoperative outcome of TMJ replacement. According to collected data, stock and custom-made TMJ replacement systems showed similar postoperative results. Clinical outcomes detected a relevant decrease of pain factor and a remarkable mouth opening index increase of about 10 mm, which improves the patients' quality of life. However, analysis of TMJ prosthesis kinematics has shown poor results of mandibular lateral excursion and protrusion (5,6). So that, compared with natural TMJ, TMJ prosthesis perform purely rotational pattern, losing translational motion. In case of

unilateral replacement, this effect induces a unilateral hypomobility and a contralateral hypermobility, so as to overload the natural contralateral TMJ. According to literature, this lack is likely related to the detachment of lateral pterygoid muscle due to condylectomy during replacement surgery (4,6,7).

TMJ natural mobility is generated by condylar movement of condyle against glenoid fossa (8-10). TMJ kinematics is considered complex because the condyle performs translation and rotation movements on the 3 conventional planes. Moreover, direction and amplitude of TMJ mobility are determined by the shape of articular surface, i.e. fossa and eminence, and by the force exerted by masticatory muscles. Therefore, the combined action of masticatory muscles generates the mandibular movements of opening and closing, of protrusion and retrusion and of lateral excursion, which gives rise to the cycles of chewing and speaking. A technique commonly used to evaluate mechanical behavior of TMJ replacement is computational simulation using Computer Aided Modeling (CAM) software (11). This computational simulation is a Finite Element Analysis (FEA) of mandible computational model subjected to masticatory muscles forces. FEA results inform on TMJ mechanical response, quantifying and characterizing stress and strain generated on mandible computational model. In this study FEA is performed in case of a unilateral bite, at incisors, and bilateral, at molars, with the action of lateral pterygoid muscle and without it, with the aim of evaluating the effect of this muscle on stress and strain distribution on mandibular bone.

## Materials and methods

Mandible computational model is created from CT data. At first, CT-data in DICOM format is segmented with Invesalio software (CTI Renato Archer, Brazil), which generates a STL file. Segmentation technique uses threshold to separate bone structures from other biological tissues and produces a surfaces model of mandibular bone. Surfaces model is then transformed into a volumetric model with CAM software, such as Solidworks (Dassault Systèmes, France) and Magics (Materialise, Belgium).

<sup>1</sup>Faculty of Chemical Engineering, Campinas State University, Campinas (SP), Brazil.

<sup>2-4</sup>National Institute of Biofabrication (INCT BIOFABRIS)Campinas State University, Campinas (SP), Brazil.

<sup>3</sup>Medical School, São Paulo State University (Unesp), Botucatu (SP), Brazil.

CAM software corrects superficial imperfection and creates a refined solid model of mandible, generating a STP file. Finally this file is transferred to Ansys Workbench software (Ansys INC, USA) where FEA is performed.

**Finite Element Model (FEM)**

Finite Element Model (FEM) of mandible is created in Ansys Workbench by discretizing solid model into linear tetrahedral elements (14628 nodes and 63112 elements) and modeling with cortical bone property. Cortical bone is considered an isotropic and linear elastic material with an elastic modulus of 13 GPa and a Poisson ratio of 0.3 and characterized by density of 1950 kg/m<sup>3</sup> (12,13). Bites simulated are bilateral Incisor bite (INC) and unilateral Molar bites on Right (RMOL) and Left side (LMOL). In unilateral molar bite working side and balancing side are distinguished. Thus, in RMOL case the working side is on right and the balancing is on left, and vice versa in LMOL case.

Figure 1a shows FEM with external forces and boundary conditions applied. Model geometry is modified on condyle and dental parts to apply boundary conditions. Thus, model is fixed on bite point in three directions, as fixed support, and condyle heads are vertically constrained, so that they can translate on x and y directions (14). To simulate bite loading forces of masticatory muscles are applied to FEM (Table 1).

Data of muscles insertion areas derived from Hylander book (8) and amplitude and direction of forces from Koriath model (15). To evaluate the effect of lateral pterygoid muscle on TMJ mechanical behaviour, FEA of three bite loading is performed with lateral pterygoid and without it, as follows: Case A): lateral pterygoid on both side; Case B): no lateral pterygoid; Case C): lateral pterygoid on left side; Case D): lateral pterygoid on right side.

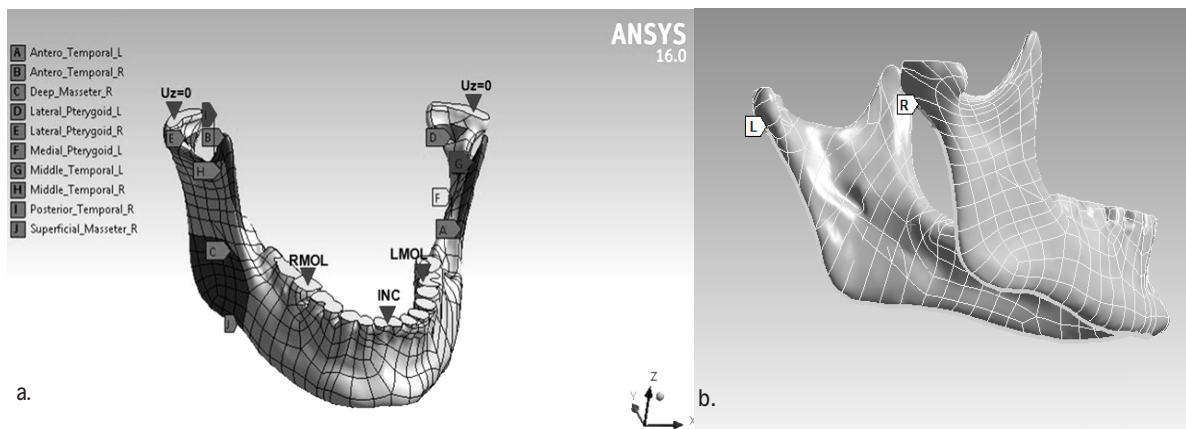


**Figure 1** – a) FEM created in Ansys Workbench with applied muscular forces and boundary conditions. b) Control line to calculate minimum principal strain from right to left condyle.

Muscles	Unilateral Molar Bite						Bilateral Incisor Bite		
	Working side			Balancing side			Fx	Fy	Fz
	Fx	Fy	Fz	Fx	Fy	Fz	Fx	Fy	Fz
Superficial masseter	-28.4	-57.4	121.3	23.6	-47.9	101.1	-15.8	-31.9	67.4
Deep masseter	-32.1	21.0	44.5	26.7	17.5	37.1	-11.6	7.6	16.1
Medial pterygoid	71.4	-54.6	116.1	-51.0	-39.0	83.0	66.3	-50.7	107.8
Anterior temporal	-17.2	-5.1	114.0	13.7	-4.0	90.5	-1.9	-0.6	12.5
Middle temporal	-13.9	31.5	52.8	14.2	32.0	53.6	-1.3	2.9	4.8
Posterior temporal	-9.3	38.1	21.1	6.1	25.2	14.0	-0.6	2.6	1.4
Lateral pterygoid	12.6	-15.2	-3.5	-27.4	-32.9	-7.6	29.9	-36.0	-8.3

**Table 1** – Masticatory muscle forces. Force values reported in Unilateral Molar Bite refer to RMOL bite. In LMOL case, working side force values are applied to left side and vice versa on balancing side, and force vector x changes direction. In Bilateral Incisor Bite the applied muscular forces are the same for both sides, only force vector x is reversed.

**Results**

This study aims to evaluate the influence of lateral pterygoid muscle on TMJ biomechanical behaviour and to predict the effect of lateral pterygoid muscle detachment in the event of TMJ replacement. Thus, distribution of equivalent (Von–Mises) stress on both condyles and pattern of minimum principal elastic strain along a control line on mandibular bone (Fig. 1b) are collected with FEA.

**Equivalent Von–Mises Stress**

As shown in Table 2, the results of stress distribution in case of bilateral INC bite show that maximum occurs near to fixed support on incisors.

	Equivalent (Von-Mises) Stress (MPa)								
	Total	INC		Total	RMOL		Total	LMOL	
		Right	Left		Right	Left		Right	Left
Case A	16.2	12.8	13.0	34.5	13.7	34.5	33.3	32.3	13.1
Case B	15.5	15.0	13.9	35.3	14.9	35.3	35.3	34.3	13.3
Case C	20.0	14.6	13.3	34.5	15.0	34.5	35.2	34.3	12.9
Case D	20.2	13.1	13.6	35.3	13.6	35.3	33.3	32.3	13.5

**Table 2** – Equivalent Von Mises Stress.

In Case A, when all muscle are acting, stress distribution is almost symmetric with a slight overload 1.7% on left side. On contrary, Case B shows a greater overload on right side of 7.3%. When only one lateral pterygoid is working (Case C and D) stress overload is registered on non-operating side, ie on balancing side. This result is reinforced in cases of unilateral bite. As shown in case RMOL and LMOL, the overloaded side is the balancing side. In natural condition (Case A–RMOL, LMOL), stress on balancing side is about 2.5 times working side. The stress overload in Case D–RMOL and in Case C–LMOL is the largest recorded with a difference between working and balancing side of about 2.6 times on balancing side and the minor difference of 2.3 times is collected in cases C–RMOL and D–LMOL. Maximum equivalent Von Mises stress are located on condylar neck and reach values of 35.3 MPa on balancing side for RMOL case and of 34.3 MPa on balancing side for LMOL case.

**Minimum principal elastic strain**

Minimum principal elastic strain informs about distribution of compressive strain along the mandibular bone. Strain distribution in INC case (Fig. 2) shows that on right side Case A and D follow the same pattern as well as Case B and C, and on left side this relation is reversed. In RMOL bite (Fig. 3), strain distribution on working side are nearly the same in all cases, but on balancing side Case A–C and Case B–D follow the same distribution. This trend is not so clear in LMOL simulation result (Fig. 4), because differences between cases are smaller. Minimum strain peaks on balancing side are detected on condyle neck and mandibular angle. On mandibular angle strain peak is  $-1.18 \times 10^{-3}$  mm/mm in case A,C–RMOL and  $-1.24 \times 10^{-3}$  mm/mm in Case B,D–RMOL, and  $-1.04 \times 10^{-3}$  mm/mm in Case A,D–LMOL and  $-1.09 \times 10^{-3}$  mm/mm in Case B,C–LMOL. During INC bite, maximum strain reaches almost half of unilateral molar bite cases.

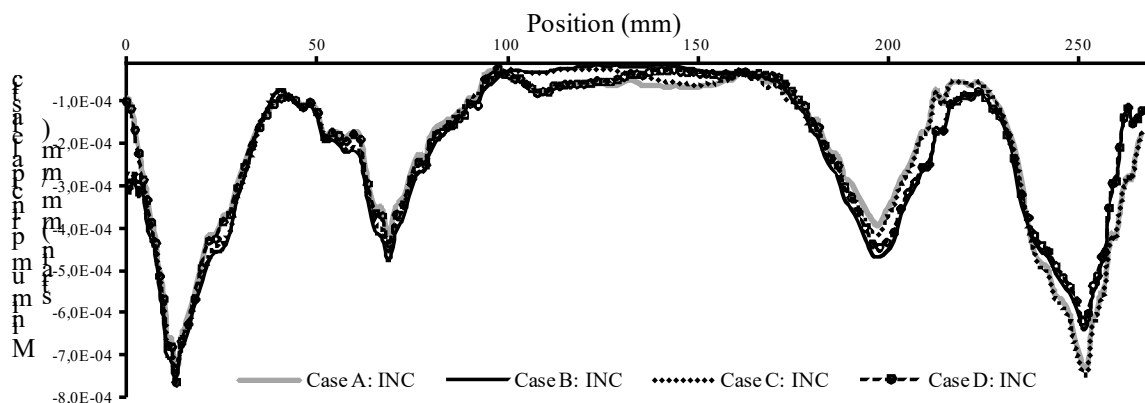


**Figure 2** – Minimum principal elastic strain recorded on control line (from right to left condyle) of INC bite simulation.

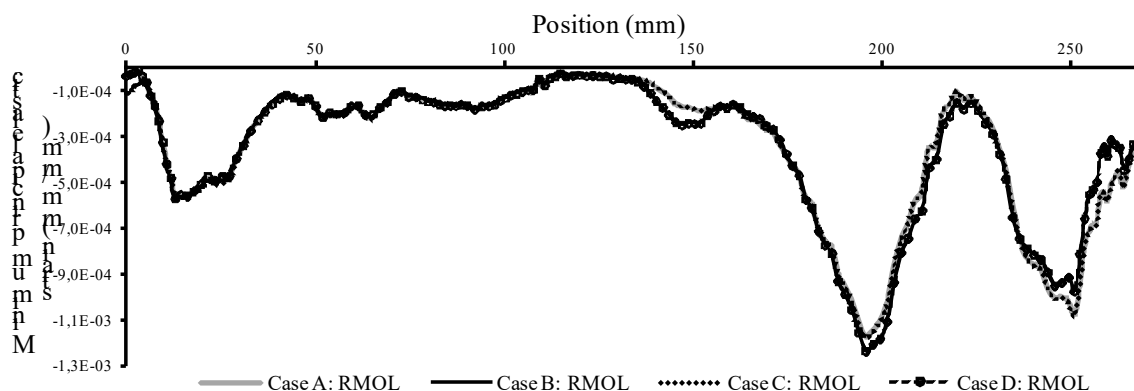


**Figure 3** – Minimum principal elastic strain recorded on control line (from right to left condyle) of RMOL bite simulation.



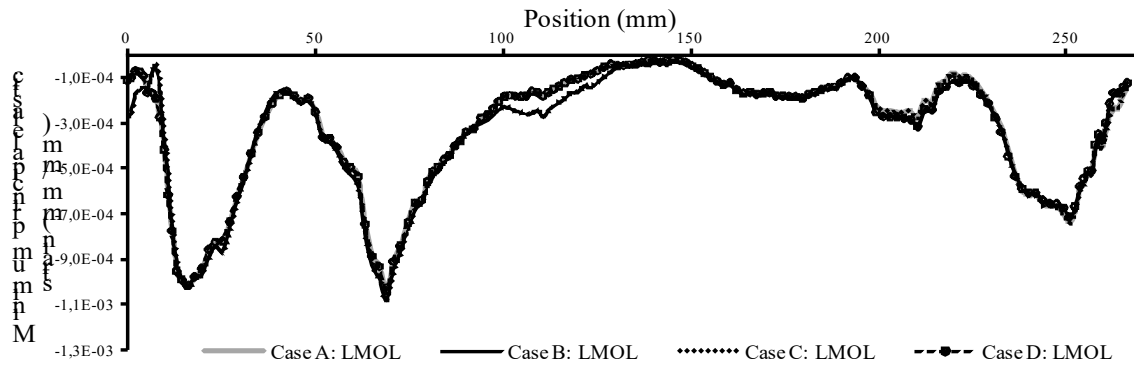


**Figure 4** – Minimum principal elastic strain recorded on control line (from right to left condyle) of LMOL bite simulation.

### Discussion

This FEA analysis performs bilateral (INC) and unilateral loading (RMOL, LMOL) bite and tests the influence of lateral pterygoid muscle on stress and compressive strain distribution. Case A simulates natural condition of bite with all masticatory muscles in action, Case B considers a total lack of lateral pterygoid muscle and Case D and C tests the influence of the left and right muscle, respectively, during the three loading bites. Stress and strain results in case of unilateral bite show that TMJ maximum functional loading occurs during molar biting<sup>(16)</sup>. During unilateral bite, maximum stress on mandibular bone increases on balancing side, or contralateral side of bite. This result coincides with several studies found in the literature<sup>(8,10,17)</sup>. The influence of lateral pterygoid muscle on working side is observed in Case D–RMOL and in Case C–LMOL, when only lateral pterygoid on working side is acting. The similarity between natural case and D–RMOL and C–LMOL informs that muscle on working side could be considered the responsible of contralateral overloading. Hylander study of TMJ mechanics<sup>(17)</sup> and in particular the human mandible, is generally thought to function as a lever during biting. This notion, however, has not gone unchallenged. Various workers have suggested that the mandible does not function as a lever, and they base this proposition on essentially two assertions: (1) found that during molar bite muscles on working side seem to be more active and so to keep TMJ system in static equilibrium reaction forces on balancing side are larger than working side. Moreover, in literature<sup>(8)</sup> balancing side is called also resting side, so that the similarity between stress and strain distribution of Case B and C in RMOL bite, and Case B and D in LMOL bite are explained. Kumazaki's clinical study of patients with unilateral disc displacement<sup>(18)</sup> observed that patients with this TMJ disorder on one side, prefer to use the unhealthy side as the working side, because it generates less pain.

Comparing results of this study with previous ones<sup>(19,20)</sup> which simulates bilateral and unilateral bite on unilateral TMJ replacement system neglecting lateral pterygoid muscle, was noticed that contralateral overloading also occurred. Moreover, the case of TMJ prosthesis implanted on balancing side is observed to be the worst in terms of maximum stress calculated on prosthesis, it reaches almost 2.8 times the value of bilateral bite. The same trend was observed by Van Loon *et al.*<sup>(21)</sup> in a three-dimensional mathematical study.

### Conclusion

In conclusion, FEA analysis performed in this study obtained result of TMJ biomechanical behaviour in agreement with data found in literature. The unilateral bite is the more critical loading because it creates a load difference between the two sides increasing loading on balancing side. This overloading increases if only lateral pterygoid muscle on working side is active. Thus, it could be predicted that TMJ replacement implanted on balancing side suffers a greater loading. However, with data collected in this study it is not possible to clearly analyze the influence of lateral pterygoid on TMJ replacement implanted on working or balancing side. As future perspectives, it should be performed a FEA simulating bilateral and unilateral bite on TMJ with implanted replacement device and the action of lateral pterygoid muscle on working and balancing side.

### Acknowledgments

The authors wish to acknowledge the financial support provided by the Scientific Research Foundation for the State of São Paulo (FAPESP – grant 2015/20630–4) and National Council for Scientific and Technological Development (CNPq – Process 573661/2008–1), and by the Coordenação de Aperfeiçoamento de Pessoal de Nível Superior (CAPES – Finance Code 001).

### References

- [1] Bayat M, Abbasi AJ, Noorbala AA, Mohebbi SZ, Moharrami M, Yekaninejad MS. Oral health-related quality of life in patients with temporomandibular disorders: A case-control study considering psychological aspects. *Int J Dent Hyg* [Internet]. 2018; **16**(1):165–70. Available from: <https://onlinelibrary.wiley.com/doi/abs/10.1111/idh.12266>
- [2] Lotesto A, Miloro M, Mercuri LG, Sukotjo C. Status of alloplastic total temporomandibular joint replacement procedures performed by members of the American Society of Temporomandibular Joint Surgeons. *Int J Oral Maxillofac Surg* [Internet]. 2017; **46**(1):93–6. Available from: <http://www.sciencedirect.com/science/article/pii/S090150271630176X>
- [3] De Meurechy N, Mommaerts MY. Alloplastic temporomandibular joint replacement systems: a systematic review of their history. *Int J Oral Maxillofac Surg*. 2018; **47**(6):743–54.
- [4] Zou L, He D, Ellis E. A Comparison of Clinical Follow-Up of Different Total Temporomandibular Joint Replacement Prostheses: A Systematic Review and Meta-Analysis. *J Oral Maxillofac Surg* [Internet]. 2018; **76**(2):294–303. Available from: <http://www.sciencedirect.com/science/article/>

pii/S027823911731145X

- [5] Linsen SS, Reich RH, Teschke M. Mandibular Kinematics in Patients With Alloplastic Total Temporomandibular Joint Replacement—A Prospective Study. *J Oral Maxillofac Surg* [Internet]. 2012;**70(9)**:2057–64. Available from: <http://www.sciencedirect.com/science/article/pii/S0278239112006738>
- [6] Briceño F, Ayala R, Delgado K, Piñango S. Evaluation of temporomandibular joint total replacement with alloplastic prosthesis: observational study of 27 patients. *Craniomaxillofac Trauma Reconstr* [Internet]. 2013/06/04. 2013;**6(3)**:171–8. Available from: <https://www.ncbi.nlm.nih.gov/pubmed/24436755>
- [7] Leandro LF, Ono HY, Loureiro CC, Marinho K, Guevara HA. A ten-year experience and follow-up of three hundred patients fitted with the Biomet/Lorenz Microfixation TMJ replacement system. *Int J Oral Maxillofac Surg*. 2013/06/19. 2013;**42(8)**:1007–13.
- [8] Hylander W. *Functional Anatomy of the TMJ*. 2006.
- [9] Kerwell S, Alfaro M, Pourzal R, Lundberg HJ, Liao Y, Sukotjo C, et al. Examination of failed retrieved temporomandibular joint (TMJ) implants. *Acta Biomater*. 2016/01/16. 2016;**32**:324–35.
- [10] Lundberg HJ. TMJ Biomechanics. In: *Temporomandibular Joint Total Joint Replacement – TMJ TJR: A Comprehensive Reference for Researchers, Materials Scientists, and Surgeons* [Internet]. Cham: Springer International Publishing; 2016. p. 3–28. Available from: [https://doi.org/10.1007/978-3-319-21389-7\\_1](https://doi.org/10.1007/978-3-319-21389-7_1)
- [11] Rodrigues YL, Mathew MT, Mercuri LG, da Silva JSP, Henriques B, Souza JCM. Biomechanical simulation of temporomandibular joint replacement (TMJR) devices: a scoping review of the finite element method. *Int J Oral Maxillofac Surg*. 2018/03/13. 2018;**47(8)**:1032–42.
- [12] Carter DR, Spengler DM. Mechanical properties and composition of cortical bone. *Clin Orthop Relat Res*. 09/01. 1978;**(135)**:192–217.
- [13] Hsu JT, Huang HL, Tsai MT, Fuh LJ, Tu MG. Effect of screw fixation on temporomandibular joint condylar prosthesis. *J Oral Maxillofac Surg*. 2011/01/11. 2011;**69(5)**:1320–8.
- [14] Ramos A, Completo A, Relvas C, Mesnard M, Simoes JA. Straight, semi-anatomic and anatomic TMJ implants: the influence of condylar geometry and bone fixation screws. *J Craniomaxillofac Surg*. 08/31. 2010;**39(5)**:343–50.
- [15] Koriath TW, Hannam AG. Deformation of the human mandible during simulated tooth clenching. *J Dent Res*. 1994/01/01. 1994;**73(1)**:56–66.
- [16] Mercuri LG, Edibam NR, Giobbie-Hurder A. Fourteen-year follow-up of a patient-fitted total temporomandibular joint reconstruction system. *J Oral Maxillofac Surg*. 05/23. 2007;**65(6)**:1140–8.
- [17] Hylander WL. The human mandible: lever or link? *Am J Phys Anthr*. 09/01. 1975;**43(2)**:227–42.
- [18] Kumazaki Y, Kawakami S, Hirata A, Oki K, Minagi S. Ipsilateral Molar Clenching Induces Less Pain and Discomfort than Contralateral Molar Clenching in Patients with Unilateral Anterior Disc Displacement of the Temporomandibular Joint. *J Oral Facial Pain Headache*. 2016/07/30. 2016;**30(3)**:241–8.
- [19] Mazzocco AG, Jardini AL, Nunes EL, Filho RM. Custom-made temporomandibular joint prosthesis: Computer aided modeling and finite elements analysis. Vol. 74. *Chemical Engineering Transactions*; 2019. p. 1489–94.
- [20] Huang HL, Su KC, Fuh LJ, Chen MY, Wu J, Tsai MT, et al. Biomechanical analysis of a temporomandibular joint condylar prosthesis during various clenching tasks. *J Craniomaxillofac Surg*. 2015/06/02. 2015;**43(7)**:1194–201.
- [21] Van Loon JP, Otten E, Falkenstrom CH, de Bont LG, Verkerke GJ. Loading of a unilateral temporomandibular joint prosthesis: a three-dimensional mathematical study. *J Dent Res*. 11/21. 1998;**77(11)**:1939–47.

# 3DBB

2020 Aug 26-28th

1st INTERNATIONAL DIGITAL CONGRESS ON  
3D BIOFABRICATION AND BIOPRINTING

NUT3D – PPGB – UNIARA

*The 1st International Digital Congress on 3D Biofabrication and Bioprinting (3DBB) is an event organized by the Postgraduate Program in Biotechnology (PPGB) at the University of Araraquara – Uniara, São Paulo State, Brazil, which took place online and free of charge during three days, from the 26th to the 28th of August 2020.*

*Due to the COVID-19 pandemic, 3DBB was performed digitally.*

*The theme of the congress was Biofabrication / 3D Bioprinting, in general, with openness to all topics related to regenerative medicine and tissue engineering in an automated way.*

*The congress was aimed at graduate and undergraduate students, academics (professors and researchers), as well as the industry, both for Brazilian and foreign participants.*

*The event organized by the University of Araraquara (Uniara) with support from the Renato Archer Information Technology Center (CTI), offered participants with lectures by world renowned scientists from the biofabrication of institutions such as CTI Renato Archer, the University of Campinas (Unicamp), Federal University of Rio de Janeiro (UFRJ), Federal University of Rio Grande do Sul (UFRGS), Brazilian Agricultural Research Corporation (Embrapa), as well as Wake Forest Medical School (USA), University of Manchester (UK), University of Maastricht (The Netherlands), University Technological University (Austria), Simón Bolívar University (Venezuela).*

*The 3DBB was divided into 7 thematic areas: Biofabrication and Bioprinting; Devices and Processes; Information Technology; Biomaterials; Cell cultures; Clinical and Industrial Applications; and Other Topics.*

*Two mini-courses were held (“3D Design for Bioprinting” and “InVesalius: Open Software for Reconstruction of Medical Images”, a panel of debates among Brazilian entrepreneurs in the bioprinting area, as well as the submission and presentation of more than 70 works – the abstracts of which are presented in this edition of IJAMB – in addition to a special digital panel with videos dedicated to solution developers with 3D printing to combat the COVID-19 pandemic.*

*I hope you enjoy the abstracts and I hope to review everybody in the next edition of 3DBB!*

**Rodrigo A. Rezende, PhD**  
**Creator and President of 3DBB.**



## Evaluation of prototype printing of national 3D bioprinter for tissue engineering

Vanessa Manchim Favaro\*; Vagner Rogério dos Santos\*; Denys Emilio Campion Nicolosi\*\*

### (Biofabrication and bioprinting (in general))

**Abstract:** The applications of three dimensional (3D) bioprinting in tissue engineering and regenerative medicine have attracted the attention of many researchers. The 3D bioprinting process can be classified in three phases, pre-processing, processing and post-processing. Pre-processing involves the conception or capture of a bioimage and its representation using a CAD software. In the processing phase, the tissue or organ is printed. Finally, in the post-processing phase, it is necessary to check the maturation and monitor the tissue or organ. As the 3D bioprinting area is relatively new, many devices, software and methods are adapted and not are duly created for bioprinting, so the development of these tools are the current challenge of the area. The aim of the work is the standardization of the national 3D bioprinter Cbot prototype printing for tissue engineering. We used the Hadron Max® 3D printer (Wietech) and the Nivea Crème as product. The standardization variables utilized were: Nivea Crème viscosity; needle diameter (4 gauges); head speed; speed that the piston goes down; accuracy of bioprinting. The standardization phases were: creation of a 3D model in STL format using FreeCAD 0.18 software; open in the printer control software (Repetier Host); monitoring of the 3D printing; registration of the final product. The initial results of the prototype show that the viscosity of the Nivea Crème was above 300,000 cp with a torque of 99% and temperature of 24.7°C. In conclusion, the product is too viscous for the viscometer utilized. Therefore, other tests are necessary to continue our protocol.

**Keywords:** Bioprinting; Bioprinter; Viscosity; Prototype; Tissue Engineering.

\* Universidade Federal de São Paulo (Unifesp), Brazil.

\*\* Instituto Dante Pazzanese, São Paulo, Brazil.



## ***In Vitro* study of polymers used for the confection of occlusive devices**

Ana Clara Hecker de Carvalho\*; Laura Hecker de Carvalho\*\*, Dayanne Diniz e Souza Morais\*\*, Renata Coelho Soares\*, Nadja Maria Oliveira\*; Maria Jacinta Arêa Leão Lopes Araújo Arruda\* ; Ana Isabella Arruda Meira Ribeiro\*

### **(Biomaterials)**

**Abstract:** Occlusal devices are widely used in dentistry and can be made from different resins (Polymethylmethacrylate [PMMA] or Polyethylene Teraftalto [PET]) by techniques that include thermopolymerization, additive manufacture by photopolymerization and thermoforming, each one with their advantages and disadvantages. In view of the advances resulting from the use of 3D printing in health, it has been suggested to make occlusal splints using this technology for patients with temporomandibular disorders (TMD) instead of thermoformed or conventional thermopolymerized plates. This study aimed to analyze and compare the characteristics of flat splints obtained from the colorless acrylic base photopolymer used in 3D Printing (Group I), PET thermoformed plates (Group II) and conventional thermopolymerized acrylic resins (Group III).

The characterization of the samples occurred through their thermal stability (TGA), glass transition temperature (Tg), water sorption and UV-visible spectroscopy. The results of thermogravimetry, which are associated with the thermal stability of the samples, indicated that the degradation of the samples it occurred in a different way (a single stage for the thermopolymerized and in two stages for the others) and that the sample from the GIII group was the most stable, starting to lose mass at approximately 360 °C. The order of thermal stability found was GIII> GI> GII. Water absorption data confirmed these results with samples from the GIII group (thermally cured PMMA) absorbing less moisture than the others. These behaviors were attributed to an incomplete polymerization of the samples of the GI group in the photopolymerization process. Despite the fact that the UV-visible absorption tests were performed on solid samples with adaptations in the display of the samples in the sample holder, structural differences were found between PMMA resins polymerized by different methods (GI and GIII) and PET ( GII). The wave lengths at which the transitions were observed decreased in the order: GI> GIII> GII. In general, displacements for longer wave lengths occur when there is more extensive conjugation. Apparently, the conjugation order was GIII> GI> GII. Thus, it can be concluded that Group III, represented by conventional thermopolymerized acrylic resins, proved to be more stable than the other groups in the proposed tests, being more suitable for the manufacture of occlusal devices.

**Keywords:** 3D Printing; Three-Dimensional; Temporomandibular Joint Dysfunction Syndrome; Occlusal Splints; Biocompatible Materials; Dental Materials.

\* Universidade Estadual da Paraíba (UEPB), Campina Grande, PB, Brasil.

\*\* Universidade Federal de Campina Grande (UFCG), Campina Grande, PB, Brasil.



## 3D cultures based on agarose micro-molds for the spheroid formation of medullary thymic epithelial cells

Ana Carolina Monteleone Cassiano\*; Janaína De A. Dernowsek\*\*; Dimitrius L. Pitol\*\*\*; João Paulo M. Issa\*\*\*; Eduardo Antonio Donadi\*; Geraldo Aleixo Passos\*\*\*

### (Cell cultures)

**Abstract:** The thymus is a primary lymphoid organ whose function is the generation of mature T cells and the induction of central tolerance. The thymic microenvironment is formed by thymocytes, medullary epithelial thymic cells (mTECs), and cortical epithelial thymic cells (cTECs). The mTECs are responsible for presenting the peripheral autoantigens (PTAs) to the thymocytes, leading to the elimination of those that recognize them. Therefore, cell aggregation and adhesion correspond to essentially biological processes in the structure and function of the thymus. The Scaffolds are biocompatible biomaterials in which cells adhere and/or interact with each other and with the extracellular matrix to produce living tissues like the original. The structure of the scaffold provides mechanical support for cell development, transport of nutrients, growth factors, and others. To increase the efficiency of T cell development, we establish and characterize a model for the formation of spheroids and promote the aggregation of TECs. We use an agarose mold with non-adherent micro-wells, making the mTEC cells, once seeded in these compartments aggregate with each other. It was possible to show the spheroid formation sequence from mTEC cells, from their deposition in the agarose microwells (0 h) until their complete structuring, after 24 h of culture. To better characterize the model, we constructed a growth and cell viability curve, comparing 2D (monolayer) and 3D (spheroid) cultures. The 2D cell curve grows exponentially faster and the viability in the early stages of both is similar, but 2D maintains the highest viability for longer. To verify the formation of the necrotic centers, we performed the LIVE/DEAD assay and observed that the red cells (dead) increase over time in the center of the spheroids, reaching almost 40% in the time of 48h. The analysis of high-resolution microscopy allowed us to observe with cuts of 1µm the internal structure of these spheroids and how they aggregate over time. We perform scanning electron microscopy to study the external cell surface in detail, which proved to be strongly compacted with a well-defined contour. These results provide us with a better understanding of the 3D mTEC-mTEC interaction. The formation of spheroids with mTEC cells is a useful model to study the aggregation and adhesion between these cells, which is a fundamental role in intra-thymic communication, the process of whose is crucial for the structuring of the thymus in vivo.

**Keywords:** 3D cell culture; Spheroid; Thymus; Mtec; Agarose Micro-Molds.

\* Faculdade de Medicina de Ribeirão Preto FMRP-USP.

\*\* National Institute of Science and Technology in Regenerative Medicine – INCT Regenera.

\*\*\* Faculdade de Odontologia de Ribeirão Preto – FORP/USP.

# 3DBB

2020 Aug 26-28th

1st INTERNATIONAL DIGITAL CONGRESS ON  
3D BIOFABRICATION AND BIOPRINTING

NUT3D – PPGB – UNIARA

## Kinetic study of plla synthesis in conditions applicable to medicine

*Samuel Diógenes Azevedo de Souza\**; *André Luiz Jardini\**; *Maria Ingrid Rocha Barbosa Schiavon\**; *Rubens Maciel Filho\**; *Viktor Oswaldo Cárdenas Concha\**; *Maria Regina Wolf Maciel\**

### **(Biomaterials)**

**Abstract:** Poly (L-lactic acid) (PLLA) is a synthetic and hydrolytically unstable aliphatic polyester, a fact that is of increasing interest in medical applications, from sutures to vascular and urological stents, and devices for orthopedic applications (such as pins), for degrading and eroding over time. The conventional routes for the polymerization of PLLA involve direct polycondensation (generating, at first, a low molar mass polymer) and the opening of the cyclic L-lactide ring (forming a polymer with the greater molar mass concerning polycondensation), however, L-lactide is a product of high added value, which is an obstacle in the process of obtaining. Since the molar mass can directly influence the degradation period and the future erosion of PLLA, gel permeation chromatography (GPC) becomes an effective ally in the characterization of the molar mass of the polymer, either by the numerical molar mass ( $M_n$ ) (for short chains), the average weight molar mass ( $M_w$ ) (for medium chains), or the molecular molar mass ( $M_z$ ) (applied to long chains). Thus, once we obtain the molar mass of samples collected during the reaction of the polymer synthesis, we can analyze conditions related to the kinetics of its formation, therefore, in this work, we evaluated the reaction kinetics in obtaining the PLLA. During the polymerization process, four sample collections were carried out over 18 hours and later characterized by gel permeation chromatography, giving the average weight molar mass necessary to present the consumption of L-lactic acid over time, and linear regression with the best fit by the integral method.

**Keywords:** Poly Lactic Acid; Degradable Polymer; Biomaterial; Integral Method; Gel Permeation Chromatography.

\* INCT-BIOFABRIS / Faculdade de Engenharia Química – Unicamp, Campinas, SP, Brasil.

# 3DBB

2020 Aug 26-28th

1st INTERNATIONAL DIGITAL CONGRESS ON  
3D BIOFABRICATION AND BIOPRINTING

NUT3D – PPGB – UNIARA

## Surgical optimization using 3D print model for orbital fracture repair: a case report

José Cleveilton dos Santos\*; Luís Fernando O. Gorla\*; Luiz Henrique S. Torres\*; Mário Francisco. R. Gabrielli\*\*; Valfrido A. Pereira-Filho\*\*;  
Marisa Aparecida C. Gabrielli\*\*

### (Applications)

**Abstract:** The orbital floor fractures are among the most common injuries in oral and maxillofacial traumatology, present in approximately 40% of facial fractures. The management of these fractures is difficult and inadequate reconstruction may lead to severe complications such as diplopia, enophthalmos, decrease of visual acuity, and limitation of eye movement. Three-dimensional printing (3DP) technologies can help surgeons in many ways and have become more accessible in the past few years. The aim of this paper is to present a case of orbital fracture where surgical optimization was obtained using a 3DP model. M A O, a female patient, 52y, victim of physical abuse was examined at Hospital Santa Casa de Araraquara by the Oral and Maxillofacial Surgery team from the São Paulo State University (UNESP). She was diagnosed as presenting a severe left orbital floor fracture extending to the medial orbital wall. Clinically, she presented soft tissue injury at the left supraorbital region, restriction of the left eye movement in infra and supraversion, subconjunctival hemorrhage, left periorbital swelling and binocular diplopia in the upper gaze. We used the computerized tomography DICOM file in the open source software InVesalius to create a Standard Triangle Language (STL) file, then printed the STL in a Digital Light Processing (DLP) printer MoonRay®. Two 3DP models were made: a) one model of the fractured orbit to evaluate the extension of the fracture and to cut the titanium mesh in the correct size and b) another model, of the mirrored right orbit, to pre-bend the titanium mesh before the surgical procedure. Surgical access was obtained via subciliary approach, the mesh was positioned and fixed with two screws in the inferior orbital rim and correct eye position was recovered. Extrinsic eye movement restriction and diplopia resolved. The patient has been symptom free since then. In conclusion using the 3DP model improved the accuracy of fit of the reconstructive titanium mesh, decreased operative time and anesthesia duration, as it has been described in the literature.

**Keywords:** Printing; Three-dimensional; Orbital fractures; Diplopia.

\* DDS, PhD Student, Department of Diagnostic and Surgery, São Paulo State University (Unesp), School of Dentistry, Araraquara.

\*\* DDS, MSc, PhD, Assistant Professor of the Department of Diagnostic and Surgery, São Paulo State University (Unesp), School of Dentistry, Araraquara.





## Production of PLLA / curcumin bioactive membranes for wound healing

Karla barbosa\*; Isabella C. P. Rodrigues\*; Mateus F. Oliveira\*; Letícia Tamborlin\*\*\*; Augusto D. Luchessi\*; Éder S. N. Lopes\*\*; Laís Pellizzer Gabriel\*

### (Biomaterials)

**Abstract:** A wound can be described as a rupture in the integrity of the skin and its healing occurs through the activation of inter and intracellular pathways, a major problem of a fissure in the continuity of the skin is the risk of bacterial infection and its complications. Tissue engineering (ET) is a multidisciplinary research field that studies the production of biological substitutes that mimic the extracellular matrix of tissues for cell adhesion and proliferation. It can assist in restoring the integrity of damaged tissues. In the present study, the processing and evaluation of polymeric membranes based on poly (lactic acid) (PLLA) and curcumin was carried out, with potential for applications in wound healing and fighting infection processes. PLLA is a biocompatible polymer and with significant importance for the pharmaceutical and biomedical areas. Curcumin is a natural compound and has antibacterial and antioxidant potential, in addition to therapeutic action on inflammations and diseases such as diabetes and cancer. Rotary jet spinning is a prominent technique in the processing of polymeric membranes due to the high rate of fiber production, thus allowing the production of these membranes on a larger scale and at a lower cost. The membranes PLLA and PLLA / curcumin were processed in the concentrations of PLLA at 8% (m / v) and curcumin at 4% (m / m), with a rotation speed of 18,000 rpm and at room temperature and were also characterized. The membrane morphology was verified using Scanning Electron Microscopy (SEM) and fibers with diameters smaller than 10  $\mu\text{m}$  were identified. Using the Fourier Transform Infrared Spectroscopy (FTIR) technique, the chemical bands characteristic of the polymer and curcumin, and the absence of the organic solvent, were identified. The performance of the thermogravimetric analysis allowed the thermal characterization, which determined the thermal stability of the membranes up to 280 °C. Hydrophobic characteristics were identified in the membranes with the contact angle technique. Cell viability was assessed using the MTT technique, which confirmed the biocompatibility of PLLA and PLLA / Curcumin membranes. The antimicrobial activity test confirmed the antimicrobial action of curcumin. With the drug release test, he verified the dispersion of curcumin in its application medium. Finally, it was found that the processed membranes are bioactive and suitable for applications in wound healing.

**Keywords:** Curcumin; Rotary Jet Spinning; PLLA; Wound Healing; Membranes.

\* Faculdade de Ciências Aplicadas, Universidade Estadual de Campinas (Unicamp).

\*\* Faculdade de Engenharia Mecânica, Universidade Estadual de Campinas (Unicamp).

\*\*\* Instituto de Biociências, Universidade Estadual Paulista (Unesp).



## Manufacture of high quality 3D scaffolds by extrusion based bioprinting technique

Verónica Passamai\*; Sergio Katz\*; Vera Alvarez\*\*; Guillermo R. Castro\*

### **Biofabrication and bioprinting (in general)**

**Abstract:** In recent years, extrusion based bio-printing (EBB) techniques have been used to produce scaffolds with controlled micro-architecture and geometry for biomedical applications, including research in drug delivery, tissue engineering and wound healing, among others. EBB is one of the most studied methods of additive manufacturing due to several advantages, such as precise deposition, cost-effectiveness, simplicity, process speed, materials availability, homogeneous distribution of bioactive components, versatility, and predictability. However, it requires specific knowledge to adapt biomaterials and equipment to the application needs. In the present work, general characteristics of EBB and biopolymer inks requirements are reviewed, printability concepts are summarized so as an approach to its analysis. An experimental application was carried out using a 3D bio-printer fabricated on NBM-CINDEFI Laboratory (La Plata, Buenos Aires, Argentina). Three pectin-based inks, two of them with celluloses addition, were formulated to obtain well defined 3D scaffolds. To evaluate the ink behavior, extrudability, printability and thermogravimetric analyses were carried out. As a result, high quality 3D printed scaffolds were obtained with different geometries. Cellulose addition, as an excipient, modifies and enhances mechanical and physical properties of biopolymer inks. Rheological measurements, and biophysical analysis of the biopolymer inks will allow to standardize the synthesis procedures, combined also with cytotoxicity assays to ensure its 3D bioprinting applications for different biomedical applications.

**Keywords:** Scaffolds; Biopolymer Inks; Printability; Extrudability; Bioprinting.

\* Laboratorio de Nanobiomateriales (NBM), CINDEFI-CONICET-Universidad Nac. de La Plata, Argentina.

\*\* Grupo de Materiales Compuestos (CoMP), INTEMA-CONICET- Universidad Nac. de Mar del Plata, Argentina.



## Perspective on current scenario of bioinks for osteochondral repair based on 3D bioprinting

Juliana Daguano\*; Ana Pereira\*\*; Fabiana Cunha Giora\*\*; Karina Santos\*; Andrea Rodas\*; Jorge Vicente Lopes da Silva\*\*

### **Biofabrication and bioprinting (in general)**

**Abstract:** Bioprinting has become a promising area for application in transplants and recovery of injuries, mainly for the skin and osteochondral tissue, because it allows the growth of human tissue independently. Characterized by the destruction of articular cartilage, the osteochondral lesion treatment has not yet been effectively addressed. Existing repair techniques often do not offer complete healing to the patient and are, therefore, inefficient, depending on the stage of the disease. **Methodology:** This study aims to present an overview and the state of the art of bioinks, relating information on 3D bioprinting by extrusion and repair of osteochondral tissue, as an alternative treatment. Academic research and the market for bioink and bioprinters were compared to prove the feasibility. Initially, scrutiny was carried out, bringing together approximately 230 publications and 16 companies, using search tools such as Scopus, Google Patents, and LinkedIn. The search results in data representative of the set of most favorable requirements for bioprinting of osteochondral tissue, such as rheology of the material, biochemistry and mechanics of the artificial extracellular matrix, and cell viability and differentiation. **Results:** From that, 23 articles were selected, among which alginate stood out as the main component of bioink (52%), and could be associated with hydrogels, such as gellan gum, GelMa (methacrylate gelatin), and cellulose. As a mineral component, Laponite appeared in most research (13%). Furthermore, the Pluronic F127 polymer has been one of the leading choices as a sacrificial component of bioinks (12.5%), and therefore its typical rheological behavior highlights its use during the printing process. As for 18 patents filed in the past six years, the USA owns 39% of intellectual property, following by China with 28%. The patents show that the innovations are concentrated in the formulation of bioinks, and new methods of 3D bioprinting. The USA also leads the bioprinting market with 37.5% of the registered companies at LinkedIn, followed by Brazil and Canada, both with 12.5% focused on this segment. CEIIIInk (USA) is the most outstanding company in the sector, with a portfolio based on materials presented by the academic area. **Conclusion:** Thus, it appears that the market and the academy are in line, focusing on the improvement of bioink formulations and 3D bioprinting methods, to create products that can biomimicry the tissue microenvironment.

**Keywords:** 3D bioprinting; Bioink; Osteochondral Tissue; Market; Bioprinting Review.

\* Universidade Federal do ABC – UFABC, Brasil

\*\*\* DITPS – Divisão de Tecnologias para Produção e Saúde – Centro de Tecnologia da Informação Renato Archer, Campinas, SP, Brasil



## Decellularized spinal cord matrix bioink production for 3D bioprinting

Marcelo Garrido dos Santos\*; João Pedro Prestes\*\*; Cristian Teixeira\*\*\*; Luiz Sommer\*\*\*; Fernanda Stapenhorst França\*\*\*; Laura–Elena Sperling\*\*\*\*; Patricia Helena Lucas Pranke\*\*\*\*

### **Biofabrication and bioprinting (in general)**

**Abstract:** Spinal cord injury (SCI) is a highly debilitating neurological syndrome that compromises the lives of patients, causing permanent loss of motor functions and sensibility, and for which there is no efficient therapy. Bioprinting is an innovative approach in regenerative medicine and the use of a bioink containing extracellular components may lead to improved functional recovery. The aim of this study has been to produce a bioink using lyophilized rat Decellularized Spinal Cord Tissue (DSCT). Methodology: The spinal cord of the animals was collected, cut in 1 cm length segments and submitted to a 9 hours decellularization process using consecutive immersions in 1% sodium dodecyl sulfate (SDS), 1% Triton X-100 and PBS. Following this, the genomic DNA content was measured. Histological sections of the samples were stained with DAPI or with hematoxylin and eosin and the collagen content was quantified by spectrophotometry. In order to assess the cytocompatibility of the DSCT, PC12 cells were cultivated on top of the decellularized tissue and cytotoxicity was analyzed using MTT assay. The DSCT was lyophilized to produce the bioink and 1.5% DSCT was mixed with 4% alginate, 3% gelatin and PC12 cells. The bioink was bioprinted in a disc with a density of  $1.5 \times 10^6$  cells per mL. The cytocompatibility of the construct was analyzed by MTT and Live/Dead assay. Results: The DNA quantification indicated that the DSCT presented 224.41 ng DNA/mg of tissue, while the control spinal cord tissue presented 12737.13 ng of DNA/mg of tissue and the histological analysis revealed only a few cells at the end of the process. The DSCT presented a decrease of 17.65% collagen content when compared to the native spinal cord. The MTT assay indicated that the DSCT did not alter the cell viability. The bioink was bioprinted and it produced a 3D structure representing a disc of 0.3 mm height and 10 mm diameter with a total volume of 50  $\mu$ L. The MTT test indicated that the bioprinted material presented a tendency towards higher cell viability and adherence in comparison with the control after 3 and 7 days. The DAPI staining indicated cell presence in multiple layers of the bioprinted material. Conclusion: It was possible to produce a bioink with the combination of alginate, gelatin, the PC12 cells and DSCT, which were able to maintain cell viability and support cell growth on a 3D structure. Therefore, this bioink may be an easily-available cell carrier for SCI treatment.

**Keywords:** Spinal cord injury; Decellularization; 3D bioprinting; Bioink.

\* Universidade Federal de Ciências da Saúde Porto Alegre (UFCSPA).

\*\* Universidade Vale do Rio dos Sinos (Unisinos).

\*\*\* Universidade Federal do Rio Grande do Sul (UFRGS).

\*\*\*\* Instituto de Pesquisa com Células-Tronco (IPCT).

# 3DBB

2020 Aug 26-28th

1st INTERNATIONAL DIGITAL CONGRESS ON  
3D BIOFABRICATION AND BIOPRINTING

NUT3D – PPGB – UNIARA

## Poly ( $\epsilon$ -caprolactone): development of a rotary jet spinning system and synthesis of porous membranes

Elcio Malcher Dias Junior\*; Tainara Lima\*; Debora Silva\*; Viktor Cardenas\*\*; Luis Adriano Nascimento\*; Carlos Emmerson Costa\*; Marcele Fonseca Passos\*

### (Biomaterials)

**Abstract:** Biodegradable polymers have attracted the attention of many researchers in recent years. Among the most well-known biodegradable polymeric materials, poly ( $\epsilon$ -caprolactone) (PCL) stands out due to its excellent biodegradability and mechanical properties, which amplify its applications in tissue engineering. Then, the objective of this work was to develop an innovative rotary jet spinning system to obtain porous PCL membranes, with potential applications as wound dressings. The system of rotary jet spinning was developed according to three components: collector, responsible for capturing the fibers formed; reservoir, the container used for the deposition of the polymeric solution and its subsequent ejection through the holes/capillaries of the wall, according to the centrifugal force and engine, with different rotation speeds. The PCL solutions were prepared at different concentrations: 15%, 17.5% and 20% w/v, using dichloromethane as a solvent. The solutions were obtained at atmospheric pressure and speeds between 3.200 and 20.000 rpm to observe the fibers' organization and plasticity. Then, the samples were dried at 45 ° C for 48 hours to remove the residual solvent. The surface morphology was analyzed using the scanning electron microscopy (SEM) technique. The results demonstrated the technical viability of the rotary jet spinning system, producing elastic and organized fibers. The concentration of 15% w/v with a rotation speed of 3.200 rpm enabled more visually elastic fibers, with an average diameter of 7.71  $\mu\text{m}$ . At this same concentration, at speeds close to 20.000 rpm, fibers were obtained with diameters between 8.33  $\mu\text{m}$  and 22.55  $\mu\text{m}$ . Lower speeds, close to 5.000 rpm, formed fibers with a greater thickness, between 7.22  $\mu\text{m}$  and 32.95  $\mu\text{m}$ , in the concentration of 17.5% w/v. The concentration of 20% w/v led to fibers' formation with diameters between 4.02  $\mu\text{m}$  and 11.54  $\mu\text{m}$ . It was also observed the homogeneous presence of micro and macropores in all samples, demonstrating the rotary jet spinning system's technical viability for obtaining porous membranes with potential use in skin dressings.

**Keywords:** Poly ( $\epsilon$ -caprolactone); Biodegradable polymers; Rotary jet spinning.

\* Universidade Federal do Pará (UFPA).

\*\* Universidade Federal de São Paulo (Unifesp).



## Three-dimensional technologies applied to the development of a customized upper limb prosthesis

Carlos Alberto M. Dos Santos Filho\*, Ketinly Yasmyne N. Martins\*\*, Rodolfo R. Castelo Branco\*\*, Isabella D. Gallardo\*\*, Anna Kellssya L. Filgueira\*\*, Lucas Vinícius A. Sales\*\*

### *(Devices and processes)*

**Abstract:** The process of acquiring three-dimensional images from 3D scanning associated with the manipulation of software that enables the development of devices compatible with reality, in the current scenario of using the Additive Manufacturing – AM, enabling considerable advances in the production of medical devices. In this perspective, with regard to customization and production efficiency, three-dimensional technologies have created a new scenario for the development of prostheses. This study aims to describe the use of three-dimensional technologies in the development of a customized upper limb prosthesis. **Methodology** This is a study developed at the Laboratory of Three-dimensional Technologies, allocated at the Center for Strategic Technologies in Health at the State University of Paraíba, with appreciation by the research ethics committee under number CAAEE 10308819.5.0000.5187. The research included a male patient, 34 years old, with transradial amputation of the left upper limb. A 3D scanner was used to capture three-dimensional images of the patient's stump, which were manipulated in the Autodesk Meshmixer software, generating a geometric mesh .STL. After that, the prosthesis was designed, including the socket, forearm and hand, together with the assembly mechanism and dynamic movement simulations of digital operation, in the Autodesk Inventor software. Finally, the prosthesis was made using the AM in the FDM process, using PLA material. **Results:** The entire production process was carried out in 200 hours, minimizing several stages of the traditional manufacturing process, requiring only a single contact with the patient in the analysis of the digital dimensioning of the stump. The prototyped real model did not show dimensional variations when compared to the digitized model, resulting in an acceptable anatomical geometric conformity. **Conclusions:** The association of three-dimensional scanning with the management of modeling software and additive manufacturing proved to be effective for the production of customized upper limb prosthesis, highlighting the optimization in the production process, when compared to the traditional process, both for the development team and for the individual. Presenting itself as a light and low cost customized device, thus enabling a possible change of design and adaptation of the patient to new fabrications of prosthesis interfaces.

**Keywords:** Imaging Three-Dimensional; Manufactures Materials; Printing, Three-dimensional; Prosthesis; Three-Dimensional Technologies.

\* Universidade Federal de Campina Grande – UFCG, Campina Grande, PB, Brasil.

\*\* NUTES – Universidade Estadual da Paraíba – UEPB, Campina Grande, PB, Brasil.



## Semi-interpenetrating network of PHEMA-PCL, interspersed with anti-inflammatory properties, for use as a skin wound dressing

Tainara de Paula de Lima Lima\*; Yan Gabriel Lima\*; Elcio Malcher Dias Junior\*; Débora Silva\*; Luís Adriano Nascimento\*; Carlos Emmerson Costa\*; Carmen Gilda Dias\*; Viktor Conchas\*\*; Marcelle Fonseca Passos\*

### (Biomaterials)

**Abstract:** The human body has “tools” that support its functioning and maintain the body’s homeostasis, and one of them is the skin. It acts as the biological system’s primary barrier, preventing external bodies from threatening its integrity. However, this “heroic” act of the skin causes damage to itself (skin wounds, for example), which requires extra care, through the wound dressing’s performance. Therefore, biomaterials such as polycaprolactone (PCL) and poly (2-hydroxy-ethyl methacrylate) (PHEMA), can be used to develop dressings with optimized properties, aiming the efficiency in the healing process. Thus, this work’s objective was to synthesize and characterize semi-interpenetrating networks (semi-IPNs) of PHEMA-PCL, interspersed with bioactive compounds, derived from vegetable oils from the Amazon region, for use as a skin wound dressing. The polymeric synthesis was realized through the rotary jet spinning process to obtain the PCL’s membranes, followed by the interpenetration process between the hydrogel (PHEMA) and the synthesized PCL’s membranes. The bioactive compound, with the anti-inflammatory property, was intercalated, in concentrations of 0.64% w / w and 1.27% w / w, in relation to the PCL mass (20 g). The obtained materials were characterized by the contact angle test, fluid absorption assays, and scanning electron microscopy (SEM). The contact angle assays emphasized that the material had hydrophilic characteristics but also a variation of PHEMA on the samples’ surface. The fluid absorption test, in saline sulfate buffer solution (PBS), showed that the semi-IPN network has swelled, with values ranging from 90.9 to 160.5%. The morphological analyzes showed dispersed fibers, with diameters between 6 to 31.31  $\mu\text{m}$ , and certain porosity, which makes it an essential characteristic for cell proliferation. Therefore, analyzing the results can conclude the potential that the material presents as a skin dressing. Even though, it is still necessary to optimize the PHEMA distribution on the surface of the PCL membranes and evaluate in vivo and in vitro features, to verify the anti-inflammatory action of the bioactive compound.

**Keywords:** Biomaterials; Wound dressing; Semi-IPN’s network; PHEMA-PCL; Polymers.

\* Universidade Federal do Pará – UFPA, Belém, PA, Brasil.

\*\* Universidade Federal de São Paulo – Unifesp, Diadema, SP, Brasil.



## Development of bioactive composites scaffolds for bone tissue–engineering

Nida Iqbal\* ; Saman Iqbal\*\*

**(Biomaterials)**

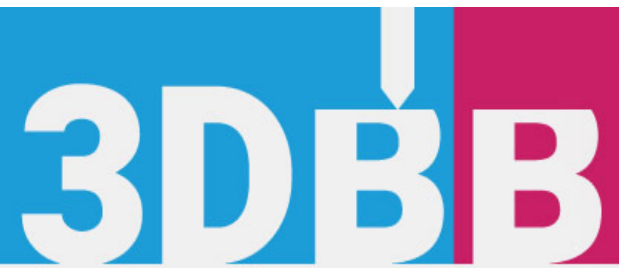
**Abstract:** Tissue engineering is an interdisciplinary field that involves the combination of biomaterials, cells, and engineering methods for the purpose of tissue regeneration. The aim of this field is to lead the organs or tissues to regenerate with the help of biocompatible and biodegradable scaffold that acts as a template for the cells to grow. Scaffolds are the main component in tissue engineering as they are used to provide support and ideal microenvironment for the incorporation of the cells and bioactive molecules in order to repair and remodel damaged tissues or organs. To help the organs regenerate better, the scaffold needs to imitate the natural extracellular matrix (ECM) behavior of that particular organs which are fibrous structure at nanoscale. The typical properties of scaffolds are porous, biocompatible and biodegradable. There are several methods to fabricate three-dimensional (3D) scaffolds which are electrospinning, phase separation, freeze dry, self-assembly, 3-D printing etc. Among all these techniques, electrospinning has attracted more attention due to its simple equipment setup, low cost, able to process various kind of polymers and synthesize long aligned continuous nanofibers. The aim of this study was to fabricate and characterize Poly (lactic acid) (PLA)–Zeolite composite nanofibers using electrospinning technique. Electrospinning was performed with an applied voltage of 12kV at 1 mL/h for 5 hours. Prepared composite scaffolds were chemically characterized using Fourier Transform Infrared spectroscopy (FTIR) and Energy Dispersive X-ray (EDX). The results indicated that the addition of zeolite resulted in the presence of silica and aluminum along with carbon and oxygen elements in the EDX spectrum and the appearance of absorption peak in the spectra of PLA–Zeolite composite fibers. The surface morphology was analyzed with Scanning Electron Microscopy (SEM) and Water Contact Angle (WCA). The results showed that relative smooth and round nanofibers were obtained and the hydrophobicity of the nanofibers decrease with the increasing of zeolite percentage. Bioactivity of the composite nanofibers was evaluated using simulated body fluid (SBF) solution and it can be confirmed through the formation of apatite precipitation on the surface of the nanofibers.

**Keywords:** Biomaterials; Bioactivity; Tissue Engineering; Scaffold; Electrospinning.

\* Bio–Medical Engineering Centre University of Engineering and Technology (UET), Lahore, New Campus, University of Engineering and Technology (UET), Lahore New Campus.

\*\* Department of Physics, University of Engineering and Technology, Lahore, Pakistan.





2020 Aug 26-28th

1st INTERNATIONAL DIGITAL CONGRESS ON  
3D BIOFABRICATION AND BIOPRINTING

NUT3D – PPGB – UNIARA

## Rheological behavior of carboxymethylcellulose (CMC) and laponite nanocomposite inks

Ingri Julieth Mancilla Corzo\*; Jéssica Heline Fonseca\*; Marcos Akira D'Ávila\*

### **Biofabrication and bioprinting (in general)**

**Abstract:** Hydrogels are materials with the ability to absorb large amounts of water, resulting in systems with unique characteristics and are widely applied in the biomedical area [1]. Among these applications, the fabrication of scaffolds by Additive Manufacturing (AM) for tissue engineering is appealing and challenging, mainly due to their rheological behavior [2]. Then, rheological properties and colloidal interactions are fundamental to define printability since they have strong influence in the shape fidelity and porous formation of printed structures. A new system of colloidal ink composed of Carboxymethylcellulose (CMC) and nanosilicate of Laponite was developed in this work. Different concentrations of CMC, Laponite, and CMC-Laponite (CMC-Lap) mixtures were studied. Rheological characterizations were carried out in a Modular Compact Rheometer (Anton Paar MCR-102, Austria) at 25 °C, with a cone-plate geometry (50 mm diameter and 1 mm the gap). Shear thinning was observed for all CMC solutions (0.25 to 4 wt.%) and the Cross viscosity model was used to fit the experimental data. On CMC-Lap mixtures, physical gels were observed even in low CMC and Laponite concentrations. The gel obtained was transparent and uniform. The addition of Laponite reinforced the polymer network by increasing its viscosity, storage ( $G'$ ) and loss ( $G''$ ) moduli of the inks. The Ostwald-de Waele model described well the viscosity behavior of the mixtures. CMC-Lap gels showed shear-thinning behavior and self-recovery characteristics due to their rapid rearrangement of the internal phase after being subjected to shear stress. Moreover, time sweep tests revealed that CMC-Lap solutions suffer aging due to increases in storage modulus. Electrostatic interactions and hydrogen bonds are the two possible types of interactions that occur between the CMC chains and Laponite nanoparticles. FTIR spectra revealed a weak hydrogen bonding between the silanol (Si-O) groups of Laponite and hydroxyl (-OH) of CMC. Hydrogels of CMC-Laponite crosslinked with CaCl<sub>2</sub> presented low cytotoxicity for fibroblasts, indicating that this system has potential for applications in AM processes for tissue engineering. References. [1] I. M. El-sherbiny and M. H. Yacoub, "Review article Hydrogel scaffolds for tissue engineering : Progress and challenges," 2013. [2] J. Malda et al., "25th Anniversary Article : Engineering Hydrogels for Biofabrication," pp. 5011–5028, 2013.

**Keywords:** Additive manufacturing (AM); Nanocomposite hydrogels; CMC; Laponite; Ink.

\* Department of Manufacturing and Materials Engineering, School of Mechanical Engineering, University of Campinas (Unicamp), Campinas, SP, Brazil.



## 3D printing cellulose-based nanocomposite ink

Jéssica Heline Lopes Da Fonseca\*; Ingri Julieth Mancilla\*; Marcos Akira D'Ávila\*

### **Biofabrication and bioprinting (in general)**

**Abstract:** In the last years, the development of cellulose-based inks for 3D printing has received significant interest due to numerous cellulose and their derivatives properties. Carboxymethyl cellulose (CMC) is an anionic water-soluble cellulose derivative widely used as superabsorbent hydrogels. Another cellulose derivative is cellulose nanocrystal (CNC), a rod-like nanoparticle that can be applied for the mechanical strengthening of hydrogels and also presents potential use in several applications in the biomedical field. Based on this, we have proposed to investigate if CMC and CNC mixtures result in cellulose-based nanocomposite gels suitable for extrusion printing. Interactions between CNC and CMC resulted in physical gels, where both rheological properties and the effects of extrusion printing parameters were studied. A Modular Compact Rheometer (Anton Paar MCR-102, Austria) with a plate-plate geometry (50 mm diameter and 1 mm the gap) at 25 °C was used to perform rheological measurements. Extrusion printing was performed on the customized 3DCloner Lab printer using a 22G nozzle tip of 25 mm in length, and a diameter of 0.70 mm (Injex, Brazil). Gels presented shear-thinning, solid-like viscoelastic behavior, viscosity recovery, and continuous filaments were obtained during printing. Tests with different print and extrusion speeds evidenced the influence of both on the geometry obtained. Therefore, among the studied parameters, we used the extrusion speed of 45 mm/s, and a print speed of 15 mm/s to obtain geometries with better shape fidelity. After printing, the geometries were submerged on citric acid (CA) aqueous solution at 2.0 wt.% for 5 minutes to obtain a crosslinked structure. Cylindrical scaffolds with 12 mm diameter and 4 mm height were lyophilized and dipped in phosphate buffer saline (PBS, pH 7.4) at 37 °C for two days to measure the swelling ratio. After two days, the swelling degree of  $726.1 \pm 25.5\%$  was measured. Moreover, low cytotoxicity to CMC/CNC crosslinked hydrogels as confirmed through MTT assay of fibroblasts.

**Keywords:** Nanocomposite Gels; Extrusion Printing; CMC; CNC; ink

\* Department of Manufacturing and Materials Engineering, School of Mechanical Engineering, University of Campinas (Unicamp), Campinas, SP, Brazil.



## Using additive manufacturing technology to assist the production of immobilization orthosis

Marlem Oliveira Moreira\*; Renata De Souza Coelho Soares\*

### ***Biofabrication and bioprinting (in general)***

**Abstract:** CAD (Computer Aided Design) technology provides materials and methods for molding and creating objects via three-dimensional printing, as well as it allows greater customization. In terms of health, it makes orthosis better adapted to the patient's anatomical shape when compared to most used accessories and thermoplastics for limb immobilization. Since scientific and technological developments influence medical decision-making, this study focuses on using software packages to mold a three-dimensionally printing device for use in rehabilitation processes, as an alternative treatment for patients with bone fractures/contusions. Methodology: This is an experimental, descriptive, and exploratory study which uses two different types of software (Makehuman® and Rhinoceros®) as tools for creating a humanoid model based on anthropometric data obtained from medical professionals, and for virtually creating a device via CAD system. This research is based on the development of an experimental device for the rehabilitation of lower limb deformity, created by researchers from the Post-Graduate Program in Health Science and Technology at Universidade Estadual da Paraíba. Orthopedic trauma physicians and physiotherapists have assisted on gathering functional and non-functional requirements. Results: For research objectives, the Makehuman® software had a satisfactory performance in creating a humanoid model, and the Rhinoceros® software provided the tools for creating and adjusting the device. The honeycomb pattern model offered a better skin-brace interface for recovering bone fracture/contusion, allowing better visualization of the injured area, and intervening in the treatment of wounds in the region; it prevents the formation of pressure ulcers, providing enough space for proper electrodes placement and other equipment use, occasioning greater agility in rehabilitation. Conclusion: Proper orthosis adjustment/adaptation, as well as its low weight, proved to be the main advantages for AM (Additive Manufacturing) technologies in fractures or contusions of the lower limbs, improving user's quality of life through innovation in treatment protocols.

**Keywords:** Additive Manufacturing; 3D printing; Software; Orthosis; Rehabilitation.

\* Universidade Estadual da Paraíba (UEPB).



## Synthesis and characterization of PCL / andiroba oil hybrid films as wound dressing

*Débora Freitas Silva\**; *Tainara de Paula Lima Lima\**; *Elcio Malcher Dias Junior\**; *Luis Adriano Santos Do Nascimento\**; *Carlos Emmerson Ferreira da Costa\**; *Marcele Fonseca Passos\**

### (Biomaterials)

**Abstract:** With the population aging and the lack of healthy practices, many citizens are affected by mechanical trauma and diseases that cause inflammations in the tissues. An alternative is to develop biomaterials able to assist in the treatment and restoration of the compromised regions. Thus, polycaprolactone (PCL) has been investigated for its biodegradable properties and versatility of application. However, hybridization studies of PCL membranes with vegetable oils, and its anti-inflammatory effects in tissues, are sparsely found in the literature. Vegetable oils, such as andiroba oil, contribute to numerous medicinal properties, participating in several stages of skin healing and acting as microbial protection in injuries. With technological potential in the health area, including natural resources of amazon basin, this project aimed to develop hybrid dressings, using the casting technique. This methodology allows us to obtain thin and low-cost membranes that assist in wound healing by releasing active principles in the polymeric matrix. Films were synthesized from a 5% w / v solution using acetone as a solvent, with different oil concentrations. The solution was prepared under constant magnetic stirring and heating to 40°C for 4h hours. The oil was added to the PCL solution and stirred for 5 minutes. Then 5 ml of each solution was deposited in molds to obtain the membranes. Drying time was four days at room temperature, followed by another four days in an oven at 40°C. Thermal analysis was performed using differential scanning calorimetry (DSC) and thermogravimetry (TGA). Contact angle measurements were also investigated. Results showed no significant macroscopic difference between control material and hybrid membranes. Despite this, the oil amorphous chain's influence on polymer structure was verified, decreasing the degree of crystallinity. The hydrophobic character of films was influenced by oil content. But, a certain degree of films' wettability was observed due to high porosity. Consequently, it is still possible to exchange gases or liquids on the surface of hybrid films. In general, results showed the feasibility of obtaining hybrid PCL / andiroba films with stable thermal character and curative potential.

**Keywords:** Polycaprolactone; Pcl; Andiroba; Amazon Oil; Wound Dressings; Biomaterials; Curative.

\* Federal University of Pará (UFPA), Belém, PA, Brazil.



## Developing and systematizing a process for the construction of personalized respiratory protection masks by additive manufacturing

Eugenio D. A. Merino\* ; Diogo Pontes Costa\* ; César N. Giracca\* ; Carmen E. M. Riascos\* ; Giselle Schmidt Andrés Díaz Merino\*

### (Devices and processes)

**Abstract:** The Sars-CoV-2 imposed unexpected challenges on society, such as, changes in the traditional models of productive systems and effective management of health system resources in diverse countries. In this context, a series of initiatives, in which the use of industry 4.0 technologies are important in the acceleration of the process of Personal Protective Equipment (PPE) development, specifically to health agents inserted in Covid-19 environments combat. However, some Respiratory Protection Masks tackle some issues, such as excessive pressure, skin lesions, discomfort, and incompatibility with the user's face surface. Therefore, this research aims to develop and systematize a process for the construction of personalized Respiratory Masks by additive manufacturing, which achieves the aforementioned demands. Methodology: The methodology was divided into four stages: 1. Problem identification considering the user demands; 2. selection, definition and application of procedures and materials; 3. equipment materialization; 4. user tests. As support, a 3D scanner, computer-aided design software, assisted manufacturing software and 3D printers were used. The mask was manufacturing using polymeric filament PLA (polylactic acid), broad elastic for fixation, and filters with activated carbon. Results: Applying this methodology, it is possible to produce a mask adjusted to the user's facial topology. With a satisfactory and personalized fit resulting from the virtual planning between the product and the user. The construction time was using four hours, included manufacture and assembly of the mask. Conclusion: The systematization of the production process demonstrated feasibility in manufacturing, agility in 3D printing, and precision in the shape of the user's face, verified in the materialized product when tested by the user. This helps to enable an expansion of this applicability and dissemination, which in the case of health, are pressing and necessary. As opportunities for advancing and improving this process, other devices for three-dimensional scanning and materialization can be incorporated, such as the use of polymeric resin SLA by UV curable or other materials, provided that do not harm the user's skin. Finally, the importance of developing research and applications of these technologies in human-centered projects is emphasized.

**Keywords:** Covid19; Additive Manufacturing; Ppe; Maks; Design.

\* Federal University of Santa Catarina (UFSC), Florianópolis, SC, Brazil



## Luminescent composite materials for 3D printing

Francisco Recco Torres\*; Hernane Da Silva Barud\*\*; José Maurício Almeida Caiut\*

### (Biomaterials)

Biopolymers have attracted great interest in tissue engineering research as they are components of living structures and have chemical and biological similarities with natural tissues. Nanofiber scaffolds developed from natural resources are interesting because of their biodegradable properties and, therefore, potentially used as temporary substrates to induce the regeneration of newly developed tissues. Gellan gum is a natural polysaccharide derived from bacteria that can be prepared in the form of a hydrogel, a versatile, functional biomaterial that can be molded into different forms of tissue. Cellulose nanocrystals, or whiskers, are crystalline domains of cellulosic fibers isolated by acid hydrolysis and are named this way due to their physical characteristics of rigidity, thickness and length. They have the potential to increase the properties of polymeric composites and serve as reinforcement for the natural fibers. It is expected that the preparation of nanocomposites based on nanocellulose dispersed in gellan gum can generate biocomposite hydrogels with tunable properties for 3D printing, allowing the manufacture of scaffolds with controllable matrix morphology and porosity. Together, the structures of both biopolymers have groups that can act as a coordination environment for lanthanide ions and the properties resulting from this interaction can allow the development of new biocompatible photonic systems. The presence of the Europium (III) ion as a spectroscopic probe in the material, through the addition of a complex already reported in biocompatibility tests in cells, can allow the study of structural change at the molecular level through changes in the coordination sphere of the lanthanide ion.

**Keywords:** Biopolymers; Scaffolds; Gellan Gum; Cellulose Nanocrystals; Lanthanide Ions.

\* Faculdade de Filosofia, Ciências e Letras de Ribeirão Preto (FFCLRP-USP), Ribeirão Preto, SP, Brazil

\*\* University of Araraquara (Uniará), Araraquara, SP, Brazil



## Genipin extration from venezuelan caruto and preparation of chitosan 3D porous scaffold for tissue engineering

Pedro Luis Rodríguez Sequera\*; Marcos A. Sabino G.\*

### **(Biomaterials)**

**Abstract:** Genipin (GN) is a secondary metabolite found in the fruits of *Genipa Americana* L, its non-toxicity, its anti-inflammatory properties and the ease of reacting with primary amino groups allowing to be used as a crosslinking agent for biopolymers such as chitosan, collagen, etc. Chitosan (CH) hydrogels are currently receiving great interest from researchers due to their interesting properties: antibacterial, biocompatible, biodegradable. However, its rapid degradation and low mechanical properties make it necessary to apply stabilizing mechanisms that at the same time improve said mechanical properties. In this sense, covalently crosslinking CH is one of the possible solutions. A possible application for these cross-linked gels is the obtaining of scaffolds for nucleus pulposus; because it can improve the biomechanics of the intervertebral disc, important for transmits the load imposed on the spine (spinal tension, torsion, compression and bending). In this work, the extraction, purification and characterization of GN was carried out from the fruit of *Genipa americana* L (Caruto Venezolano) obtained on Venezuelan soil and to evaluate its use as a cross-linking agent to prepare CH/GN hydrogels and scaffolds. The pulp of frozen unripe fruits were grated and macerated in chloroform under constant mechanical stirring for 4 h. The chloroformic extract was filtered and the solvent was removed by distillation under reduced pressure. From the oil obtained the GN was obtained by extraction with organic solvents, the solid was purified by recrystallization, obtaining maximum yields of 4 mg GN/g of pulp. The product was characterized by FT-IR, <sup>1</sup>HNMR and <sup>13</sup>CNMR spectroscopy. Chitosan and CH/GN hydrogels at 0.1%, 0.5% and 1% were formed by incorporating GN into a 1% solution of CH in acetic acid. After 3D porous structures were obtained by lyophilization (-48 °C, 72 h and 0.075 torr). Chemical crosslink of CH was confirmed by FTIR, the morphology of the structures was studied by SEM. Hydrogel swelling studies showed that increasing the concentration of GN decreases the capacity of CH to absorb water. Additionally hemolysis tests demonstrated that the incorporation of GN in CH gels does not affect the hemocompatibility of them. The results show how the pore size depend on the concentration of GN, generating 3D scaffold-like structures, which have potential for use in tissue engineering, and possibly as a substitute gel for the nucleus pulposus of the intervertebral disc.

**Keywords:** Biopolymers; Porous Scaffolds Chitosan; Genipin, S.

\* Departamento de Química, Grupo B5IDA, Universidad Simón Bolívar, Caracas, Venezuela



## Biotech-educated platelets platform creating value: ingrowth-bio hydrogel mimics crowded shape of microvascular environmental, with tissue

Sheila Siqueira Andrade\*; Alessandra V.s. Faria\*\*

### (Biomaterials)

**Abstract:** Biotech-educated platelets are conceptual and technological innovations that provide platelets with versatile biotechnological roles as a central scientific system with molecular and biomimetic bases to consider platelet-based solutions (hybrid materials) for therapeutic use and experimental insights into translating platelet technology to the market. While regenerative medicine is expected to ultimately improve patient safety, our knowledge of natural extracellular matrices (ECMs) has increased considerably; we have learned about platelet function and its unexpected biochemistry, especially in regenerative medicine. As a result, we developed of human platelet-based fibrinogen-, fibronectin-, and vitronectin-rich hydrogel, named InGrowth-Bio, which improves micro-vascularization in a complete 3D endothelial cell culture support or Bioscaffold. By incorporating multiple platelet-angiogenic growth factors, this hydrogel supports the proliferation of endothelial cells in 2D cultures (2D-projected images obtained by optical microscopy), and the formation of a microvascular network/structures ex vivo in 3D cultures without requiring the addition of recombinant growth factors (3D images acquired by confocal microscopy). In addition, this compound may be polymerized at body temperature through the proteolytic action of proteases secreted from target cells, offering a fully human option from a Biotech-educated platelet platform. Importantly, the InGrowth-Bio promotes blood-vessel structures formation, which is required in the context of tissue repair. InGrowth-Bio stiffness, degradability and 'stickiness' can all spur cells that form blood vessels to switch between multicellular and single-cell modes of migration. Single cells quickly invade new regions, but the multicellular mode is needed to cells collectively form a blood vessel and its maturation. Ideally, InGrowth-Bio mimics a "crowded cellular environment" led to biomimetic changes in cytoskeletal rearrangement and coordinates the migration of cells during 3D angiogenesis.

**Keywords:** Platelets; Biomimetics; Ingrowth-Bio; Biotechnology; growth factors

\* PlatelInnove Biotechnology

\*\* University of Campinas, UNICAMP





## Development And Characterization Of Membranes Based On Chitosan/ Genipin–Oil For Biomedical Applications

Erick De Freitas\*; José Ramón Domínguez\*\*; Dinorah Herrera\*\*\*; Marcos A. Sabino G.\*

### (Biomaterials)

**Abstract:** Genipin (GP) is a natural cross-linking agent that is used to cross-link chitosan (CH). From the pulp of a fruit known as Venezuelan Caruto (Genipa American L.), an oil extraction process was carried out. The extracted oil (GP-oil) was characterized and used as a reticulation agent with CH for the preparation of membranes (solvent casting) in three different formulations, contained the oil in a concentration of: 0 %, 0.05% and 0.1% w/w. The surface morphology of the membranes was evaluated by scanning electron microscopy (SEM), where an absence of superficial pores was observed. These membranes were characterized by Fourier transform infrared spectroscopy (ATR-FTIR). Accordingly, to the FTIR results, a chemical change was observed in the proportion of deacetylated units in relation to acetylated units, which determining the effect of the cross-linking process between the GP-oil and CH. Subsequently, permeability tests using Nitrogen, Argon and Air gases were performed (at 8 and 16 psi) of the membranes, which showed an impermeable character. During these permeation tests, an interesting deformation was observed in the membranes, which allowed to relate said deformation with mechanical resistance. The mechanical resistance was evaluated at high pressure rupture tests (48–56 psi), determining that the resistance to rupture increases and the elastic deformation decreases in function of % GP-oil. Swelling tests were performed to determine the water sorption of the membranes, finding a decrease in % of swelling as the GP-oil concentration increased. Using the thermal stimulation current density (TSDC) technique, the influence of oil cross-linking was determined by the mobility of the polymer chain. TSDC results indicated that in function of the GP-oil concentration increase, the mobility of the polymer chain decreased. The results by FTIR, TSDC, permeability and swelling are promising results because they show that it is not necessary to have purified GP to achieve the crosslinking of CH. The evaluation of hemocompatibility of the oil into the membranes was carried out, where it was proved that it is not cytotoxic. All these results obtained on the reticulation capacity of the GP-oil extracted from the Venezuelan Caruto, its hemocompatibility and improve mechanical resistance, open a window for its use in biomedical applications: for example in the development of 3D scaffolds for the nucleus pulposus.

**Keywords:** Biopolymers; Chitosan; Genipin; Membranes.

\* Departamento de Química, Grupo B5IDA, Universidad Simón Bolívar, Caracas, Venezuela

\*\* Departamento de Química, Laboratorio de Absorción Atómica, Universidad Simón Bolívar, Caracas, Venezuela

\*\*\* Departamento de Física, Laboratorio de Física del Estado Sólido, Universidad Simón Bolívar, Caracas, Venezuela



## Rapid 3D prototyping biomodel as an auxiliary surgical planning method for facial tumor resection

Luiz Henrique Soares Torres\*; Marisa Aparecida Cabrini Gabrielli\*; Valfrido Antônio Pereira Filho\*

### Biofabrication and bioprinting (in general)

**Abstract:** ameloblastomas are slow growing, high recurrence and locally invasive facial tumors. Thus, an accurate surgical approach guaranteed satisfactory clinical results and less patient morbidity. The additive manufacturing technique allows to making three-dimensional models from 3D image data that a physical replica of the patient's anatomy, assisting in planning and ensuring surgical predictability. Methodology: male patient, 32 years old, with no previous medical history, attended the ambulatory of maxillofacial surgery, with swelling on the right side, painless, with evolution of 08 months. Imaging exams showed an intraosseous trabecular lesion in the right body and mandibular angle. In histopathological analysis by incisional biopsy, the diagnosis of multicystic ameloblastoma was obtained. We opted for making a 3D model by additive manufacturing for planning tumor resection and previous modeling of osteosynthesis titanium plate. Results: the tumor resection regarding the installation of the fixation device was performed under general anesthesia. Following an 8-month follow-up, the titanium plate was fractured. A new digitally preformed and more robust device was installed. Bone grafting of autogenous origin was performed in the same session. Currently in follow-up for 01 year, he continues without recurrence or complications. Conclusions: the additive manufacturing is an effective auxiliary method in the planning of tumor resections, since it allows the visualization of the lesion margins, in addition to providing a pre-modeling of the bone fixation devices and reduction of the surgical time.

**Keywords:** Three-Dimensional Printing; Ameloblastoma; Neoplasms; Technology; Facial Neoplasms .

\* Universidade Estadual Paulista "Júlio de Mesquita Filho", Faculdade de Odontologia de Araraquara, UNESP/FOAr.

The logo for 3DDBB features the letters '3D' in white on a blue background, followed by 'DBB' in white on a pink background.

2020 Aug 26-28th

1st INTERNATIONAL DIGITAL CONGRESS ON  
3D BIOFABRICATION AND BIOPRINTING

NUT3D – PPGB – UNIARA

## Development of a 3D microextrusion bio printer

Diego Silva Batista\* ; Hernane Da Silva Barud\*\*

### Biofabrication and bioprinting (in general)

**Abstract:** Three-dimensional (3D) printing or additive manufacturing is an emerging technology that has recently been gaining significant attention in the area of medical and tissue engineering. However, commercial bioprinting platforms still have a high cost for small research facilities, especially in the academic environment. In addition, to use this technique, it is also necessary to produce hydrogels and functional bioinks that aim to match the properties, chemical, physical and biological of human tissue. In the present work, a low cost homemade 3D bioprinter was designed and built using the piston microextrusion process by adapting a commercial Fused deposition modeling (FDM) printing head of the ReprapPrusa i3 model, for bioprinting using bioinks and hydrogels. To validate the developed bioprinter, aiming at possible applications in tissue engineering, scaffolds were printed using hydrogels of different compositions. The scaffold was dimensioned in a cylinder shape, with a diameter of 10.75 mm and a thickness of 5 mm. Demonstrating its ability to manufacture 3D structures with good spatial accuracy along the X, Y and Z axes and presenting the ability to follow the projected project. The printing results demonstrate scaffolds with structural stability similar to those reported in the literature, showing that bioprinter is promising for applications in additive manufacturing and tissue engineering.

**Keywords:** Bioprinting; Microextrusion; Additive Manufacturing; Tissue Engineering; Homemade.

\* MedTech Lab Solutions.

\*\* University of Araraquara (Uniará), Araraquara, SP, Brazil.



## Biomimetic structures development from chitosan–graft–amino acids as potential biomaterial for cell culture

Jesús Campos\*; Ramón Coronado S.\*\*; Marcos A. Sabino G.\*

### (Biomaterials)

**Abstract:** Biopolymers are important for tissue engineering and potential for artificial organs area. The polysaccharide Chitosan is one of them because contain interesting characteristics of biodegradability and biocompatibility, but has problems of application in biological systems due to its limited solubility in neutral aqueous solution. Its applicability in biotechnological and medical areas may be accomplished by chemical modification to open more possibilities to be apply in the biofabrication of 3D structures or gels for bioextrusion. In this project, chitosan (CH) was chemically modified with two amino acids (L–leucine, L–tyrosine) using carbodiimide chemistry. With the functionalized CHs (FCHs), the aim was to prepare (using electrospinning technique) biomimetic structures (scaffolds) as models for cell culture. Initially, the chemical characterization of the FCHs was performed using Fourier–transform infrared spectroscopy (FT–IR) and nuclear magnetic resonance (NMR). Follow, the solubility properties of the derivatives obtained were also studied. In the case of chitosan, this study was relevant to demonstrate that its solubility was enhanced in a physiological pH solution. Subsequently, polyblends (from solution) were prepared between the modified chitosans (FCHs) and poly (vinyl alcohol) (PVA) in proportion 25/75 FCHs/PVA. These polyblends permitted to study the experimental conditions in the electrospinning process for to obtain the scaffolds, formed by micro/nano fibers, with a morphology of interconnected pores. This morphological characterization was performed using scanning electron microscopy (SEM) and permit to observe that these structures mimic an extracellular matrix. Also, the hydrophilicity/hydrophobicity property of the FCHs and polyblends was studied using the contact angle test. Finally, biocompatibility studies were carried out in two way: using the hemocompatibility test on human erythrocytes, and in vitro viability cellular test using a hemocytometer with trypan blue. As a result, a percentage of hemolysis less than 5% point that they are not cytotoxic, and the experimental complement using cell culture in vitro shown that both biomaterials are biocompatible: but the CH graft L–leucine is better than CH graft L–tyrosine. All results were relevant to propose future potential of these biomimetic structures for cell culture, tissue engineering, bioprinting techniques, development of bioinks and other biomedical applications.

**Keywords:** Biomimetic structures; Biomaterial; Chitosan; Chemical Modification; Amino Acids.

\* Departamento de Química, Grupo B5IDA, Universidad Simón Bolívar, Caracas, Venezuela

\*\* Lester Smith Medical Research Institute, USA



## Development of a polycaprolactone scaffold functionalized with nanocapsules containing heparin for use as a vascular graft

Bruna Borstmann Jardim Leal\*; Daikelly Iglesias Braghirolli\*\*; Patricia Pranke\*\*\*

### (Biomaterials)

**Abstract:** Synthetic vascular grafts are widely used clinically in large diameter vessels. However, in vessels < 6 mm of diameter, they have a high failure rate due to thrombus formation. Electrospun scaffolds functionalized with biomolecules, such as heparin (Hep), can be an interesting tool for use as a vascular graft. For blood vessel regeneration, the establishment of vascular endothelium is the initial goal for the success of the grafts, which can be achieved using endothelial progenitor cells (EPCs). Aim: Develop a polycaprolactone (PCL) scaffold functionalized with nanocapsules (NC) containing Hep. Methodology: PCL scaffolds were produced by electrospinning and were functionalized with NC containing Hep by electro spraying, from an emulsion of poly(lactic-co-glycolic acid) (PLGA) and Hep. Following this, the EPCs were cultivated on the scaffolds. PCL fibers and Hep NC were characterized by morphology and diameter. For biological characterization, three groups were evaluated: PCL without NC (PCL/ControlNC), PCL with NC containing Hep (PCL/Nhep) and a culture plate treated with collagen (control group). The morphology and adhesion of cells were evaluated. The EPC morphology was analyzed by staining the nuclei and cytoskeleton with DAPI and phalloidin, respectively. For cell adhesion, following the nuclei staining with DAPI, nine random fields from each sample were analyzed under fluorescence microscopy and the number of adhered cells/sample was estimated. Results and discussion: The PCL scaffolds presented smooth, homogeneous and randomly distributed fibers, with diameter of  $0.682 \pm 0.21 \mu\text{m}$ . The NC containing Hep presented round and homogeneous morphology, with diameter of  $440 \pm 172.4 \text{ nm}$ . In the cell adhesion test, the control group showed  $1,191 \pm 412.6 \text{ cells/sample}$ . The scaffolds groups showed similar cell adhesion: PCL/ControlNC  $697.5 \pm 309.7$  and PCL/Hep  $692.5 \pm 145.1 \text{ cells/sample}$ . Through this test, it was observed that the presence of NC did not interfere in cell adhesion on the scaffolds. Moreover, after 7 days of cultivation, the EPCs showed elongated morphology on the scaffolds, indicating that the cells had a good adaptation on these structures even with low adhesion. Conclusion: The scaffolds favor the adhesion and adaptation of EPCs. In addition, the presence of NC did not alter these parameters. These results demonstrate that the developed scaffolds can be an interesting alternative for vascular tissue engineering.

**Keywords:** Tissue engineering; Regenerative Medicine; Nanocapsules; Heparin; Vascular Graft.

\* Hematology and Stem Cell Laboratory, Faculty of Pharmacy, Universidade Federal do Rio Grande do Sul (UFRGS), Porto Alegre, RS, Brazil

\*\* Physiology Post-graduation Program, UFRGS, Porto Alegre, RS, Brazil

\*\*\* Stem Cell Research Institute, Porto Alegre, RS, Brazil



## Influence of glycerol content on the mechanical properties of thermoplastic starch films produced by tape casting

Karen De Souza Do Prado\*; Maria N. Castanho\*\* ; Jane Maria Faulstich De Paiva\*\*

### (Biomaterials)

**Abstract:** Starch is a biomaterial extensively studied for preparing films due to its abundance, biodegradability, and low cost. Thermoplastic starch (TPS) is obtained by mixing starch with plasticizers such as glycerol and water, and TPS films are generally produced by casting. However, due to the small size of the films produced and the lack of thickness control, casting is generally unfeasible for large-scale production of TPS films. A promising alternative is the tape casting technique, traditionally used for ceramics but not yet widely explored for molding TPS films. The aim of this study was to determine the influence of composition on the mechanical properties of TPS films produced by tape casting, aiming at large scale production. Methodology: Starch/glycerol/water suspensions were prepared with 5 wt% of corn starch and four concentrations of glycerol (20, 30, 50, and 100 wt% in relation to the mass of starch). The mixtures were stirred at 80°C until gelatinization, and the films produced by tape casting with 0.15 ( $\pm$  0.04) mm thickness had their mechanical properties evaluated according to ASTM D882. Results: It was observed that the increase in glycerol content resulted in decreasing trends in Young's modulus and tensile strength, which follow power functions with a coefficient of determination greater than 0.992. The increase from 20 to 30 wt% in the glycerol content reduced Young's modulus by 75 wt% and maximum strength by 56%, and increased the elongation of TPS films by 50%. TPS films with 5 wt% starch and 50 wt% glycerol (in relation to starch) resulted in higher Young's modulus (19.3 MPa) and lower rupture elongation (12.1%) than values previously reported in the literature for films produced by conventional casting, which can be explained by the orientation of the polymer chains during processing. The tensile strength value (1.3 MPa) was comparable to that reported in the literature for films produced by casting. Conclusion: Therefore, the results of this work show that tape casting is a viable technique to be used in the large-scale production of TPS films for different applications, especially those that require materials with greater stiffness.

**Keywords:** Starch; Glycerol; Film; Tape Casting; Mechanical Properties.

\* Materials Science Program, Federal University of São Carlos, PPGCM/UFSCar, Sorocaba Campus, Sorocaba, SP, Brazil.

\*\* Production Engineering Department, Federal University of São Carlos, UFSCar/DEP-So. Sorocaba Campus, Sorocaba, SP, Brazil.



## Perspectives of bioprinting in regenerative medicine

Anna Kellssya Leite Filgueira\*; Ketinlly Y. N. Martins\*; Rodolfo R. Castelo Branco\*; Isabella D. Gallardo\*; Carlos A. M. Dos Santos\*\*; Lucas V. A. Sales\*\*

### Biofabrication and bioprinting (in general)

**Abstract:** Regenerative medicine makes it possible to repair or replace damaged organs, tissues and cells. The future potential of this area grows in association with the development protocols of biocompatible artificial tissues and 3D bioprinting, which has provided new evolutionary strategies for the area. In this context, the present study aims to review the currently available literature and analyze the bioprinting perspectives in regenerative medicine. Methodology: It refers to an integrative literature review in order to generate a consolidated overview of the topic addressed. The elaboration of the study respected the PICO (Patient, Intervention, Comparison, Outcome) strategy based on the guiding question "What are the perspectives of bioprinting (I) in the current scenario of three-dimensional printing (P) for improving regenerative medicine (O)?". The literature survey was conducted in two electronic databases – ScienceDirect (Elsevier) and the Virtual Health Library: VHL (Bireme). The search strategy used was the association of the descriptors "Regenerative Medicine", "Bioprinting", "Three-dimensional Printing", and after of their respective correspondents in English, duly registered in DeCS (Health Sciences Descriptors), through the Boolean operator 'AND', respecting the individuality of each electronic base. The inclusion criteria were: allowing access to the full text and respecting the thematic approach. The exclusion criterion used was to be presented in languages other than English, Portuguese and Spanish. The articles' selection was made by reading titles, reading abstracts, and finally, reading the full text. Results: The literature survey offered 209 documents. Of these, 185 articles provided only the abstract and did not participate in the research. Eight articles met the proposed exclusion criteria. Sixteen articles were analyzed regarding the thematic approach and, after reading the title and abstracts, six duplicates were found. Finally, 10 articles were reviewed. Of these, no clinical research was found. Conclusions: Advances in bioprinting have a diversity of applicability, enhancing the scenario of regenerative medicine. The lack of clinical studies of high methodological rigor, may be associated with factors that characterize the method (customization and biocompatibility) and cases absence that address the specificities of randomization, however, restricts the reliability and effectiveness of the technique.

**Keywords:** Tissue Engineering; Three-Dimensional; Regenerative medicine; Skin, Artificial; Bioprosthesis.

\* NUTES – Universidade Estadual da Paraíba – UEPB, Campina Grande, PB, Brasil.

\*\* Universidade Federal de Campina Grande – UFCG, Campina Grande, PB, Brasil.



## A new protocol for obtaining platelet–leukocyte aggregate for use as bioink

Gabriela Moraes Machado\*; Kalita R. Grubert\*, Marcos A. do Couto\*; Natasha Maurmann\*\*; Patricia Pranke\*\*; Caren Serra Bavaresco\*

### (Biomaterials)

**Abstract:** The development of bioink is a challenge in tissue engineering. Platelet aggregates have been used since the 1990s and currently represent an alternative for application in 3D bioprinting as they are an autogenous material and because of the release of growth factors. Therefore, this work aims to develop and test a new protocol for obtaining platelet–leukocyte aggregate. Methodology: The blood of two patients was collected in tubes without anticoagulants, centrifuged at 300 rpm for 10 minutes, pressed and polymerized, and the biomaterial was placed in 48 well culture plates (approval protocol CAAE 20111519.9.0000.5349). Fibroblasts (MRC5 cell line) were seeded on the membranes and macroscopic, microbiological (Tryptic Soy Broth, TSB), and cellular tests [3–(4,5–dimethylthiazol–2yl)–2,5–diphenyl tetrazolium, MTT and fluorescence microscopy] were performed to assess the presence and viability of the cells. Results: The results showed that the protocol developed using low rotation generated a rigid final membrane, although with irregular edges and with the presence of red blood cells. After 6 days of incubation of the biomaterial in nutrient medium for microorganisms TSB, microbiological evaluation was made through the turbidity test, which did not demonstrate the growth of microorganisms. The biomaterial demonstrated biocompatibility with the presence of viable cells after 7 days of cultivation using the MTT test. The mean values of absorbance  $\pm$  standard deviation in this test were  $0.420 \pm 0.048$  in the control group, where the cells were grown directly in the culture wells and  $0.396 \pm 0.049$  in the group where the cells were grown in the platelet–leukocyte aggregate ( $p = 0.205$ ). In both the control and biomaterial groups, detection was made of viable cells stained with fluorescein diacetate and dead cells with propidium iodide. Conclusion: This protocol can be used as a bioink because its initial composition can favor bioprinting and, after polymerization, obtain favorable rigidity. Protocols for obtaining platelet–leukocyte aggregate, such as fibrin–rich plasma, use higher rotation (about 3000 rpm); the protocol for obtaining the biomaterial studied in this work showed promising results for clinical practice and also for use in surgical manipulation. However, it would be interesting to make tests comparing the release of growth factors and to make an evaluation of the membrane eluate obtained by this protocol and the protocols already described.

**Keywords:** Biocompatible Materials; Bioprinting; Tissue Engineering; Transplantation; Regenerative Medicine.

\* Universidade Luterana do Brasil (ULBRA), Canoas.

\*\* Federal University of Rio Grande do Sul (UFRGS)



# 3DBB

2020 Aug 26-28th

1st INTERNATIONAL DIGITAL CONGRESS ON  
3D BIOFABRICATION AND BIOPRINTING

NUT3D – PPGB – UNIARA

## Implantation of galantamine microparticles for reducing oxidative stress in spinal cord injury in rats

Fernanda Stapenhorst França\*; Cristian E. Teixeira\*; Marcelo G. Dos Santos\*; Gabriele G. Dido\*; Cristina C. Carraro\*; Laura Elena Sperling\*\*;  
Adriane B. Klein\*; Patricia Helena Lucas Pranke\*\*\*

### (Biomaterials)

**Abstract:** Spinal cord injury (SCI) is a serious condition that currently has no effective treatment and can lead to gross loss of body sensitivity, potentially leading to debilitating paralysis. Previous studies from our group have indicated that galantamine improves recovery after SCI. Drug release characteristics are improved with the use of biodegradable polymer carriers, which sustain the release of encapsulated drugs. Hence, the aim of this study has been to produce galantamine microparticles and to evaluate galantamine effects on oxidant parameters after SCI. Methods: The microparticles were produced by electrospraying, with 2.5% of galantamine hydrobromide in a 4% PLGA solution or 4% PLGA alone. The morphology of the particles was evaluated by scanning electron microscopy (SEM) and the diameter and zeta potential of the particles were measured by dynamic light scattering. For the SCI model, Wistar rats were submitted to a contusion injury on the thoracic spinal cord, using MASICS impactor (CEUA 35781). The animals were divided into the following groups: (1) Sham (laminectomy only), (2) only SCI, (3) SCI with intraparenchymal galantamine treatment; (4) SCI with implant of PLGA particles and (5) SCI with implant of PLGA particles containing galantamine (PG 2.5%). Three days and six weeks after the injury, the animals were euthanized and the spinal cords were collected. Reactive oxygen species (ROS) production in the spinal cord was assessed by DCF analysis, and lipid peroxidation was analyzed by measuring thiobarbituric acid reactive substances (TBARS). Results: The average particle diameter was  $3,247.6 \pm 1,290.7$  nm for the 4% PLGA particles and  $568.3 \pm 172.5$  nm for the PLGA particles with 2.5% of galantamine. The zeta potential of the particles was  $-50.05 \pm 10.3$  mV for the 4% PLGA particles and  $-23.59 \pm 4.6$  mV for the particles containing 2.5% of galantamine. The group treated with PG 2.5% showed significantly decreased ROS production when compared to the injury group after 3 and 42 days post injury. Furthermore, all the treatment groups presented a decreased TBARS production when compared to the injury group after 3 days, but not after 42 days. Conclusion: The present study shows that galantamine treatment, PLGA particles, and PG 2.5% were able to decrease lipid peroxidation 3 days after the injury, but only the treatment with PG 2.5% was able to reduce the oxidative stress at 3 and 42 days after spinal cord injury, decreasing ROS production.

**Keywords:** Spinal Cord Injury; Galantamine; Electrospraying; Antioxidant Effect.

\* Universidade Federal do Rio Grande do Sul (UFRGS).

\*\* Universidade Vale do Rio dos Sinos (Unisinos).

\*\*\* Instituto de Pesquisa com Células-Tronco (IPCT).



## Study of bioink formulation and influence of bioprinting in cell viability

Luiza Silva de Oliveira\*; Natasha Maurmann\*; Juliana Girón\*; Maurício Felisberto\*; Patricia Pranke\*

### (Biofabrication and bioprinting (in general))

**Abstract:** Bioprinting is an emerging technology with biomedical applications that allows for the production of scaffolds with cells, materials, and molecules. The aim of this research has been to study the composition of bioinks of alginate hydrogels and to compare production by manual deposition or bioprinting. Viability of keratinocytes (HaCat) and stem cells, by the 3-(4,5-dimethylthiazol-2-yl)-2,5-diphenyltetrazolium bromide test (MTT) were tested to formulate the bioink. The solvents, water, sodium chloride (NaCl) or phosphate-buffered saline (PBS) and the concentration of alginate were compared. The bioprinter Octuplus™ (3DBS – 3D Biotechnology Solutions) was used. The results of manual deposition did not demonstrate statistical difference when the stem cells were cultivated in 2.5% of alginate with the different solvents ( $p=0.55$ ), showing mean absorbance  $\pm$  standard error of the mean (SEM) of  $0.13\pm 0.01$  when PBS was used,  $0.14\pm 0.01$  using water and  $0.14\pm 0.01$  with NaCl, after six days. The mean absorbance  $\pm$  SEM at HaCat cultivated in 3% alginate was  $0.53\pm 0.01$  (control),  $0.53\pm 0.02$  (NaCl),  $0.58\pm 0.04$  (PBS) and  $0.63\pm 0.03$  in water, showing an increasing non-statistically tendency with the use of water as a solvent ( $p=0.07$ ). The presence of 0, 2.5 and 3% alginate in stem cell viability was evaluated and the mean absorbance was respectively  $0.09\pm 0.01$ ,  $0.14\pm 0.01$  ( $p<0.01$ ) and  $0.18\pm 0.01$  ( $p<0.01$ ), showing that the higher concentration of alginate increases cell viability ( $p=0.027$ ). The chosen bioink used in the comparison of manual deposition and bioprinting was composed of 3% alginate in water. The MTT results show that mean absorbance after 1 and 20-days was,  $0.16\pm 0.02$  and  $0.23\pm 0.01$  ( $p=0.0071$ ), respectively when the bioprinter was used, showing cell proliferation and  $0.29\pm 0.02$  and  $0.19\pm 0.00$  ( $p=0.0018$ ) when manual alginate deposition with a syringe was used, showing a decrease in cell viability. The highest cell viability obtained with manual deposition on day one ( $p=0.0001$ ) can be related to the viability decrease caused by the higher resistance of the needle walls in the bioprinter. After twenty days, the greater viability in the bioprinted scaffolds ( $p=0.0134$ ) can be justified by the better homogeneity and integrity of this biomaterial. Due to the fragile mechanical properties of alginate, the association of the bioprinted alginate hydrogel with 3D printed scaffolds and/or electrospun nanofibers can be a promising strategy for hard tissue regeneration.

**Keywords:** Alginate; Biomaterial; Stem Cells; Keratinocytes.

\* Federal University of Rio Grande do Sul (UFRGS), Porto Alegre, RS, Brazil.

# 3DBB

2020 Aug 26-28th

1st INTERNATIONAL DIGITAL CONGRESS ON  
3D BIOFABRICATION AND BIOPRINTING

NUT3D – PPGB – UNIARA

## Production and testing of 3D o-rings for tissue engineering

Bruna Govoni\*; Natasha Maurmann\*\*; João Alvarez Peixoto\*; Patricia Pranke\*\*

### (Cell cultures)

**Abstract:** Tissue engineering uses biomaterials as well as cells and growth factors for tissue regeneration. In order for scaffolds to remain at the bottom of the culture wells and in contact with the cells, O-rings are used. Polylactic acid (PLA), a synthetic, biocompatible polymer, can be used in additive manufacturing. The aim of this research has been to produce PLA O-rings using the three-dimensional (3D) printing technique and to test them. The O-rings were printed on the printer 3DCloner, printing volume of 150 mm x 150 mm x 150 mm, melting temperature up to 220°C, and fused filament with a diameter of 0.2 mm, generating layers in this thickness. The modeling was performed by the FreeCAD software. Each O-ring was printed with an external diameter of 15.2 mm and an internal diameter of 12 mm, height of 3 mm, and manually sanded. The materials were sterilized by autoclave or glutaraldehyde. The keratinocytes (cell line HaCat) were seeded in a density of 10,000 per well in 24-well tissue culture plates. After 6 days, the cell viability test was performed by the reduction assay 3-(4,5-dimethylthiazol-2-yl)-2,5-diphenyltetrazolium bromide (MTT). As a result, the O-rings printed in additive manufacturing presented smooth and uniform surfaces. Most of the O-rings fitted into the wells of the culture plates; however, some were tight and others were loose. In the cytotoxicity test, no statistically significant difference was found between the control wells and the wells with the printed and autoclaved O-ring, indicating that the viability of the cells in the wells with this material was similar to the wells without materials ( $p = 0.1469$ ). The values of the normalized results in relation to the mean  $\pm$  standard deviation (SD) control were  $100 \pm 15$  for the control and  $88 \pm 9$  for the O-ring. Regarding the comparison of the sterilization method, the use of glutaraldehyde decreased cell viability in relation to the control ( $p < 0.0001$ ), with a mean absorbance  $\pm$  SD of  $0.04 \pm 0.01$  while the autoclaved material was  $0.65 \pm 0.07$ . It can be concluded that the PLA O-ring obtained by additive manufacturing was not cytotoxic. In order for the O-rings to be more effective, the flexible PLA will be tested. Regarding the sterilization method, although glutaraldehyde is used, residues may have remained even with two washes; however, the autoclave did not cause toxicity to the cells.

**Keywords:** Polylactic acid; Cytotoxicity; Keratinocytes; Additive manufacturing.

\* Universidade Estadual do Rio Grande do Sul (UERGS)

\*\* Universidade Federal do Rio Grande do Sul (UFRGS)



## Production of decellularized rat skin as a substitute for skin lesions treatment

Gabriele Gulielmin Didó\*; Marcelo G. Dos Santos\*; Fernanda S. França\*; Laura–Elena Sperling\*\*; Patricia Helena Lucas Pranke\*\*\*

### (Biomaterials)

**Abstract:** One of the main bioengineering goals is the production of biomaterials able to replace damaged tissues while promoting the natural repair process. The number of Brazilians that need a skin transplant has been constantly increasing over the last 10 years. Many dermal substitutes are available nowadays, and they are mostly acellular. Considering the high price of dermal substitutes available on the market, new alternatives must be sought to lower costs. Decellularized skin presents a great potential as a skin substitute. In this study, the aim has been to develop a protocol for decellularization of murine skin and analyze its structure to produce a dermal substitute. **Materials and Methods:** Discarded rat skin (CEUA 32510) was decellularized by incubation in a series of hypertonic solutions, using Triton X-100 and trypsin under continuous agitation. To establish the protocol, three different incubation times were tested during a five day, eight and a half day and twelve day period. The genomic DNA was quantified and compared to control the skin. In order to confirm the protocol efficacy, histological analyses were performed. The samples were sectioned on microtome in 5  $\mu$ m thickness and stained with DAPI and Masson's Trichrome. The microtomography was substituted by haematoxylin and eosin (HE) staining to realize macro and microgeometry analyses. **Results:** The protocol that presented better decellularization efficacy was made in 5 days. The DNA quantification analysis showed that the control skin presented a much higher DNA amount ( $111.8 \pm 7.02$  mg gDNA/mg tissue) compared with the decellularized samples, which exhibited a low presence of DNA ( $3.026 \pm 1.06$  mg gDNA/mg tissue). The histological sections stained with DAPI presented normal nuclear distribution of the control skin, but cell nuclei were not detected on the decellularized samples. The HE staining of the decellularized samples exhibited a conserved matrix structure, with the maintenance of the dermis extracellular matrix. The samples stained with Masson's Trichrome showed a structure consisting predominantly of collagen. **Conclusion and perspectives:** It was possible to establish an efficient decellularization protocol of the rat skin. This can serve as a matrix for developing a skin substitute. Future studies will be performed to test the decellularized tissue biocompatibility by the MTT test and cell adherence tests with ker

**Keywords:** Rat Skin Regeneration; Decellularization Curative.

\* Universidade Federal do Rio Grande do Sul (UFRGS).

\*\* Universidade Federal de Ciências da Saúde Porto Alegre (UFCSPA).

\*\*\* Instituto de Pesquisa com Células–Tronco (IPCT).



## How microfluidics and 3d printing can revolutionize pharmaceutical and medical research

Harrison Silva Santana\*; Mauri S. A. Palma\*\*; Mariana G. M. Lopes\*; Giovanni A. S. Lima\*\*\*; João L. Silva Jr.\*\*\*\*; Osvadir P. Taranto\*

### (Devices and processes)

**Abstract:** The pharmaceutical industry is one of the most important sectors in the industry, with research and development (R&D), innovation, manufacturing and marketing of medicines for human and animal health as objectives. In R&D and innovation processes, pharmacists, molecular biologists and other health professionals cooperate to obtain drugs with greater specificity and potential. The drug discovery and development process is accompanied by toxicological and clinical tests. The literature tells us that the total cost of screening drugs and developing safe and effective therapeutic assets can exceed 2 billion dollars. The development of new technologies is one of the weapons of the pharmaceutical industry to reduce costs in the development of medicines and to decrease the use of in vivo animal models. These technologies are being used in the synthesis of active pharmaceutical ingredients (API) and also in systems that mimic living tissues for toxicological and clinical tests. Among these new technologies, Microfluidics and Additive Manufacturing, also known as 3D printing, are enabling faster research and development in the pharmaceutical and medical fields, supporting new solutions for active pharmaceutical production and clinical testing without the need for in vivo animal models. In this presentation I will discuss two areas of work in our research group: API synthesis using microfluidic devices; 3D printing of microdevices combined with 3D bioprinting of solutions e.g., hydrogels, bioinks and catalysts. For the manufacture of these 3D printed microfluidic devices with solutions in their channels, we propose and build an automatic equipment consisting of a modified 3D printer with two independent systems, a module with a syringe for injection of solutions/hydrogels and a conventional head with a Fused Deposition Modeling mechanism. This automatic system allows the manufacture of microfluidic devices with channels filled with solutions in a single manufacturing step. We believe that Microfluidics and 3D Printing will expand the frontiers of pharmaceutical and medical research, as it will allow professionals from other areas to contribute to the development of the pharmaceutical industry, a fundamental sector for humanity.

**Keywords:** Microdevices; Medicine Drugs; Active Pharmaceutical Ingredients; Bioprinting; 3d Printing.

\* School of Chemical Engineering, University of Campinas, Albert Einstein Av. 500, 13083–852 Campinas, SP, Brazil.

\*\* Department of Biochemical and Pharmaceutical Technology, Sao Paulo University, 05508–000 Sao Paulo, Sao Paulo, Brazil.

\*\*\* Institute of Environmental, Chemical, and Pharmaceutical Sciences, Federal University of Sao Paulo, 09972–270 Diadema, Sao Paulo, Brazil

\*\*\*\* Federal University of ABC, CECS – Center for Engineering, Modeling and Applied Social Sciences, Alameda da Universidade, s/n., 09606–045 São Bernardo do Campo, SP, Brazil.



## Production of nanoparticles with controlled release by the electrospraying method

Luiz Carlos Sommer Ferreira\*; Laura Elena Sperling\*\*; Patricia Helena Lucas Pranke\*\*\*

### (Devices and processes)

**Abstract:** The number of nanotechnology studies has increased substantially during the last decades and are playing a major role in the pharmaceutical industry. Nanoparticles represent an important formulation for controlled drug release. Electrospraying technology represents a relatively simple method for producing nanoparticles. This study has aimed to establish an electrospraying protocol to produce poly (lactic acid-co-glycolic acid) (PLGA) particles with a neuroprotective compound called drug X (in the process of registering for intellectual protection), for future application of these particles in a rat model of spinal cord injury. Particles of 2 different concentrations of PLGA 50/50 (2% and 4%) and two different solvents acetonitrile (ACT) and hexafluor (HXF) were produced. Nanoparticles were produced in a device with a built-in controlled environment to help to evaporate HXF or ACT. To reduce the likely residual presence of solvents, after production the particles standing on the samples desiccator. Drug X was added at 1% to the PLGA 4% solution in both solvents. The particles were electrosprayed using a flow rate of 0.1 to 0.5 ml/h and voltage ranging from 23 to 29 kV. The particle morphology was analyzed by scanning electron microscopy (SEM). The particle size and zeta potential were analyzed through dynamic light scattering. Particles of PLGA alone were first tested at different concentrations and different solvents. SEM morphological analysis showed that 2% PLGA presented morphological irregularity in both ACT and HXF, whereas PLGA 4% showed greater morphological stability in both ACT and HXF. Hence, PLGA 4% was considered to be the better suited concentration for the production of microparticles. The addition of drug X to the 4% PLGA particles in ACT led to the occasional presence of fibers and irregular morphology. However, in HXF, the addition of drug X did not alter the morphology significantly. Therefore, the optimal formulation of drug X particles was 4% PLGA in HXF. The average diameter of 4% PLGA and 4% PLGA with drug X particles was  $428.27 \pm 77.90$  nm and  $842.1 \pm 59.66$  nm, respectively. The zeta potential was  $-15.33 \pm 3.4$  for the PLGA 4% particles and  $-16.27 \pm 1.56$  for the particles with drug X. With this study, it was possible to standardize the production of PLGA microparticles with and without drug X by electrospraying, as well as to physically characterize the particles. The optimal formulation was found to be PLGA 4% and 1% drug X in HXF.

**Keywords:** Electrospraying; Nanotechnology; Pharmacological Developing.

\* Universidade Federal do Rio Grande do Sul (UFRGS).

\*\* Universidade Federal de Ciências da Saúde Porto Alegre (UFCSPA).

\*\*\* Instituto de Pesquisa com Células-Tronco (IPCT).

# 3DBB

2020 Aug 26-28th

1st INTERNATIONAL DIGITAL CONGRESS ON  
3D BIOFABRICATION AND BIOPRINTING

NUT3D – PPGB – UNIARA

## Development of a nanostructured drug for the treatment of spinal cord injury

Rafaela Zimmermann\*; Daikelly Iglesias Braghirolli\*\*; Patricia Pranke\*\*\*

### (Biomaterials)

**Abstract:** Spinal cord injury (SCI) is a serious condition that leads to a sudden loss of motor, autonomic and sensory function. Tissue injury associated with SCI is determined by a cascade of pathophysiological events that impair neural regeneration and restoration of motor function. Therefore, it is extremely important to develop new therapeutic strategies in this area that prevent the increase of severity of the tissue damage. Nanocapsules (NCs) are a promising drug delivery system that are being used in regenerative medicine. NCs can increase the bioavailability and concentration of the encapsulated drug in a determined target. Therefore, the use of NCs can be interesting in the treatment of spinal cord injury. In this work, a variety of systems have been developed with the aim of encapsulating a drug which has been researched (named "X") for the treatment of SCI and comparing it in terms of diameter, polydispersity index (Pdl) and zeta potential. Methodology: All the NCs were prepared using the technique of interfacial polymer deposition, where the emulsions are formed by deposition of an oil phase (OP) on an aqueous phase (AP). Following this, all the NC emulsions were concentrated under reduced pressure. The polymer poly (lactic-co-glycolic acid) (PLGA) was used because it is biodegradable and biocompatible. Group I was composed of PLGA, castor oil and acetone in OP and distilled water, Triton X100 and drug X in AP. Group II was formed of PLGA, sorbitan monoesterate, TCM and acetone in OP and distilled water, polysorbate 80 and drug X in AP. Group III was formed of PLGA, copaiba oil and acetone in OP and distilled water, Triton X100 and drug X in AP. Group IV was composed of PLGA, açai oil and acetone in OP and distilled water, Triton X100 and drug X in AP. The characterization of the NCs was conducted in ZetaSizer equipment. Results: The NCs of group I exhibited an average diameter of 138 nm, Pdl of 0.450 and zeta potential of -27.7 mv. Group II presented the average values: diameter of 214 nm, Pdl of 0.343 and zeta potential of -24.5 mv. The NCs of group III exhibited average values: diameter of 584 nm, Pdl of 0.618 and potential zeta of -6.35 mv. Group IV presented the average values: diameter of 602 nm, Pdl of 0.547 and zeta potential of -3.37 mv. Conclusions: These results reveal that the nanocapsules of groups I and II have a more suitable size and polydispersion in relation to groups III and IV, and also present values of zeta potential that reveal that the charges present on the surface of the nanocapsules prevent coalescence between them, thereby avoiding agglutination, which attests to their stability. The next phase will be the evaluation of the efficiency of encapsulation.

**Keywords:** Spinal Cord Injury; Nanocapsules, Poly (Lactic-Co-Glycolic Acid).

\* Hematology and Stem Cell Laboratory, Faculty of Pharmacy, Federal University of Rio Grande do Sul (UFRGS), Porto Alegre, RS, Brazil.

\*\* Post-Graduate Program in Physiology, UFRGS.

\*\*\* Stem Cell Research Institute, Porto Alegre, RS, Brazil.



## Methodology for developing assistive technology devices from medical images

Lucas Vinícius Araújo Sales\* ; Ketinlly Yasmyne Nascimento Martins\*\* ; Rodolfo Ramos Castelo Branco\*\* ; Isabella D. Gallardo\*\* ; Carlos Alberto M. Dos Santos\*\* ; Anna Kellssya L. Filgueira\*\* ; Júlia M. R. Da Costa\*\*

### (Devices and processes)

**Abstract:** The search for precision in the modeling of Assistive Technology (AT) devices, especially orthoses, has made technological strategies that integrate the areas of medical sciences and engineering indispensable. In this scenario, three-dimensional technologies have stood out for being able to generate a customized manufacturing process. The potential advancement in medical image acquisition equipment, mainly Computed Tomography (CT), in turn, allowed the expansion of this panorama even more, enabling, together with CAD systems (computer aided design), the development and modeling of devices manufactured based on medical exams. Therefore, this study aims to present a methodology for developing AT devices from medical images. Methodology: From medical image exams in DICOM format, preferably from CT, the treatment is performed in the InVesalius software, aiming to remove possible noise generated by artifacts during the exam, as well as analysis and choice of anatomical regions of interest. Soon after, the images are exported in STL format in mesh manipulation software, Autodesk Meshmixer, in which it is possible to perform orthosis device modeling using specific tools for mesh editing and finalization of the digital model. After that, is possible manufacturing by Additive Manufacturing and subsequent testing of the AT device on individuals. Results and Conclusion: The association of medical images with the development of AT devices using three-dimensional technologies, allows the acquisition of an equally accurate model, or even superior, to conventional processes. It is also possible to provide repeatability of this methodology, as well as offering a simplified process with open access software. This association may have advantages for the development of these devices, especially in individuals with conditions that make contact with third parties unfeasible or difficult. However, care should be taken to perform CT scans exclusively for obtaining orthoses, due to the exposure to radiation involved, and it is ideal and feasible that this methodology should be used after taking images that initially aim at the diagnosis of the patient.

**Keywords:** Assistive Technology; Orthoses; Additive Manufacturing; Medical Images; Computed Tomography.

\* Universidade Federal de Campina Grande – UFCG, Campina Grande, PB, Brasil.

\*\* NUTES – Universidade Estadual da Paraíba – UEPB, Campina Grande, PB, Brasil.





## Digital twin model for the fabrication of porous scaffolds using masked stereolithography

Ivannova Michelle Jumbo Jaramillo\*; Karolina Estefanía Serpa Andrade\*; Stefany Alejandra Pusda Quiroz\*

(Digital / Information Technology)

**Abstract:** Accurate process models is a fundamental keystone as additive manufacturing technologies are being generated and deployed. Validated models reduce the need for real-world testing of materials and processes and give bioproduct designers a predictive capability for optimizing part designs. Objective: This study evaluates a digital twin model in order to define conceptual guidelines to support the implementation of process modeling for the fabrication of porous scaffolds using masked stereolithography (M-SLA). Methods: The proposed digital twin model includes physics-based approach (fundamental M-SLA process equations), geometrical approach (triply periodic minimal surface equations) and statistical approaches (statistical process control), all of them embedded in a virtual platform in order to predict the material properties and process behavior during the manufacturing of porous structures which will be used as scaffolds in tissue engineering. Results: Preliminary results show that it is possible to optimize the design of porous structures (porosity, pore size, strut size, and orientation during fabrication) and process parameters (light intensity and pull-up velocity) to maintain the accuracy and reliability of the M-SLA process. Conclusions: A comprehensive digital twin of M-SLA process can improve porous scaffolds' product quality, through the reduction of variation in product properties, and faster product development time. Functional implications of the proposed digital twin model regard the possibility to reduce the number of trial and error tests to obtain desired porous structures attributes and reduce the time required for scaffold qualification in tissue engineering.

**Keywords:** Digital Twin; Stereolithography; Digital Manufacturing; Process Modeling.

\* Universidad de las Fuerzas Armadas ESPE, Ecuador



## Development and evaluation of natural biomaterial made of chitosan for use as a bioink

Rafaela Hartmann Kasper\*; Gabriela Machado\*; Natasha Maurmann\*\*; Caren Bavaresco\*; Patrícia Pranke\*\*; Luciano Pighinelli \*\*\*

### (Biomaterials)

**Abstract:** The use of natural polymers in the production of structures used to stimulate cell development and tissue regeneration is proving to be a promising strategy in biofabrication. Chitin is an abundant polysaccharide in nature and chitosan is obtained by the process of deacetylation of chitin. Methodology: In this study, chitosan was dissolved, filtered and crowded. Following this, Buriti oil and fish scales were added to the chitosan. Chitosan and chitosan associated with the Buriti oil and Salmon fish scales were tested regarding their influence on the viability of human keratinocyte cells. The cells from the immortalized keratinocyte line (HaCaT) were seeded at a density of 5,000 cells per well, directly in 96-well tissue culture plates (TCPs). After 24 hours, the cells were treated with culture medium (control), 0.13% of chitosan; 0.13% of chitosan conjugated with salmon fish scales, or 0.30% of chitosan conjugated with Buriti oil. Cell viability was tested based on 3-(4,5-dimethylthiazol-2-yl)-2,5-diphenyltetrazolium bromide assay (MTT) after four days of cultivation. Results: The results of mitochondrial activity in relation to cell viability showed statistical significance between the cells cultivated in the well plate (control group) and chitosan tested alone. The mean and standard deviation values obtained from the results related to control of the cell viability (%) of the treated groups compared to the TCPs (used as a control group) were  $100.0 \pm 10.1\%$  and the chitosan only was  $87.6 \pm 9.7\%$  ( $p < 0.01$ ). In contrast, the cultivation of both types of conjugated chitosan were higher than the chitosan alone and similar to the control. The value obtained for chitosan conjugated with Buriti oil was  $100.3 \pm 6.8\%$  (ns) and  $95.9 \pm 15.2\%$  (ns) with the fish scales. Conclusion: It is possible to affirm that the association of chitosan with Buriti oil and Salmon scales was beneficial for the viability of the cultivated cells, being promising biomaterials for tissue regeneration. These associated biomaterials can be used as bioink in bioprinting studies as these materials presented biocompatibility.

**Keywords:** Biocompatible Materials; Tissue Engineering; Regenerative Medicine; Buriti oil; Fish scale.

\* Universidade Luterana do Brasil.

\*\* Universidade Federal do Rio Grande do Sul (UFRGS).

\*\*\* Biomater P&D Ind. de biomateriais LTDA.



## Synthesis and characterization of polymeric hydrogel based on corn starch by click chemistry reaction (Diels Alder) for application in regenerative medicine

Bruna Fernandes Antunes\*; Alessandro Gandini\*\*; Antônio J. F. Carvalho\*\* Eliane Trovatti\*

### (Biomaterials)

**Abstract:** The search for new materials derived from biopolymers has received increasing attention due to its potential applicability in several sectors, including the health area. However, biopolymers still find little application in this area due to the limited mechanical properties and the rapid biodegradability under physiological conditions, which is the case of starch, for example. Starch is a polymer from a renewable natural source, of high availability, high biocompatibility and biodegradability in physiological medium and at low cost. The presence of hydroxyls in its structure allows its chemical modification, thus allowing the crosslinking of the polymeric chains. Thus, this project deals with the application of the click chemistry reaction of Diels Alder (DA) for the crosslinking of starch, in order to obtain a material with a longer biodegradation time in the physiological environment aiming at application in the health area. For this, modifications were made to the starch through gelling, oxidation, esterification and cross-linking, which were proven through Optical Microscopy (MO), Fourier Transform Infrared Electroscopy (FTIR), conducting titration and Proton Nuclear Magnetic Resonance (NMR-1H). Through the FTIR it was possible to observe that in the control starch sample, the peak  $1600\text{ cm}^{-1}$  corresponding to the C=O group is in accordance with the characteristic; oxidized starch, on the other hand, shows an increase in this peak suggestive of an increase in COOH, and in the sample of esterified starch there is a decrease in it, and in addition, the peak appears in  $885\text{ cm}^{-1}$  corresponding to furan rings, being suggestive of the replacement of COOH in furan. It was quantified that the substitution was 13%. Confirmed through the NMR-1H in which furan groups were visualized, in positions 7.4; 6.2 and 6.4 ppm corresponding to the H5, H4 and H3 protons of furan. In addition, the crosslinking of the material was successful after visual analysis of the increase in viscosity. Therefore, a new material with viscosity alteration properties has been synthesized and new studies can be carried out with a view to promising applications, mainly in the area of regenerative medicine.

**Keywords:** Modified starch; Biomaterial; Biopolymers; Tissue engineering.

\* University of Araraquara (UNIARA).

\*\* University of São Paulo (USP).



## Standardization and automation of tumor spheroid production

Guilherme de Almeida Miranda\*; Leonardo Boldrini\*; Leandra Santos Baptista\*\*

### (Biofabrication and bioprinting (in general))

**Abstract:** Cancer is one of the most lethal diseases in the world, with high rate of morbidity and mortality in several countries. In Brazil, for example, studies show that probably more than five thousand cases will appear per year from 2020 (INCA). This increase in the number of cases may be due to the increase in life expectancy along with people's eating habits and lifestyle. As a result, there is a need to develop new approaches that provide a better reproduction of the tumor microenvironment for carrying out studies that allow the discovery of new efficient treatments. In this context, spheroids are an excellent experimental model for the study of cancer due to their 3D organization combined with the possibility of long periods in culture and their ability to reproduce the extracellular medium with greater precision. In addition, the application of spheroids becomes an interesting strategy in this scenario, since they can be biofabricated automatically by robotization, which provides the standardization and dimension of this micro-tissue. Currently, many studies have used the production of spheroids from tumoral cell lineages for in vitro drug screening. However, these spheroids have high deformity and inefficiency in the reproducibility of their characteristics, even within the same experiment. The large-scale production of cellular spheroids in a reproducible way and with established safety standards is still something that needs advances in bioengineering and metrology. Due to this current problem, the standardization, reproduction and efficiency in the production of cellular spheroids on a large scale are of great importance for studies and their applications in cancer research. Thus, the aim of our study is to combine biological, physical and metrological parameters in a proposal for scaling and standardizing the production of multicellular tumor spheroids in an automated way. The evaluation of the mechanical properties of tumor spheroids can provide us with relevant information about the viability and structure of these spheroids, something that is still poorly explored. Besides, through quantitative and qualitative analyzes, we can evaluate the reproducibility and programming of the production method. The preliminary results obtained in this work demonstrate the potential of the automated spheroid production platform, making it possible to produce up to 3072 in a single process. It was also analyzed that different tumoral cell lineage present ideal parameters for production. Therefore, the proposed technology provides advantages of scaling, reproducibility and repeatability of the 3D culture using the micro-molded agarose hydrogel technique for the application of the manufactured spheroid as an alternative for the development of new treatments and in drug monitoring tests in cancer chemotherapy.

**Keywords:** Cancer; Spheroids; Production; Automation.

\* Inmetro.

\*\* UFRJ.



## Development of an experimental analysis system for tissue bioprinting

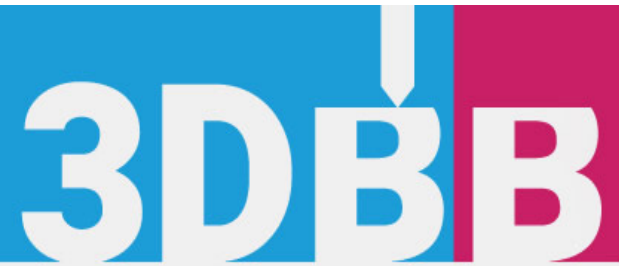
Solange Rodrigues De Oliveira\*; John Paul Hempel Lima\*

### (Biofabrication and bioprinting (in general))

**Abstract:** According to the Ministry of Health, in the year 2019 alone, only 33% of the family members of potential donors authorized the donation of organs, thus contributing to an increase in the demand for transplants already high in the country. Thinking about these issues and taking into account the durability and quality of transplanted organs today, medicine has been advancing in the technological field to make possible, in the near future, the production of personalized organs through a bioprinters. In this work the construction of an extruder-type bioprinter was carried out from a 3D printer model Ender from PCyes. As this is an experimental analysis, a microscope was attached to the bioprinting head in order to capture images during the entire printing process of the Bioink . The ImageJ software was also used for the analysis of these images in which it was effective in quantifying cells. The survey of effectiveness is an important step for research involving tissue production. Besides helping to eliminate possible noise at the time of manufacture, this technique can be used in the future to analyze parameters during bioprinting not observed without the aid of a microscope. The steps of the bioprinting process include a modeling that can be performed in specific software such as Autocad, Blender, Freecad (the same used in traditional 3D printing) then exported to other slicing software; this modeling can be of data images such as magnetic resonance imaging or CT scans sequentially choosing the material and type of cell grown. The bioprint by extrusion is the deposition of the Bioink that is propelled in filament form through a nozzle extruder layer by layer until forming a construct with good stabilization, at the moment of its bioprint , this material must have good rheology or good fluidity and after printed must remain stable. The filling patterns for bioprinting can be of the type, rectilinear, grid, hexagonal or concentric; respecting the characteristics of the filament such as diameter, spacing and uniformity; with an adequate topography the cells will be properly nourished, having among them communication, migration, proliferation and differentiation.

**Keywords:** Bioinks; Bioprinting; Tissue engineering; Organoids; Bioengineering.

\* Departamento de Engenharia da Faculdade de Ciências Exatas e Tecnologia Pontifícia Universidade Católica de São Paulo (PUC-SP).



2020 Aug 26-28th

1st INTERNATIONAL DIGITAL CONGRESS ON  
3D BIOFABRICATION AND BIOPRINTING

NUT3D – PPGB – UNIARA

## Functionalized nanotubular surfaces on Ti-6Al-4V ELI alloy cellular structures made by additive manufacturing

Guilherme Arthur Longhitano\*; André Luiz Jardim\*\*; Rubens Maciel Filho\*\*

(Biomaterials)

**Abstract:** The increase in life expectancy and the constant demand for better quality of life make the development of new materials and techniques a constant requirement. Customized implants, functionalized surfaces and biological mimetic morphologies are some current trends in medicine. In orthopedics, an implant must present biocompatibility, low stiffness and high mechanical and corrosion resistance. Additive manufacturing (AM) made it possible to produce Ti-6Al-4V ELI alloy customized implants with complex geometries, such as porous cellular structures. These structures provide better conformity of bone and implant stiffness, bypassing the bone resorption (stress shielding) process and promoting faster and longer lasting adaptation. The Ti-6Al-4V alloy may also have its surface modified by the anodizing technique. As a result, functionalizations by improving corrosion resistance, incorporation of beneficial ions and drug incorporation for in situ delivery become possible. The combination of these techniques results in reduced surgery risks, faster patient recovery, longer implant durability, better aesthetic and ergonomic results and, above all, improvement in patient's quality of life. This work produced Ti-6Al-4V ELI alloy cellular structures by Direct Metal Laser Sintering (DMLS), a metal AM technique. The surfaces were functionalized by electrochemical anodization technique in a 1 M  $\text{NH}_4\text{H}_2\text{PO}_4$  and 0,3 M  $\text{NH}_4\text{F}$  solution. Geometric, mechanical, and surface characterization techniques were used for analysis. Cellular structures with open porosity, which mimic bone tissue, were successfully obtained. The samples presented a 71.1% porosity with a stiffness of  $2.39 \pm 0.23$  GPa. The surfaces presented a topography composed by nanopores and nanotubes. Fluorine ions were incorporated into the surfaces during the processes, obtaining concentrations of ~ 9.9 at%. The results suggest that the use of combined technologies for manufacturing customized and functionalized orthopedic implants can reduce infection risks and improve implants lifespan.

**Keywords:** Ti-6Al-4V; Additive Manufacturing; Functionalization; Nanotubes; Cellular Structures.

\* Renato Archer Information Technology Center (CTI).

\*\* School of Chemical Engineering, State University of Campinas.



## Rheological evaluation of cellulose nanofibers\gelatin composite hydrogels potentially applicable to bioprinting

Lucas Noboru Fatori Trevizan\*; Hernane Da Silva Barud\*

### (Biomaterials)

**Abstract:** 3D bioprinting technology is directly related to the deposition of biomaterials, cells, biological structures and growth factors layer by layer. Studies currently carried out use hydrogels based on polymeric associations to obtain the bioinks. Hydrogels applied to bioprinting must satisfy requirements of both conventional and biological materials for optimized, functional applicability, and to reduce the rejection rates of the target organism. Generally, all of these hydrogel formulations use a viscous polymer solution for its printing. However, the properties related to this material are directly correlated with the printability, mechanics, degradation, functionalization, and must meet the biological requirements, as biocompatibility, cytocompatibility and bioactivity. One aspect of these properties is the ability to print and self-arrange three-dimensionally. Therefore, the rheology of its materials is an essential factor in determining a hydrogel applicability for bioprinting. Thus, the objective of the current work was to evaluate the rheological properties of hydrogels with different concentrations of cellulose nanofibers (PCNF) and gelatin (Gel), analyzing their viscosity property and their behavior using the rheometry. Thus, hydrogels with different concentrations in percentage of Gel/PCNF were prepared (100/0; 75/25; 50/50; 25/75; 0/100). Their rheological characterizations were performed at 25°C using a 40 mm diameter plate-plate geometry in a TA Instruments AR 1500ex Rheometer. The Ostwald-de Waele power law model was used to calculate the viscosity and the  $n$  index as a function of shear rate. In conclusion, the formulations showed that the increase of gelatin percentage affected directly the hydrogel viscosity. Furthermore, the characteristic of medium viscosity in comparison to the other formulations indicates that the formulation with 25%PCNF / 75%Gel can be considered promissory to be applied to 3D bioprinting.

**Keywords:** Hydrogel; Cellulose Nanofiber; Gelatin; Rheology.

\* University of Araraquara (Uniar), Araraquara, SP, Brazil.



## Biospeckle´s application: an analytical monitoring contribution to fungi inoculation first hours

José Francisco Ferreira de Oliveira\*; Inacio Maria Dal Fabbro\*\*

### (Applications)

**Abstract:** Researches based on the application of Speckle, a technique based on the relationship of statistical interference originating at random, when the laser beam is applied to surfaces, has its appearance connected to the theory of light scattering, and this theory involves the process of interaction of light with matter. When the result of monitoring these analyzes of rough surfaces comes from one with biological activity, it is called Biospeckle. Our research proposal was to demonstrate the application of Biospeckle as a viable tool for monitoring and analyzing the possibility of biology activity in fungi on its first hours of inoculation. In order to demonstrate it, we used three indexes of biological activity analysis, namely: Moment of Inertia (IM), Differences of Absolute Values (AVD) and Speckle Space-Time (STS). By getting these indicators results, we obtained different fungi images in the first days of their incubation, evolving for the first hours, to measure the development of fungi in Petri dishes. When conducting the research, the used procedures were aiming to obtain results that could assist and help in the application of the Biospeckle in many stages of fungal incubation, but essentially on its first hours. The isolation of all filamentous fungi in their growth environment, used in this research work, was performed under aseptic conditions in the Vertical Laminar Flow Safety Chapel. It can be inferred that fungi inoculated in Petri dishes were radially developed in their early days. This process can be well observed by applying the randomly selected points distribution technique following a Gaussian distribution, which is a literature area analysis methodology, then it allows to present a new correction in the growth curve. Therefore, it is possible to follow the displacement of the nucleus of biological activity by varying the focus, applying the Gaussian distribution. All in vitro experimental research procedures were performed at the Mycology Laboratory of the Faculty of Food (FEA / UFLA) and at the Optics Laboratory (FEAGRI / UNICAMP). The fungi were provided by the library of the Collection of Culture of Microorganisms (CCDCA), located in the Laboratory of Mycology and Mycotoxins within the Department of Food Science at UFLA.. The developmental analysis showed to be quite fruitful, demonstrating that the laser Biospeckle technique revealed to be a good monitoring tool in the first hours of growth for both genus *Aspergillus* and *Penicillium*.

**Keywords:** Biospeckle; IM; STD; AVD; Fungos.

\* Instituto Federal de São Paulo IFSP.

\*\* Universidade Estadual de Campinas (Unicamp).





## Films obtention from recovery of expanded polystyrene

Ingrit Daniela Pardo Mendoza\*; Jeffrey León Pulido\*

(Biomaterials)

**Abstract:** Expanded polystyrene (EPS) is a plastic obtained from the polymerization of styrene, and represent the fourth most used plastic along the world. EPS is used in industries such as construction, food packaging and transport of delicate materials among other applications. Due to the fact that it is composed of more than 95% air. Within applications is a thermal–acoustic insulator, shock absorber and a light and durable filling material, since it is not hygroscopic, nor does it represent a substrate for microorganisms. However, have a slow degradation rate, this added to the fact that it is a single–use plastic and one of the least recycled due to its low density, it is generating significant problems for the environment since most of their waste ends up accumulating in landfills. This work presents a sustainable alternative for EPS recycling, using eucalyptus oil and limonene as natural solvents. Experimental practices were carried out where the dissolution potential was evaluated at different proportions of EPS (1:10, 1: 3, 1: 2, 3: 4, 1: 1, 1.25: 1 and 1.5: 1) in a controlled environment and the saturation point of each solvent was determined. Additionally, the influence of the temperature between 294 K and 323 K they were studied. A relation for overall composition was obtained that eucalyptus oil and limonene (1:1 and 1.5: 1 respectively) including variables such as weight and solvent properties. The result present on average both solvents can reduce the volume of waste by 96–97%. In addition, in this work was done with the obtained resins, adding ethanol in order to precipitate the polystyrene (PS), then the solvents were separated by vacuum filtration and rotary evaporator to be reincorporated in other process, the recovered PS was dried in an oven at 343 K to remove alcohol residues and obtain a polymer with high hardness if limonene is used and a polymer with characteristics of flexibility and elasticity using eucalyptus oil.

**Keywords:** Sustainable; dissolution y polystyrene.

\* Chemical Engineering, Faculty of Engineering – EAN University, Bogotá, Colombia.



## Fabrication of a biomaterial with gelatin, alginate and $\beta$ -TCP for the treatment of fractures caused by osteoporosis

Thaís Pezza de Souza\*; Antonio Carlos Guastaldi\*; Rodrigo Fernando Costa Marques\*\*

### (Biomaterials)

**Abstract:** Considering the increase of the life expectancy and the number of osteoporosis cases, the development of materials that can be used as support in bone fractures treatment decurring from this disease is necessary. With the progress in biomaterials area, there is the potential of using gelatin and alginate in their formulation, because they have good biocompatibility, low toxicity and can be used as drug delivery. It is known that  $\beta$ -TCP (beta tricalcium phosphate) has bioactivity and bone growth inducing properties and could compose the biomaterial formed of gelatin and alginate. Thus, the objective of this work is to obtain a biomaterial composed of gelatin, alginate and  $\beta$ -TCP to be used as a 3D printer ink aiming the treatment of fractures caused by osteoporosis. Methodology:  $\beta$ -TCP, tri-sodium citrate 2-hydrate (PA, Panreac), sodium alginate (PA, Exodo) and powdered gelatin (Synth) were dispersed in aqueous solution and then mixed in a magnetic stirring at temperature of 55°C degrees. The presence of sodium citrate ensure that agglomeration is not formed. Different concentrations were studied and the influence of each compound was evaluated by FTIR-ATR (Frontier Dual Range, PerkinElmer), DSC (2910, TA Instruments) and rheological test (rheometer AR 2000ex, TA Instruments). Results: FTIR spectra showed the bands of  $\beta$ -TCP ( $\nu_4$  PO<sub>4</sub> – 750–500 cm<sup>-1</sup>;  $\nu_3$  PO<sub>4</sub> – 1100–900 cm<sup>-1</sup>), gelatin and alginate chains (C–O carboxylic acid – 1400 cm<sup>-1</sup>; C=O carboxylic acid – 1700–1500 cm<sup>-1</sup>) and an increase of intensity after crosslinking was observed. By DSC analysis, it was observed that, when adding  $\beta$ -TCP and sodium citrate, the melting point temperature is shifted to lower temperatures, indicating an increase in the order of the material generated by the addition of  $\beta$ -TCP, that make it possible to increase the interaction between polymer chains. The rheological test showed that  $\beta$ -TCP increases the values of G' and G'' and that the elastic behavior is predominant, indicating that the addition of phosphate contributes to the material structure obtained, enabling an increase in the polymer chains interaction. Conclusion: The addition of  $\beta$ -TCP provides an increase in the mechanical properties of the material obtained and presents a viable alternative to compose the biomaterial that will be used as ink for 3D printing.

**Keywords:** Biomaterials; Osteoporosis; Gelatin; Alginate;  $\beta$ -TCP.

\* Instituto de Química – UNESP Araraquara.



## Development of films and filaments containing $\beta$ -TCP and bacterial cellulose based on a polymeric matrix for 3D printing

Gabriel Cardoso Pinto\*; Miguel Jafelicci Junior\*; Antonio Carlos Guastaldi\*

### (Biomaterials)

**Abstract:** Considering the aging of the population, increase in life expectancy and quality of life, increase in accident rates, economic and technological aspects, the development of biomaterials for bone tissue regeneration is of great importance and its demand is increasing every day. However, the complex structure and properties of natural bone limit the use of synthetic materials and manufacturing techniques, currently available, which could be used as custom implants or Scaffolds for the treatment of bone defects or guided bone regeneration. This challenge can be overcome by using 3D printing technology, which is an excellent approach to overcome the limitation that supports the efficient and rapid manufacture of customized complex bone substitutes. Natural and synthetic polymers associated with calcium phosphates allow the development of important composites to be used in the manufacture of 3D Scaffolds, due to their composition, combining favorable properties of both phases. The objective of this research was to study the use of bacterial cellulose (BC) and synthesized calcium phosphates ( $\beta$ -TCP), in the nano and microstructure for the development of films and filaments to be used in obtaining 3D Scaffolds. To determine the best way to interact  $\beta$ -TCP with bacterial cellulose, it was initially proposed to obtain the film containing these two materials, with the PCL (Polycaprolactone) polymer being the binding agent. Another method proposed to interact  $\beta$ -TCP with BC was through obtaining filaments of these materials with PLA (PolyLactic acid) as polymeric matrix in the NuLEEN laboratory extruder (UFSCar). For the films and filaments synthesized, characterizations techniques as thermogravimetry, scanning electron microscopy (SEM) and infrared confirmed the mass proportion used, the morphology and the presence of the main functional groups of  $\beta$ -TCP, PCL and PLA components. Due to the insolubility of CB, in polar and nonpolar media, there was the formation of a CB aggregate in the films synthesized, but for filaments a greater homogeneity was observed, confirming then that filaments based on PLA/ $\beta$ -TCP/CB are a promising alternative for an biomaterial that can be used in 3D printing for regenerative engineering.

**Keywords:** Calcium Phosphate; Scaffolds 3d; Regenerative Engineering; Biomaterial, Bone.

\* Instituto de Química – Unesp Araraquara.



## Biofabrication and the medical field: which is the scenario for 2030?

Emanuel S. Serrano\*; Liliana Coutinho Vitorino\*; Henrique De Amorim Almeida\*\*

### (Biofabrication and bioprinting (in general))

**Abstract:** Nowadays, Additive Manufacturing is more and more a frequent topic of discussion, due to its effects and causes, not only at a technological level, but also in terms of economic, social and political levels and its impact has been observed on several sectors, especially in the medical field. These technologies have created a specific technological field, namely biofabrication / biomanufacturing which is capable of producing medical devices with the combination of biomaterials, drugs and growth factors with or without the inclusion cells for the production of biomedical implants for both permanent or temporary applications. These technologies have shown to be capable of meeting the requirements demanded by the medical sector. However, the significance of these technologies can't be based only on the current context, but also need to be assessed in the future context. This study intends to develop reliable future scenarios for this technology, for a very specific and important sector, namely the medical field. Concerning this prediction, academic studies dedicated to additive manufacturing and the medical field are non-existent. In this context, the Delphi method combined with the PEST analysis was applied to world experts in the field of biomanufacturing with the goal of presenting the impacts related to this technology for the horizon of 2030, concerning four different dimensions: political, economic, social and technological. The results made it possible to obtain projections for the next decade, revealing satisfactory levels of agreement among the specialists in the four dimensions that are included in this analysis, with the highest values related towards the technological dimension. This study also provides an awareness of the needs and concerns of the usage of this technology in the medical domain.

**Keywords:** 3D Printing; Biofabrication; Medical Applications; Delphi Method; PEST Analysis.

\* Escola Superior de Tecnologia e Gestão (ESTG), Politécnico de Leiria (IPL), Leiria, Portugal.

\*\* Centro de Investigação em Informática e Comunicações (CIIC), Politécnico de Leiria (IPL), Leiria, Portugal.



## Synthesis and characterization of L-lactide for poly-L-lactic acid production aiming its application in the medical field

*Bruna Letícia de Carvalho Cunha\**; *Maria Ingrid Barbosa Rocha Schiavon\*\**; *Letícia Xavier\**; *Viktor Oswaldo Cárdenas Concha\**

### (Biomaterials)

**Abstract:** The search for polymers from natural sources increased exponentially since they have potential to replace petroleum derived polymers. Some of these biopolymers are biodegradable, which have wide application as a biomaterial in the health area. Among them, Poly Lactic Acid (PLA), stands out for being a biodegradable polyester with excellent physical and biological characteristics. The main route for high molar mass PLA has the Lactide as starting monomer, commonly produced by depolymerizing the PLA. Currently, there is a deficiency in knowledge about the lactide obtaining process and divergences about reaction parameters. In addition, the synthesis of PLA from this dimer has a high production cost, since the monomer has high added value. In this context, L-Lactide production process is fundamental for your use as a monomer for the synthesis of high molar mass PLA, which is widely used in medical applications. Therefore, this work aims to evaluate the effect of temperature, pressure and reaction time in the L-lactide synthesis process, in order to obtain a high molar mass PLA. For this, a 23 factorial design was carried out, with central point triplicate, considering a temperature variation of 170 to 200 ° C, pressure of 50 to 200 mmHg, and reaction time of 2 to 6 hours. The L-lactide produced had its thermal and spectroscopic properties characterized by techniques of Differential Scanning Calorimetry (DSC), Thermogravimetry (TGA), Fourier-transform infrared spectroscopy (FTIR) and X-ray powder diffraction (XRD). Previous results showed the formation of L-Lactide in some system points (connector between reactor and round bottom flask, round bottom flask and condenser), whose properties were compatible with L-Lactid standard sample (PURASORB® L).

**Keywords:** L-Lactide; Poly-L-Lactic Acid; Biopolymer; Synthesis; Characterization.

\* Universidade Federal de São Paulo (Unifesp).

\*\* Universidade Estadual de Campinas (Unicamp).



## A natural extracellular matrix hydrogel derived from decellularized bovine cornea: a new biomaterial for the development of 3D models

Jordana Andrade Santos\*; Artur Christian G. Da Silva\*; Marize Campos Valadares\*

### (Biomaterials)

**Abstract:** The use of 3D cellular models to mimic biological microenvironments has been considerably increased in the last years. The development of 3D models is based on the proliferation of cells in a scaffold similar to the extracellular matrix, which generates a favorable condition for cell proliferation. Usually, the scaffolds are composed of polymers or/and matrix elements, such as collagen type 1. The marketed collagen is generally produced from rat tails, at high cost and, to improve its functionality, it is necessary to add other matrix elements and growth factors. The use of decellularized Extracellular Matrix (dECM) hydrogels from food industry waste can be more sustainable, representing a lower cost alternative and mimicking more closely the complexity of the extracellular matrix better than the isolated Collagen or any other material. In addition, can contribute to the reduction of animal use in research, which is aligned with the 3R's principle in the context of the 21st century Toxicology. This work aims to develop a new hydrogel source for future applications in the construction of 3D tissue models. **Methodology:** Bovine corneas, were collected in a slaughterhouse in Goiania, Brazil. The corneas were subjected to decellularization by 0.5% Sodium dodecyl sulfate, maceration with tissue grinder, lyophilization and neutralization to obtain hydrogel. The sample was evaluated for decellularization extension by H&E staining. The structural and compositional change of dECM hydrogel components were analyzed using alcian blue stain to visualize GAGs, azan blue stain to visualize collagen, scanning electron microscopy to visualize the ultrastructure, total proteins (BCA) and Turbidimetric gelation kinetics. Hydrogel were compared with native corneas and decellularized cornea. **Results:** The hydrogel obtained from bovine cornea showed the concentration of total proteins was similar between different batches of samples ( $p = 0.0956$ ). the decellularization method was effective and biochemical components (collagen and GAGs) were preserved, however in visually smaller quantities than in the native matrix. Gelation kinetics of cornea dECM hydrogel and collagen type 1 showed that collagen reach first gelation compared to hydrogel, but all samples were cross-linked at the end of the analysis. **Conclusions:** The bovine cornea is a natural source of matrix components and can be applied as biomaterial in the field of different tissue engineering in future applications.

**Keywords:** Extracellular Matrix; Hydrogel; Tissue Engineering; Biomaterial; Cornea.

\* Laboratory of Education and Research in *In Vitro* Toxicology, Tox In, Faculty of Pharmacy, Federal University of Goiás (UFG), Brazil.

# 3DBB

2020 Aug 26-28th

1st INTERNATIONAL DIGITAL CONGRESS ON  
3D BIOFABRICATION AND BIOPRINTING

NUT3D – PPGB – UNIARA

## Rheological effects of laponite clay in gellan gum gels aiming biomaterial inks for 3d bioprinting

Mayté Paredes Zaldivar\*; Lucas Noboru F. Trevizan\*; Diego Silva Batista\*; Hernane Da Silva Barud\*

### (Biomaterials)

**Abstract:** The 3D bioprinting or additive manufacturing is a growing technology used in tissue engineering. It is used to deposit layer-by-layer biological inks to obtain 3D objects. These inks can be composed by biomaterials, cells and support components. The most commonly used inks are viscous polymer solutions (gels) that after printing and gelling processes became hydrogels, maintaining the 3D object structure. The gellan gum (GG) is a high molecular weight and water-soluble anionic polysaccharide produced by the bacteria *Sphingomonas elodea*. It is biocompatible, biodegradable and can form very viscous gels even at low concentrations. The laponite (Lp) is a synthetic nanosilicate clay used as a rheology modifier of water solutions. It is also non-toxic and enhances biological activities like cell adhesion and proliferation. Thus, the objective of this work was to study the rheological effects of laponite in gellan gum gels aiming to define the better gel-ink composition for 3D bioprinting. Gels with concentrations of 3% (m/V) in distilled water and different GG/Lp compositions (100/0; 90/10; 50/50) were prepared. Their rheological characterizations were performed at 25 °C using a 40 mm diameter plate-plate geometry in a TA Instruments AR 1500ex Rheometer. The Ostwald-de Waele power law model was used to calculate the viscosity and the n index as a function of shear rate. The results indicated that laponite addition affected the shear-thinning and the solid-like behaviors of GG gels. The pristine GG formed a very viscous gel, hard and slightly brittle that after laponite addition showed a significantly decrease in their viscosity. The data was successfully fitted to the Ostwald-de Waele model and all the n indexes were less than 1, indicating the pseudoplastic behavior of gels. We can conclude that effectively the laponite acts as a rheology modifier in gellan gum gels solutions and that the gel composition with 90 % of gellan gum and 10 % of laponite (90/10) showed the better viscosity characteristics. This gel composition of GG/Lp will be used as biomaterial ink in 3D extrusion bioprinting.

**Keywords:** Biomaterial Inks; 3d Bioprinting; Gellan Gum; Laponite; Rheology.

\* University of Araraquara (Uniará), Araraquara, SP, Brazil.



## Study of in-vitro degradation of poly (butylene adipate co-tereftalate) based polymers processed by FFF 3D printing

Bruno da Costa Oliveira\*; Luis Alberto Loureiro Dos Santos\*

### (Biofabrication and bioprinting (in general))

**Abstract:** The growing advance in the tissue engineering area makes it necessary to study and develop new materials for application as a three-dimensional support for tissue growth (scaffold). In this context, the knowledge of mechanical properties and the degradation rate of materials is of paramount importance, as they are determining factors in the application as a scaffold. In this work, the behavior of the copolymer poly (butylene adipate co-terephthalate) (PBAT) and its blend with poly (lactic acid) (PLA), in different proportions, were studied in a degradation test in PBF solution. The raw materials in the pellet form were produced and supplied by BASF, under the brand names ecoflex (neat PBAT) and ecovio (PBAT+PLA blend in different proportions). The filaments were produced by extrusion, when it were determined the optimal parameters. The parts were processed in a FFF 3D printing equipment, varying parameters such as nozzle and bed temperature, in order to determinate the best printing profile. Variations in mechanical properties (young's modulus/tensile strenght/elongation at break), mass loss and changes in surface morphology of printed samples were evaluated over 60 days of immersion. The printed PBAT samples showed high elongation at break and low elastic modulus compared to the blend. Parts were affected by the degradation period, with greater reductions in mechanical properties.

**Keywords:** Bioprinting; Biomaterials; Scaffold; Tissue Engineering.

\* Federal University of Rio Grande do Sul (UFRGS), Porto Alegre, RS, Brazil.





## Planning and execution of orthodontic traction using a printed biomodel: clinical case report

Marlos Eurípedes de Andrade Loiola\*; Luiz Gonzaga Gandini Junior\*

### (Other topics)

**Abstract:** Advances in digital technology have been changing the orthodontic routine. The incorporation of technologies such as three-dimensional printing assists the professional in making clinical and surgical decisions in some situations, in addition to the possibility of developing orthodontic appliances such as clear aligners that promote tooth movement. **Methodology / Results:** This paper presents the report of a clinical case that illustrates the applicability of this important technology in the dentist's clinical routine. For this, a three-dimensional biomodel printed from files (DICOMs) obtained by computed tomography of an 11-year-old patient was used, with no permanent incisors in the oral cavity that bothered him. This model helped in the planning and execution of extraneous teeth removal surgery, in addition to the correct positioning of accessories for traction of teeth retained in the jaw bone. **Conclusion:** The visualization of anatomical changes through three-dimensional printed models facilitates communication between the team and patients, anticipating decision making, increasing the chances of success and decreasing complications in the execution of treatment.

**Keywords:** Orthodontics; Imaging, Three-Dimensional ; Printing, Three-Dimensional ; Tomography ; Dentistry.

\* FOAR/UNESP, Araraquara, SP, Brasil.

# 3DBB

2020 Aug 26-28th

1st INTERNATIONAL DIGITAL CONGRESS ON  
3D BIOFABRICATION AND BIOPRINTING

NUT3D – PPGB – UNIARA

## Biomodulatory effect of laser radiation on multicellular spheres for application in cellular therapy and bioprinting

Gabriela Gomes Cardoso Gastaldi\*; Sandro B. Moreira\*; Rodrigo A. Rezende\*; Jorge V. L. Da Silva\*\*; Fernanda De F. Anibal\*\*\*; Cynthia A. De Castro\*\*\*; Renata A. De Carvalho\*; Nivaldo Antonio Parizotto\*; André Capaldo Amaral\*

### (Cell cultures)

**Abstract:** The use of mesenchymal stem cells (MSC) is a promising strategy for regenerative medicine (MR) and tissue engineering (TE) for the treatment of tissue and organ injuries. Multicellular spheroids (MS) represent an excellent alternative for cell carriers, both for cell therapy (CT) and/or bioprinting (BP) in MR and TE applications. Using biomodulating resources during the process of constitution of MS, such as low-level laser radiation (LILR), could enhance the biological response. However, research aimed at identifying the effectiveness of this proposal is scarce. Objective: The aim of this study was to analyze the biomodulating influence of LILR on MS from MSC for use in cell therapy and bioprinting. Methodology: Human subacromial bursa MSC (hSBMSC), collected in an arthroscopic procedure, were isolated, characterized and seeded in agarose molds containing microwells ( $3.5 \times 10^5$  cells/mL). The molds were irradiated, during the 5 days of constitution, with LILR at the wavelength ( $\lambda$ ) of 685 nm, power density of 9 mW/cm<sup>2</sup> and doses of 0.5, 1.0 and 1.5 J/cm<sup>2</sup>. The biomodulatory influence was determined by assessing cell viability, the potential for osteogenic differentiation and the cytokine production profile of irradiated MS compared to non-irradiated ones. Cell viability was quantified using the Resazurina colorimetric method after the end of the irradiation protocol. To determine the differentiation potential, MS were transferred to wells in culture plates and kept under the influence of osteogenic differentiation induction medium for 14 days. At the end of this period, a histomorphometric analysis was performed to detect the bone matrix produced and stained with alizarin red. The cytokine production profile was established by the quantification of interleukins 1 beta (IL-1 $\beta$ ), 6 (IL-6), 10 (IL-10) and tumor necrosis factor alpha (TNF- $\alpha$ ) using an immunodetection procedure. Results: The results showed that there was no biomodulatory influence on cell viability and osteogenic differentiation and there was a dose-dependent biomodulatory influence of LILR on the production of cytokines, with a reduction in IL-6 at doses of 1.0 and 1.5 J/cm<sup>2</sup>. Conclusion: It is concluded that LILR exerted a dose-dependent biomodulatory influence on cytokine production by hSBMSC grown as MS. This potential can be exploited to influence the microenvironment in TC and BP.

**Keywords:** Photobiomodulation; Immunomodulation; Regenerative Medicine; Cell Therapy; Bioprinting.

\* University of Araraquara – UNIARA, Araraquara, SP, Brazil.

\*\* Renato Archer Information Technology Center (CTI), Campinas, SP, Brazil.

\*\*\* Federal University of São Carlos – UFSCar, São Carlos, SP, Brazil.



## Rapid 3D prototyping biomodel as an auxiliary surgical planning method for facial tumor resection

Luiz Henrique Soares Torres\*; L. F. O. Gorla\*; Marisa Aparecida Cabrini Gabrielli\*; Valfrido Antônio Pereira Filho\*

### (Biofabrication and bioprinting (in general))

**Abstract:** ameloblastomas are slow growing, high recurrence and locally invasive facial tumors. Thus, an accurate surgical approach guaranteed satisfactory clinical results and less patient morbidity. The additive manufacturing technique allows to making three-dimensional models from 3D image data that a physical replica of the patient's anatomy, assisting in planning and ensuring surgical predictability. Methodology: male patient, 32 years old, with no previous medical history, attended the ambulatory of maxillofacial surgery, with swelling on the right side, painless, with evolution of 08 months. Imaging exams showed an intraosseous trabecular lesion in the right body and mandibular angle. In histopathological analysis by incisional biopsy, the diagnosis of multicystic ameloblastoma was obtained. We opted for making a 3D model by additive manufacturing for planning tumor resection and previous modeling of osteosynthesis titanium plate. Results: the tumor resection regarding the installation of the fixation device was performed under general anesthesia. Following an 8-month follow-up, the titanium plate was fractured. A new digitally preformed and more robust device was installed. Bone grafting of autogenous origin was performed in the same session. Currently in follow-up for 01 year, he continues without recurrence or complications. Conclusions: the additive manufacturing is an effective auxiliary method in the planning of tumor resections, since it allows the visualization of the lesion margins, in addition to providing a pre-modeling of the bone fixation devices and reduction of the surgical time.

**Keywords:** Three-Dimensional Printing; Ameloblastoma; Neoplasms; Technology; Facial Neoplasms.

\* Universidade Estadual Paulista "Júlio de Mesquita Filho", Faculdade de Odontologia de Araraquara, UNESP/FOAr.

# 3DBB

2020 Aug 26-28th

1st INTERNATIONAL DIGITAL CONGRESS ON  
3D BIOFABRICATION AND BIOPRINTING

NUT3D – PPGB – UNIARA

## Production of polymeric scaffolds by fdm from phbv polymer reinforced with ZrO<sub>2</sub>

Júlia de Carvalho\*; Noelle Cardoso Zanini\*; Amanda Claro\*\*; Nayara Do Amaral\*\*; Hernane Barud\*\*; Daniella Regina Mulinari\*

### (Biomaterials)

**Abstract:** Additive manufacturing has been one of the great technologies that emerged with the fourth industrial revolution, which reached emerging areas of rapid prototyping. The 3D printing technique, layer by layer, using FDM (Fused Deposition Modeling) has consolidated itself as cheap and accessible, using design software to personalize the printed object. Thus, regenerative medicine gained a tool to obtain small three-dimensional structures of detailed geometry with interconnected pores, the scaffolds, which act as a support for tissue regeneration. To mimic the tissues of a living organism, the scaffold material must have biocompatibility, non-toxicity, and biodegradability. A biopolymer that fits these characteristics is polyhydroxybutyrate-cohydroxyvalerate (PHBV). Hybrid organic-inorganic materials can improve the properties of pure polymers. Inorganic zirconium oxide (ZrO<sub>2</sub>), besides having good thermal, chemical, and mechanical stability, is also highlighted in regenerative medicine, for its ability to stimulate the growth of osteoblastic cells. In this work, composite filaments reinforced with ZrO<sub>2</sub> (1 to 10% w/w) were obtained and characterized for the manufacture of scaffolds. The ZrO<sub>2</sub> was obtained by the Conventional Precipitation Method (CPM) and mixed with PHBV in a mini-extruder. For the filaments (PHBV and composites), the morphology was evaluated by the stereomicroscopy technique, and the microhardness by the Vickers hardness test (HV). SolidWorks was the software chosen to develop the 3D designs of cylindrical scaffolds to be printed by FDM. However, it was not possible to print the 10% ZrO<sub>2</sub> composite due to the fragility (causing fracture) and the non-linearity of the filament length, confirmed by stereomicroscopy, which exposed changes in the sample surface: the roughness was increased by the agglomeration of the oxide in the surface, making printing impossible. As for the mechanical properties, except for the 7.5% ZrO<sub>2</sub> composite (162 MPa), the addition of oxide in the polymeric matrix did not cause major changes in the microhardness of the composites, which obtained a range of 90 to 105 MPa, similar to pristine PHBV (105 MPa), revealing that there was possibly a weak interaction between matrix and reinforcement (due to the hybrid nature of the material). It was concluded that ZrO<sub>2</sub> changed the filament morphology, but the mechanical properties did not show significant changes.

**Keywords:** PHBV; ZrO<sub>2</sub>.nH<sub>2</sub>O; Filamentos Compósitos; Manufatura Aditiva; Scaffolds.

\* Universidade do Estado do Rio de Janeiro (UERJ), Faculdade de Tecnologia (FAT).

\*\* Universidade de Araraquara (Uniará).



## Valorization of palm residue as phbv reinforcement for scaffold printing by FDM

Noelle Cardoso Zanini\*; Emanuel Da S. Carneiro\*\*; Lívia R. De Menezes\*\*\*; Hernane Da S. Barud\*\*\*\*; Daniella Regina Mulinari\*\*

### (Biomaterials)

**Abstract:** One route for the reconstruction of damaged bone tissues is the scaffolds, structures with interconnected pores of temporary support for cell growth. Surgical interventions for prostheses of conventional materials cause infections, pain, and immunological rejections. To remedy such side effects, the use of biopolymers in scaffolds stands out for their compatibility with the living organism. However, one of the disadvantages of biopolymers, such as polyhydroxybutyrate-co-hydroxyvalerate (PHBV), is the high price, discouraging their use. The incorporation of natural fibers can be stimulating to decrease the cost and at the same time improve the properties of the biopolymeric matrix. By associating the filler function with the reuse of a natural fiber considered as agro-industrial waste, the scaffold gains a green character, re-signifying a waste for a noble purpose. The production of scaffolds by Fused Deposition Modeling (FDM), is a practical additive manufacturing technique for printing complex custom 3D shapes and more financially advantageous. The FDM printer needs extruded filaments to deposit the porous structure of the scaffolds in thin layers. Thus, this work aimed to elaborate and characterize PHBV filaments reinforced with bleached fibers from the palm residue (in percentages varying from 1 to 10% w/w) for the manufacture of scaffolds by the FDM technique. Fibers from palm residue before and after bleaching (FRP and FBRP, respectively), and filaments (pure PHBV and biocomposites) were analyzed by Scanning Electron Microscopy (SEM), Infrared Spectroscopy (FTIR), Contact Angle (CA) and Cytotoxicity. SEMs of the filaments revealed a tendency for FBRP to clump at the ends during extrusion, which later corroborated the impossibility of FDM printing of the filaments with a higher FBRP content. FTIR showed that bleaching promoted the -OH band of FBRP cellulose, facilitating fiber-matrix interaction. Biocomposite filaments revealed small decreases in the characteristic bands of PHBV, showing slight matrix-reinforcement interaction. The addition of FBRP increased the hydrophilicity of biocomposites ( $CA > 90^\circ$ ) and favored cell viability (from 95% after 7 days) classifying all filaments as biocompatible. Pristine PHBV scaffolds and 1% FBRP had cylindrical structures with interconnected pores, desirable for application in tissue engineering.

**Keywords:** PHBV; Bleached Fibers; Residue; Fdm; Scaffold; Tissue Engineering.

\* Universidade do Estado do Rio de Janeiro (UERJ), Faculdade de Tecnologia (FAT).

\*\* Instituto de Ciência e Tecnologia, Universidade Federal Fluminense (UFF).

\*\*\* Instituto de Macromoléculas (IMA), Universidade Federal do Rio de Janeiro (UFRJ).

\*\*\*\* Universidade de Araraquara (Uniará).



## Mandibular reconstruction with prototyping after resection of multicystic ameloblastoma

*Giovanni Cunha\**; *Valfrido A. Pereira-Filho\**; *Mário Francisco Real Gabrielli\**; *Marisa Aparecida Carbini Gabrielli\**

### **(Biofabrication and bioprinting (in general))**

**Abstract:** The multicystic ameloblastoma is a benign tumor relatively common of the jaw. It is clinically similar to other pathologies that affect the bones of the face. In the present report, the reconstruction of the affected mandible was performed using prototyping and the use of pre-shaped plaque. The patient was referred to the Maxillofacial Surgery service with main complaining of pain in the right retromolar region. The radiograph showed the root resorption in “knife blade” form in the second lower right molar. Moreover, there was an extensive multiloculated radiolucent area in the mandible body. The first diagnostic hypothesis was Ameloblastoma. With the computed tomography the case was planned, and the mandibular model was constructed in the 3D printing. After a second histopathological analysis, performed in the hospital, with the full lesion, the diagnosis was confirmed as multicystic ameloblastoma. In the second surgical time, reconstruction was performed with autogenous bone grafting from the anterior iliac crest. The literature reports the aggressive characteristic of the ameloblastoma, the necessity of radical treatment and reconstruction with biomaterials or grafts, such as the anterior iliac crest, which allows adequate quantity and quality of bone to restore form and function. However due to the large area that ameloblastomas and other jaw lesion can affect, the digital planning with prototyping allow a better understanding of the extent of the tumor as well as the amount, type, and location of the fixation material, which allowed predictability of the case. Reconstruction using this type of technique with 3D models could create the necessary framework to the second time surgery with bone graft, it saves surgical time and increase the possibility of correcting facial symmetry. At this moment, the patient is under follow up without tumor recurrence.

**Keywords:** Prototyping; Mandibular Reconstruction; Ameloblastoma.

\* São Paulo State University (Unesp), School of Dentistry (FOAR), Araraquara FOAr UNESP.

# 3DBB

2020 Aug 26-28th

1st INTERNATIONAL DIGITAL CONGRESS ON  
3D BIOFABRICATION AND BIOPRINTING

NUT3D – PPGB – UNIARA

## Fabrication of a biomaterial with gelatin, alginate and $\beta$ -TCP for the treatment of fractures caused by osteoporosis

Thaís Pezza de Souza\*; Bruno E. Amantea\*; Rodolfo D. Piazza\*; Gabriel C. Pinto\*; Rodrigo Fernando C. Marques\*; Antonio Carlos Guastaldi\*

### (Biomaterials)

**Abstract:** Considering the increase of the life expectancy and the number of osteoporosis cases, the development of materials that can be used as support in bone fractures treatment decurring from this disease is necessary. With the progress in biomaterials area, there is the potential of using gelatin and alginate in their formulation, because they have good biocompatibility, low toxicity and can be used as drug delivery. It is known that  $\beta$ -TCP (beta tricalcium phosphate) has bioactivity and bone growth inducing properties and could compose the biomaterial formed of gelatin and alginate. Thus, the objective of this work is to obtain a biomaterial composed of gelatin, alginate and  $\beta$ -TCP to be used as a 3D printer ink aiming the treatment of fractures caused by osteoporosis. Methodology:  $\beta$ -TCP, tri-sodium citrate 2-hydrate (PA, Panreac), sodium alginate (PA, Exodo) and powdered gelatin (Synth) were dispersed in aqueous solution and then mixed in a magnetic stirring at temperature of 55°C degrees. The presence of sodium citrate ensure that agglomeration is not formed. Different concentrations were studied and the influence of each compound was evaluated by FTIR-ATR (Frontier Dual Range, PerkinElmer), DSC (2910, TA Instruments) and rheological test (rheometer AR 2000ex, TA Instruments). Results: FTIR spectra showed the bands of  $\beta$ -TCP ( $\nu_4$  PO<sub>4</sub> – 750–500 cm<sup>-1</sup>;  $\nu_3$  PO<sub>4</sub> – 1100–900 cm<sup>-1</sup>), gelatin and alginate chains (C–O carboxylic acid – 1400 cm<sup>-1</sup>; C=O carboxylic acid – 1700–1500 cm<sup>-1</sup>) and an increase of intensity after crosslinking was observed. By DSC analysis, it was observed that, when adding  $\beta$ -TCP and sodium citrate, the melting point temperature is shifted to lower temperatures, indicating an increase in the order of the material generated by the addition of  $\beta$ -TCP, that make it possible to increase the interaction between polymer chains. The rheological test showed that  $\beta$ -TCP addition increases the values of G' and G'' and, in the same time, that the elastic behavior is predominant (G'>G'') for this sample, indicating that the addition of phosphate contributes to the material structure obtained, enabling an increase in the polymer chains interaction. Conclusion: The addition of  $\beta$ -TCP provides an increase in the mechanical properties of the material obtained and presents a viable alternative to compose the biomaterial that will be used as ink for 3D printing.

**Keywords:** Biomaterials; Osteoporosis; Gelatin; Alginate;  $\beta$ -TCP.

\* Instituto de Química – UNESP Araraquara.



## Modeling and 3D printing of biomechanical prosthesis for dogs

Luciana Lopes de Oliveira\*; Jessé Ribeiro Rocha\*; Henrique José Da Silva\*

### (Biofabrication and bioprinting (in general))

**Abstract:** This work aims to model and develop, through 3D printing, a biomechanical prosthesis for a female dog. Which is justified by the lack of specialized services in the development of prostheses in Brazil. For the development of the prosthesis, characteristics such as the amputated area, sensitivity and pain tolerance were respected. It is expected that the dog's adaptation time will be reduced. This study has the support of the Veterinary Hospital of UNIFRAN of a small, female, adult, SRD, canine patient, with partial amputation of the left pelvic region which was submitted and accepted by the ethics committee and authorized by the tutor. The patient was clinically evaluated general, orthopedic, muscular, biomechanical and neurological plaster bandage and plastic film were used. The plastic film was used to isolate the patient's skin and hair in order to ensure comfort and facilitate the removal of the mold, and then the plaster bandage was applied over the plastic film. The plaster bandage was dipped in warm water and the excess was removed, so that the plaster hardening time was shortened. Then, for removal in the model, silicone rubber and catalyst were used, which were used in the following proportion, for each 100 g of silicone rubber, 02% Catalyst (by weight) was added, after the partial curing time After 4 hours, the silicone model was removed from the mold, corresponding to the region of the stump to which the prosthesis will be fitted. Photographs of the model of the amputated pelvic region were taken, where the perspectives used for were: outer (thigh), frontal (knee) , interior (thigh), posterior (hock), front and rear diagonal. Based on these perspectives, the computational modeling of the stump was performed using the Blender software. In the current stage of the work, 3D modeling of the prosthesis is being made in conformity to silhouette of the pelvic region, at the end of the prosthesis modeling it will be printed on the Ender-3 printer, using 1.75mm thick PLA filament, then the prosthesis will be fitted to the stump and the dog's gait will be followed by a veterinarian. The process of adapting the dog to the prosthesis will be introduced gradually, respecting the patient's limits and tolerance.

**Keywords:** 3D Printing; Blender; Prosthesis; Amputation; Dogs.

\* Universidade de Franca – UNIFRAN.





## Three-dimensional drug printing

José Alberto Paris Junior\*; Maurício Cavicchioli\*\*; Antonio Carlos Massabni\*

### (Biofabrication and bioprinting (in general))

**Abstract:** The pharmaceutical industry is heading for the Fourth Industrial Revolution. The growing interest in new medical devices or customized pharmaceutical and biomedical products has significantly impacted on the increase and interest in three-dimensional application. This technology is reshaping the way pharmaceuticals are designed, produced and used, allowing the development of new formulations and more complex dosages, making the production of personalized medication a reality in contrast to traditional pharmaceutical processes in terms of flexibility and customization in the manufacturing process. This pharmaceutical customization aims to maximize therapy in search of better clinical responses increasing patient safety and reducing side effects. In the Oncology area and in the researches focused on cancer treatment, this vision of more specific, individual, personalized and more efficient treatments becomes a great attraction and a necessity for the use of this new tool. The objective of this work is to develop new studies on pharmaceutical formulations based on bioactive binders and metal complexes for the controlled release of these compounds, following the procedure described by Öblom et al (1) for 3D printed isoniazid formulations in combination with pharmaceutical polymers possessing suitable properties for oral drug delivery. We hope to develop similar 3D printing tablets for selected bioactive ligands and their complexes with metals like zinc, silver, platinum and vanadium. 1. Öblom, H., Zhang, J., Pimparade, M., Speer, I., Preis, M., Repka, M., & Sandler, N. (2019). 3D-Printed Isoniazid Tablets for the Treatment and Prevention of Tuberculosis—Personalized Dosing and Drug Release. *AAPS PharmSciTech*, 20(2), 1–13. <https://doi.org/10.1208/s12249-018-1233-7>

**Keywords:** Binders; Metal Complexes; Pharmaceutical Formulations; Biomedical Products; Bioprinting.

\* University of Araraquara (Uniar), 1217 Carlos Gomes St., Araraquara, São Paulo, Brazil.

\*\* Department of Inorganic Chemistry, Institute of Chemistry, São Paulo State University (Unesp), 55 Professor Francisco Degni St., 55, Araraquara, São Paulo, Brazil.



## Biospeckle´s application: an analytical monitoring contribution to fungi inoculation first hours

José Francisco Ferreira de Oliveira\*; Inacio Maria Dal Fabbro\*\*

### (Applications)

**Abstract:** Researches based on the application of Speckle, a technique based on the relationship of statistical interference originating at random, when the laser beam is applied to surfaces, has its appearance connected to the theory of light scattering, and this theory involves the process of interaction of light with matter. When the result of monitoring these analyzes of rough surfaces comes from one with biological activity, it is called Biospeckle. Our research proposal was to demonstrate the application of Biospeckle as a viable tool for monitoring and analyzing the possibility of biology activity in fungi on its first hours of inoculation. In order to demonstrate it, we used three indexes of biological activity analysis, namely: Moment of Inertia (IM), Differences of Absolute Values (AVD) and Speckle Space–Time (STS). By getting these indicators results, we obtained different fungi images in the first days of their incubation, evolving for the first hours, to measure the development of fungi in Petri dishes. When conducting the research, the used procedures were aiming to obtain results that could assist and help in the application of the Biospeckle in many stages of fungal incubation, but essentially on its first hours. The isolation of all filamentous fungi in their growth environment, used in this research work, was performed under aseptic conditions in the Vertical Laminar Flow Safety Chapel. It can be inferred that fungi inoculated in Petri dishes were radially developed in their early days. This process can be well observed by applying the randomly selected points distribution technique following a Gaussian distribution, which is a literature area analysis methodology, then it allows to present a new correction in the growth curve. Therefore, it is possible to follow the displacement of the nucleus of biological activity by varying the focus, applying the Gaussian distribution. All in vitro experimental research procedures were performed at the Mycology Laboratory of the Faculty of Food (FEA / UFLA. The”) and at the Optics Laboratory (FEAGRI / UNICAMP). The fungi were provided by the library of the Collection of Culture of Microorganisms (CCDCA), located in the Laboratory of Mycology and Mycotoxins within the Department of Food Science at UFLA. The. The developmental analysis showed to be quite fruitful, demonstrating that the laser Biospeckle technique revealed to be a good monitoring tool in the first hours of growth for both genus.

**Keywords:** Biospeckle; fungos; “Moment of Inertia (IM); Differences of Absolute Values (AVD) and Speckle Space–Time (STS)”.

\* Instituto Federal de São Paulo IFSP.

\*\* Universidade Estadual de Campinas (Unicamp).



## Developing a new file standard for bioprinting

Juliano Marcello\*; Rodrigo Alvarenga Rezende\*\*

### Biofabrication and bioprinting (in general)

**Abstract:** Biofabrication is a multidisciplinary research area that has several challenges to be overcome in all areas of knowledge involved in the process so that in the future it is possible to obtain biofabricated tissues and organs. In the area of computing, much has been adapted to 3D printing systems, such as software, methods and files, making the integration and interoperability of data complex and still inefficient, requiring improvements and innovations. A classic example of the use of adapted methods is the use of design software for modeling the design of the fabric that will be biofabricated. Another example is the use of traditional “.STL” files (Stereolithography format) to transfer information related to the project to the (bio) 3D printer. However, the STL standard has a limitation in carrying other more specific information and, therefore, is a format that will not be very efficient in the process of bioprinting complex living structures. Even within the scope of Additive Manufacturing, alternatives to STL files have already emerged, as is the case with AMF (Additive Manufacturing File format) files. The creation of this pattern brought advantages in relation to the STL, making it possible to include information such as the representation of colors, textures, materials, substructures and other properties of the objects to be manufactured. As for the “non-living” objects to be printed three-dimensionally, there is a need for some properties to be incorporated into the project file for bioprinting with specific characteristics of the tissue or organ to be biofabricated. In this sense, the objective of the work is to understand which parameters will be necessary for bioprinting considering, for example, the rheological behavior of biotints, as well as equipment parameters, and to create a file format that includes this information and can be imported and interpreted by the bio-printer making it possible to build living structures that are organized, maturable and implantable. For this, it is intended, among a wide range of computational resources, to use free and open source software InVesalius dedicated to the treatment of medical images, and to create a necessary extension so that the essential properties can be inserted in the project and generate the data in the new format.

**Keywords:** Bioprinting; Biofabrication; Design; STL File.

\* Post-Graduate Program in Biotechnology (PPGB), University of Araraquara (Uniar), Araraquara, SP, Brazil.

\*\* Renato Archer Information Technology Center (CTI), Campinas, Sp, Brazil.



## Swab development study by additive manufacturing: open access design selection and preliminary testing

João Pedro I. Varela\*; Alex F. De Lima\*; Ygor C. M. De Lucena\*\*; Vanderlino B. S. Júnior\*\*; Nadja M. Da S. Oliveira\*\*\*; Wanderley F. De A. Júnior\*

### (Devices and processes)

**Abstract:** Nasopharyngeal (NP) swabs are necessary to collect samples for COVID-19 testing. The aim of this research is the preliminary open source design swab study manufactured by 3D print: design and preliminary tests. For development of the first prototype in this research, it was used a methodology that consists: informational design, conceptual design, preliminary design, detailed design, manufacturing and testing. Then, two prototypes were generated, one is the open source design swab, available in a research carried out by CTC with the Virtual Hospital Valdecilla, and a device that was used in one of the tests. For manufacturing, 3D printing equipment model Anycubic Photon and 3D resin Odorless green, supplied by 3D Fila, were used. Finally, handling tests were performed (Swab bending tests at 90 and 180 degrees, head bending test, breakpoint rupture test and absorption test). This methodology was based on the tests presented in the literature to support this research. The 90° and 180° bending tests were successful, showing the tough of swab stem to bending. The head bending test showed there isn't so much deflect due to high stiffness, reaching a value at about 6.5 degrees before rupture. The breakpoint test was performed in two ways and both occurred correctly. Finally, the absorption test, which the swab showed a fluid absorption at about 0.1g (50% less than a common swab, used as a control group). Thus, it was possible to carry out, in the first stage of this research, requirements, specifications, dimensions, design, simulation analysis, experimental methodologies and swab parts functions. In addition, on the second stage of research, it was carry out design selection, first swab prototype additive manufacturing and initial preliminary tests.

**Keywords:** COVID-19; Swab; Open Source Design; Handling Tests; Additive Manufacturing.

\* Universidade Federal de Campina Grande.

\*\* Phaser Studio 3D Print.

\*\*\* Fundação Parque Tecnológico da Paraíba.